Annual Report

October 1, 1978 to September 30, 1979

PRINCETON PLASMA PHYSICS LABORATORY

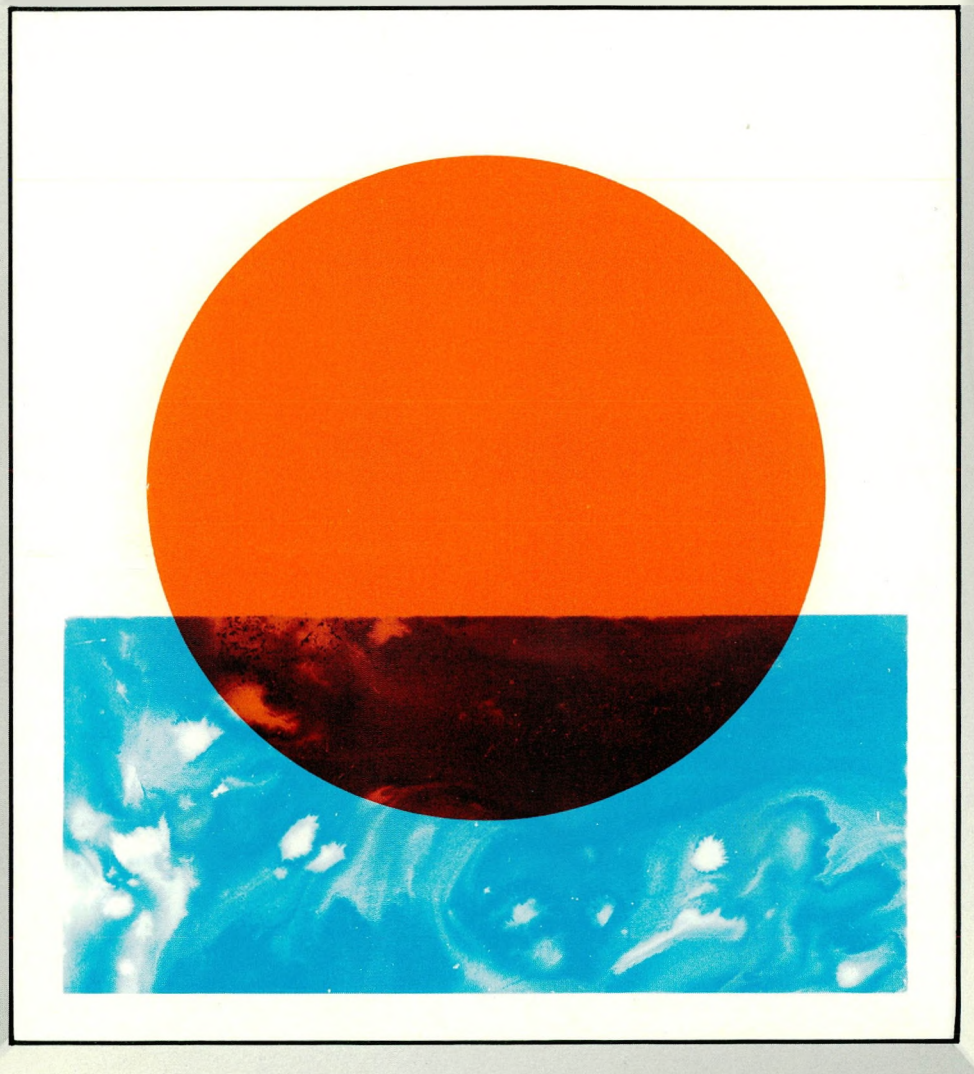

PPPL-Q-37

Notice

Available from
National Technical Information Service
U.S. Department of Commerce
5285 Port Royal Road
Springfield, Virginia 22151

Price: Printed Copy $*; Microfiche $3.50

*Pages	NTIS Selling Price
1-25	$ 5.00
26-50	6.50
51-75	8.00
76-100	9.50
101-125	11.00

Annual Report

Princeton University
Plasma Physics Laboratory
Princeton, New Jersey

PPPL-Q-37

Covering the Period
October 1, 1978 to
September 30, 1979

Issued March 1981

Unless otherwise designated, the work in this report is being funded by the United States Department of Energy under Contract DE-AC02-76-CHO-3073.

Printed in the United States of America

Contents

Cover by James W. Edwards

Preface

The Poloidal Divertor Experiment (PDX) came into operation this year with first plasma on November 29, 1978. Full-scale circular cross-section experiments began in February, 1979, and quickly led to low-q, low-z, long confinement plasmas. The full design current of 500 kA was achieved early in the spring. The next six months were occupied by the installation of hardware for divertor experiments. Meanwhile, the 6-MW PDX neutral-beam system was in fabrication at Oak Ridge National Laboratory with installation scheduled for FY80. The PDX device, operating with neutral-beam heating, is expected to provide a definitive test of the magnetic poloidal divertor concept, and to explore MHD beta limits of plasmas with optimally shaped cross sections.

The Princeton Large Torus (PLT) redirected its emphasis from neutral-beam heating to rf-heating. In the neutral-beam area, the principal new results related to the viscosity of rotating plasmas and the enhancement of thermal transport by field ripple. Fast-wave heating in the ion cyclotron range of frequencies (ICRF) was tried with a single half-turn antenna at moderate input power (typically 350 kW). Substantial ion heating (up to 600 eV) was found for D-H mixtures. Ultimately, 3-5 MW of rf power will be applied. Preparations are also being made to explore the lower hybrid frequency range on PLT.

Smaller devices at PPPL carried out a variety of investigations on wave phenomena and the gas divertor concept. The desirability of steady-state operation for tokamaks gives particular significance to the newly completed Advanced Concept Torus (ACT-1), which will undertake current-drive experiments.

Fabrication of the Tokamak Fusion Test Reactor (TFTR) proceeded throughout the year, with a 1981 target date for initial operation. A project sponsored by the Electric Power Research Institute studied the possibility of incorporating a blanket-module experiment into TFTR. The results were encouraging and work will proceed in FY80.

Design studies for new devices during FY79 included PPPL contributions to the national Engineering Test Facility (ETF) and to the International Tokamak Reactor (INTOR) effort. In view of favorable prospects for implementation of a tokamak ETF/INTOR reactor facility, further design of the short-pulse ignition experiment at PPPL (the PITR) was held in abeyance. Design studies for a long-pulse, superconducting hydrogen device were expected to proceed in parallel with the ETF/INTOR work. In the area of advanced concepts, fabrication of a spheromak device (S-1) was undertaken.

Major theoretical investigations of the year included quantitative assessment of the effect of turbulence on confinement, the effect of toroidal geometry on drift waves and on ballooning modes, and the possible relation between micromagnetic turbulence and the tearing mode.

Princeton Large Torus (PLT)

The Princeton Large Torus (PLT), shown in Fig. 1, began operations in December 1975. The initial experiments addressed the ohmic-heating regime, at plasma currents ranging up to 650 kA. Special emphasis was given to the study of MHD stability, plasma confinement scaling, and the identification and control of impurities. In 1977, neutral-beam injection capabilities were introduced. In 1978, ion temperatures of 6.5 keV were reached by high-powered neutral-beam heating. Concurrently, a new experimental program of rf-heating in the ion-cyclotron range of frequencies (ICRF) was undertaken.

MAJOR ACTIVITIES

Summary

Preparations began in October 1978 for more powerful rf heating at 25 MHz and for operation at higher frequencies. New antennas were installed and various diagnostic changes were made. During the fall and winter, the four neutral beam injectors were sequentially upgraded by the installation of new sets of beam-accelerating grids. This resulted in somewhat higher beam power and considerably reduced impurity evolution from the beam-line walls. At the end of January, toroidal field coil #6 was accidentally overheated. Machine downtime was about four months. Operations were resumed in June at reduced toroidal field. Much of the ICRF work could be carried out as planned, because the primarily desired resonance field values were 17 and 25 kG. Principal experimental results of FY79 are summarized in the following paragraphs and are presented more fully in subsequent sections.

With neutral-beam injection in one direction (either parallel or anti-parallel to the plasma

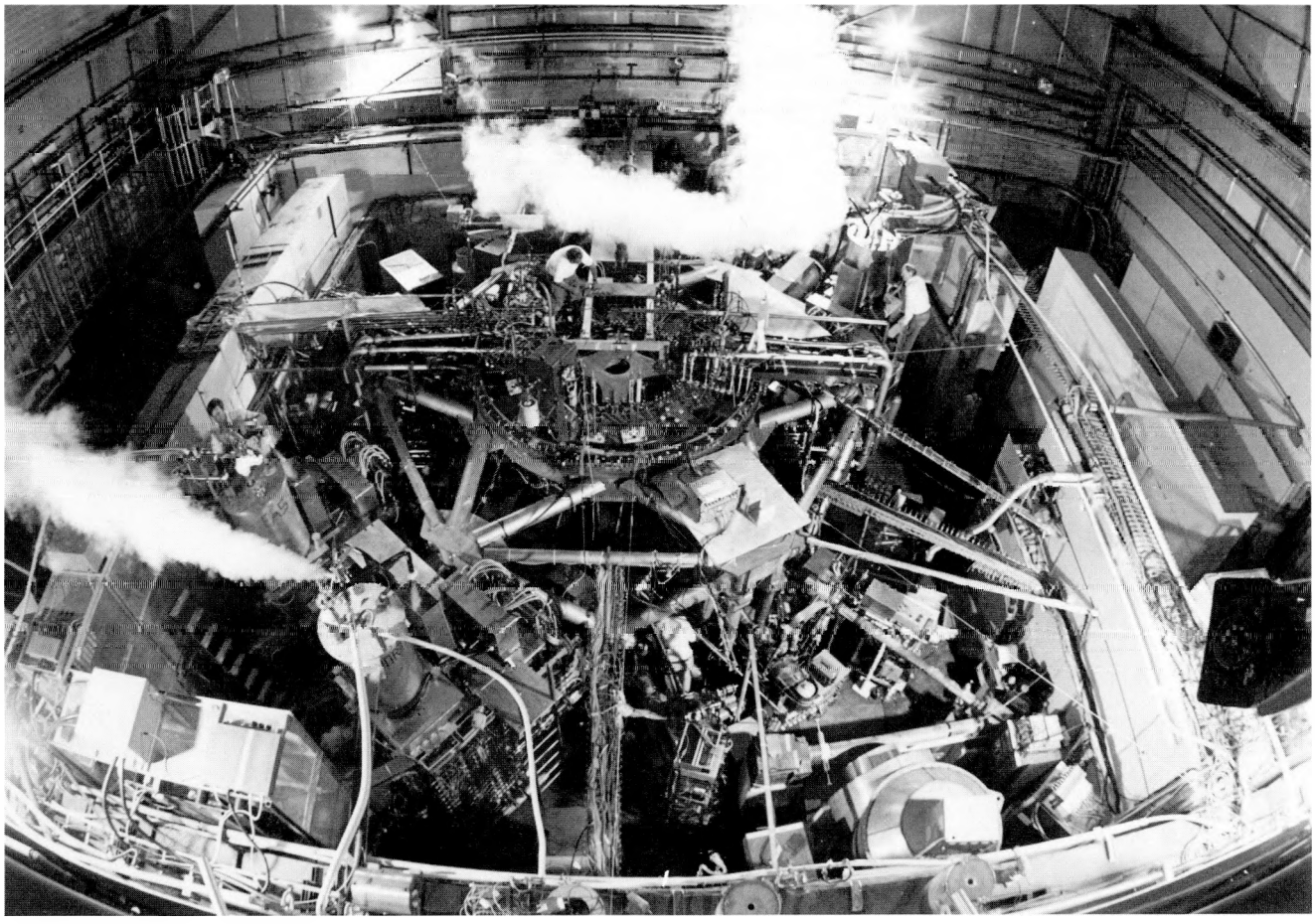

Figure 1. The PLT machine.

current) toroidal plasma rotation due to the injected beam momentum was observed. The measured plasma viscosity was about 10^4 cm^2/sec, much higher than predicted by theory. These observations should give some fundamental new insights into the anomalous transport processes in hot tokamak plasmas.

Wave heating power in the ion cyclotron range of frequencies was increased to ~350 kW absorbed in the plasma. The important minority species heating regime was investigated, and a theoretical model developed that is consistent with the experiments and indicates favorable scaling to higher powers. A heating efficiency $n_e \Delta T_i / P_{rf}$ of 3×10^{13} cm^{-3} eV/kW was obtained for proton minorities in deuterium, and 6×10^{13} cm^{-3} eV/kW for ^{3}He minorities. These efficiencies compare favorably with those obtained with neutral beam heating. In the minority-heating process, high-energy protons (up to 60 keV) were found to be generated and contained, and to equilibrate with the deuterium majority. This high-energy particle confinement has optimistic implications for scaling to higher power in PLT and for future rf-heating in larger tokamaks.

Measurements on neutron energy spectra with co and counter neutral deuterium and proton beams have confirmed the thermonuclear origin of the observed neutron emission. Observation of 14-MeV neutrons with a deuterium plasma has shown that 1-MeV tritium ions have been produced and contained for a time of order 50 ms; these measurements provide the first direct evidence for the confinement of ions with MeV energies in a tokamak—a requirement for ignition in larger machines.

An improved soft x-ray diagnostic system has shown that m = 1 oscillations can persist through and after an internal disruption, in contrast to the theoretical prediction in which complete reconnection and resymmetrization occur during the disruption.

Wavelengths of a number of highly ionized atoms of titanium, chromium, iron, and nickel were measured either for the first time or with improved accuracy—an important contribution to atomic physics. These lines were then used to measure radial profiles of ion temperatures with both neutral beam and wave heating.

Observation of the radial profiles of the line intensities of Fe XXV, XXIV, XXII, and Ti XX showed variations ascribable to charge-exchange-recombination with beam-injected hydrogen atoms. It was estimated that this effect reduces by a factor of about 5 the acceptable density of metal atoms in large tokamaks that rely on neutral beam heating.

Time-resolved measurements were made of the K_α resonance line of heliumlike iron (Fe XXV) and its dielectronic satellites. These measurements have allowed a detailed comparison with theory and have been used to determine the central ion and electron temperatures. They also have been used to investigate ionization equilibrium, and show evidence of nonclassical ion transport.

Measurements on ordinary-mode microwave absorption near the fundamental electron cyclotron frequency were found to be in substantial agreement with theory, and were used to determine local electron pressure. The results are attractive for electron cyclotron resonance heating (ECRH) because they show that the waves can be launched from the low-magnetic-field side of the torus.

New diagnostics were developed for PLT to measure the energy distribution of hydrogen atoms and ions that leave the plasma edge and strike the walls and limiters. Ion impact on the limiters is important for power and particle losses, as well as for impurity generation in low-density, ohmically-heated plasmas. Sputtering of the walls (away from the limiters) by charge-exchange neutrals is found to introduce 2×10^{13} Fe atoms/cm^2-sec at discharge initiation, but only 2×10^{12} during the steady-state phase.

PLT Neutral-Beam Injection

Following the achievement of record plasma temperatures in the summer of 1978, new sets of ion-beam accelerating grids with tapered apertures, based on a Pierce geometry, became available from the ORNL Fusion Energy Division's beam development group. The experimental program was oriented toward the investigation of moderate-temperature physics during this upgrading period of November 1978 to January 1979.

An important effect that accompanies unidirectional neutral beam injection is toroidal rotation of the target plasma. This rotation was measured from the Doppler shifts of ultraviolet impurity lines under different beam and target plasma conditions.

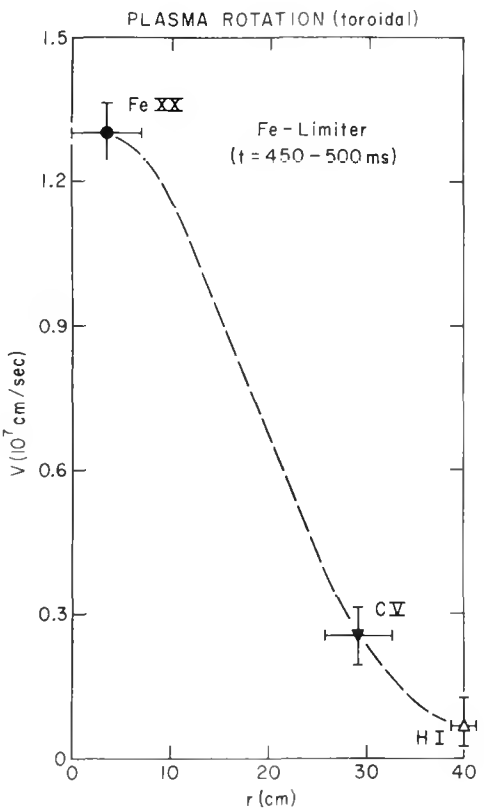

Figure 2. Radial distribution of toroidal plasma velocity at 100-140 ms after beginning neutral beam injection.

A radial profile of rotational velocity was obtained from the characteristic locations of the emitting ions (Fig. 2). In Fig. 3 measurements of the central rotational speed are plotted as a function of the corresponding beam momentum input. The rotational speed increases linearly with momentum input up to the maximum value of unidirectional beam power achieved. Fig. 4 shows the central rotational speed plotted as a function of the corresponding electron density at a constant beam power, i.e., constant momentum input level, both for D^0 beams into an H^+ plasma and H^0 beams into a D^+ plasma. According to simple classical theory, the case with D^0 beams into H^+ plasma should produce 2.8 times greater toroidal rotation velocity; the observed difference of only 20% can be interpreted as indicating better momentum confinement for $H^0 \rightarrow D^+$ injection than for $D^0 \rightarrow H^+$; in both cases the momentum transport is clearly much faster than expected from theory. In terms of time behavior, the rotation builds up in 30-50 ms and then saturates; after the beams are shut off, the rotation decays on a similar time scale. (The data of Figs. 3 and 4 cannot be compared directly, because they were taken under somewhat different conditions.)

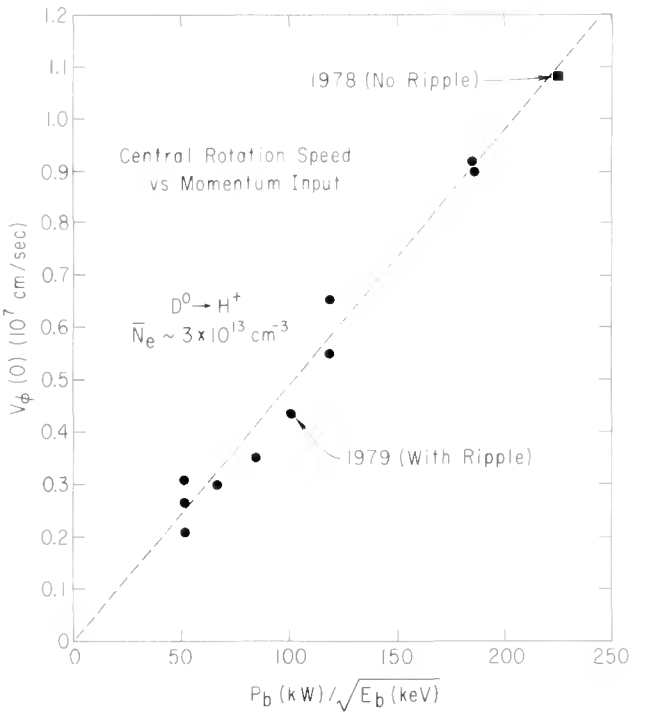

Figure 3. Central toroidal rotation velocity vs. net neutral beam momentum input.

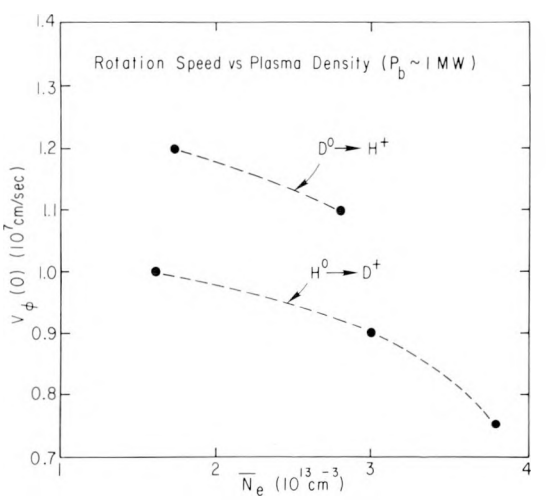

Figure 4. Central toroidal rotation velocity vs. plasma density with beam power ~1 MW.

The damping mechanism of the rotational momentum is not understood at the present time. Charge exchange with neutral ("thermal") hydrogen provides the only known damping mechanism that is significant, but it is too small by at least a factor of two, even at the lowest density, and by a larger factor as n_e increases. The momentum input from beam ions to the target plasma was calculated for a number of $D^o \rightarrow H^+$ cases, using the Monte Carlo Beam Orbit code developed to analyze neutral beam heating experiments. Comparison of the calculated time evolution and radial distribution of toroidal velocity with the measured values gives a plasma "viscosity" of order 10^4 cm^2/sec, much higher than the neoclassical prediction. The central momentum confinement time was found to be approximately 20 ms, and the volume integrated value was approximately 10 ms.

High injection power levels with four beams (~2 MW) became available again in March 1979, but the toroidal field coil accident prevented beam injection experiments until June 1979. While the effectiveness of the coil repair was being evaluated, operation was restricted to toroidal fields of 20-25 kG and there was a non-axisymmetric local dip in the field of 2.7% peak-to-peak on axis (Fig. 5). The lowered field values entailed operation at lower plasma current for fixed values of q. Calculated local ripple contours and regions of enhanced particle trapping are shown in Fig. 5.

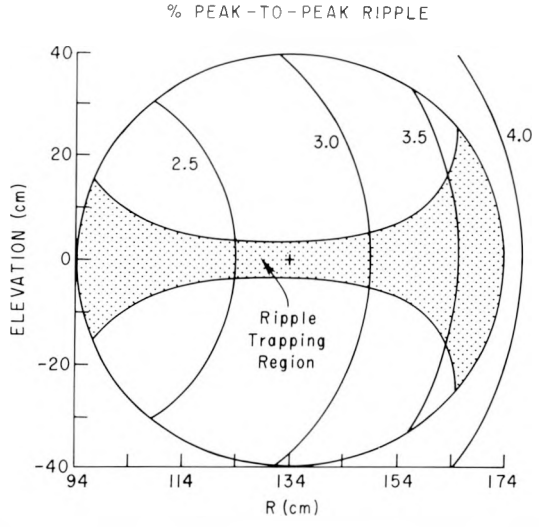

Figure 5. Ripple contours and regions of ripple trapping for PLT resulting from coil damage of early 1979.

Beam heating experiments performed at the lowest densities and highest power in the latter part of 1979 failed to achieve the ion heating efficiency $n_e \Delta T_i / P_. \simeq 4 \times 10^{13}$ cm^{-3} eV/kW observed in similar experiments performed in 1978. A summary of ion heating for the two years is shown in Fig. 6. Electron heating experiments with hydrogen beam injection at $\bar{n}_e = 4 \times 10^{13}$ cm^{-3} also showed an efficiency of only 0.3 eV/kW rather than the 0.5-0.7 eV/kW observed previously.

While the toroidal field ripple represents an easy mechanism to blame for the reduced heating efficiencies, no direct proof was obtained that this is the case, and a number of other factors having to do with different wall conditions and the conflicting requirements of the ICRF program may well be responsible.

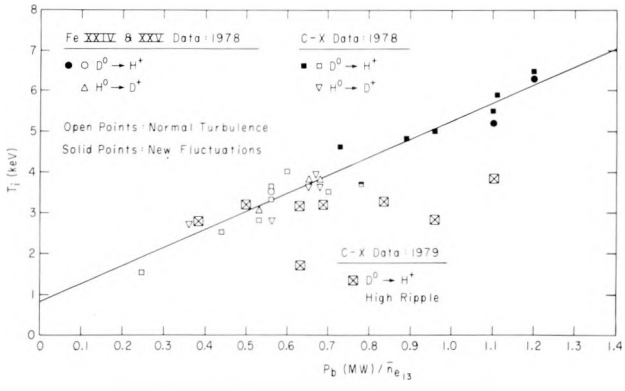

Figure 6. Peak ion temperature vs. beam power per particle including 1978 negligible ripple cases and 1979 high (2.7% on axis) ripple.

ICRF Heating in PLT

A. MINORITY HEATING REGIME

Radio-frequency plasma heating in the ion cyclotron range is being studied on PLT for the purposes of optimizing heating in various possible wave regimes of large tokamaks and providing scaling information that will permit extrapolation to reactor conditions. During FY79, the delivered rf wave power was increased substantially (to ~ 350 kW), with corresponding increases in the bulk ion temperature. Extensive study of the wave-damping physics and the kinetics of the ion heating helped develop a theoretical model that is consistent with the

experiments and indicates a favorable scaling to higher powers in PLT.

Attention was focused during this period on heating a two-ion mixture, where one ion species (minority) forms a small percentage of the total density. The wave damping rate into this minority species is observed to be particularly effective relative to fundamental majority heating.

Waves were excited by a half-turn loop fitted with an electrostatic shield to reduce edge plasma loading of the antenna. The excitation frequency was 25 MHz, matching the cyclotron frequency for minority hydrogen at B_ϕ = 16.4 kG or for ^{3}He at 25 kG on axis. Maximum forward powers of 450 kW for 150 ms were developed; with 80% coupling efficiency, 360 kW was delivered to the plasma by a single coil.

B. HYDROGEN MINORITY

Measurements of the rf-driven proton energy distributions with a mass-sensitive charge-exchange system indicated that virtually all the rf power was deposited directly into the hydrogen. The resulting proton tail was well confined, and its equilibration with the bulk deuterons and electrons was consistent with Fokker-Planck theory when the losses due to charge exchange were included (Fig. 7). Moreover, the proton distribution was observed to be nearly isotropic up to 40-60 keV, as shown in Fig. 7; the fast-ion diagnostic data include both perpendicular and parallel ion channels. As a consequence of Coulomb coupling to the protons, the deuteron temperature increased from 500 to 1200 eV, and the deuteron distribution was observed to be Maxwellian (Fig. 8); the absence of a high-energy tail indicates that direct second-harmonic heating of the deuterium was negligible in these experiments. The time evolution of the charge-exchange-deduced central deuteron temperature shown in Fig. 9 indicates a rise and fall consistent with the energy confinement time of the ohmic case. Charge exchange, Doppler broadening of impurity radiation, and neutron measurements are combined to give the deuterium temperature profile of Fig. 10 for $P_{rf} \sim 350$ kW. The heating profile is centrally peaked although somewhat broad and is found to be consistent with the power deposition model based on minority-dominated wave damping.

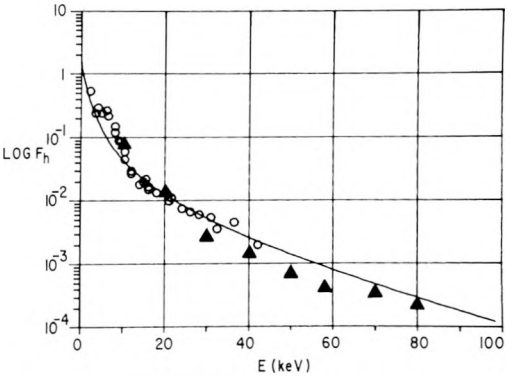

Figure 7. Hydrogen charge exchange spectrum on axis with $P_{rf} \simeq 350$ kW; o data from perpendicular charge exchange analyzer; Δ data from angle-scanned fast ion diagnostic including both perpendicular and parallel ion channels. The curve is calculated from Fokker-Planck theory with charge exchange.

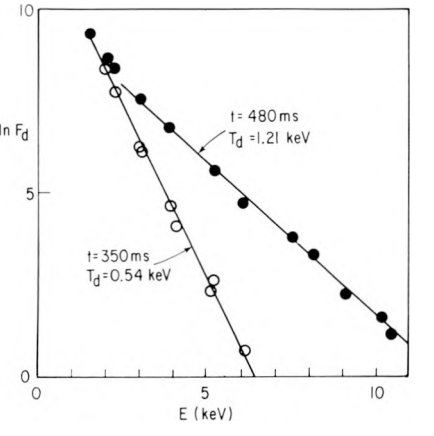

Figure 8. Deuterium charge exchange spectrum for the case shown in Fig. 7. $N_e = 2 \times 10^{13}$ cm^{-3}, B_ϕ = 17 kG; I_A = 300 kA; P_{in} = 350 kW.

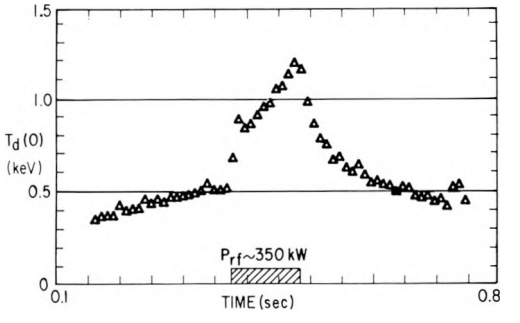

Figure 9. Time evolution of the central deuteron temperature with proton minority for the conditions of Fig. 8.

C. ^{3}He MINORITY

The use of a ^{3}He minority in PLT had a two-fold advantage for the minority heating process: (1) due to the higher charge and mass the ^{3}He was more strongly coupled to the bulk deuterons than the hydrogen minority; (2) higher toroidal field and consequently higher plasma current could be utilized, which led to substantial improvement in the fast ion confinement. The experimental result was that the overall heating efficiency was a factor of two higher for the ^{3}He case, as indicated by the central ion temperature increase as a function of normalized power (Fig. 11).

The degree of confinement of energetic ions in PLT was found to play an important role in the overall heating efficiency: as the current was lowered below a critical level, the peak deuteron temperature during the rf pulse decreased (Fig. 12), and an increased wall impurity influx was observed, presumably due to sputtering caused by the loss of fast ions. The bulk ion heating and minority tail production (measurable directly in the hydrogen minority case) scaled with density, concentration, and rf power in close agreement with Fokker-Planck theory and indicated a favorable scaling of this regime to higher power levels in PLT.

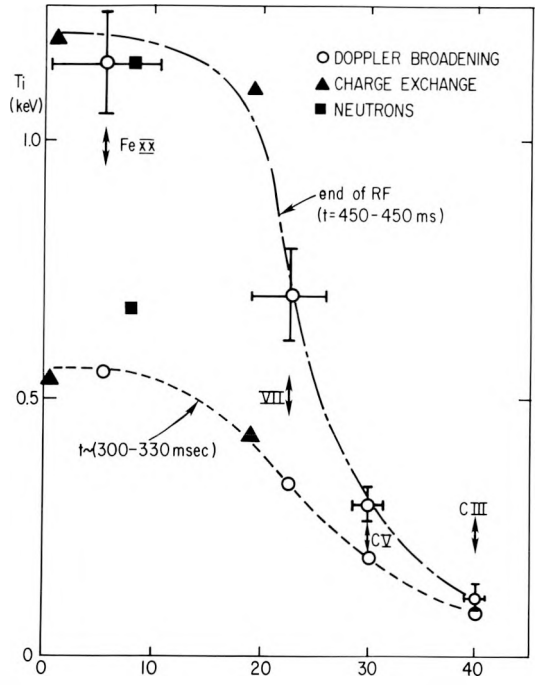

Figure 10. Radial ion temperature profile for $P_{rf} \sim$ 350 kW via charge exchange, neutron, and spectroscopic measurements.

Fusion Reaction Measurements

The PLT produces two orders of magnitude larger fusion reaction rates ($\sim 10^{14}$ d(d,n) ^{3}He reactions/sec) than any other tokamak and has a neutron yield per pulse ($\sim 2 \times 10^{13}$ neutrons/pulse) one order of magnitude beyond that of any previous laboratory fusion device. With these large reaction rates, neutron diagnostics are easier and more informative than on smaller devices.

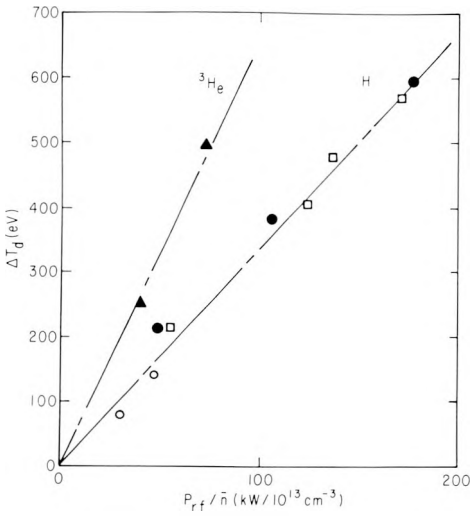

Figure 11. Deuteron temperature increase on axis for the proton and ^{3}He minority cases versus the normalized rf wave power.

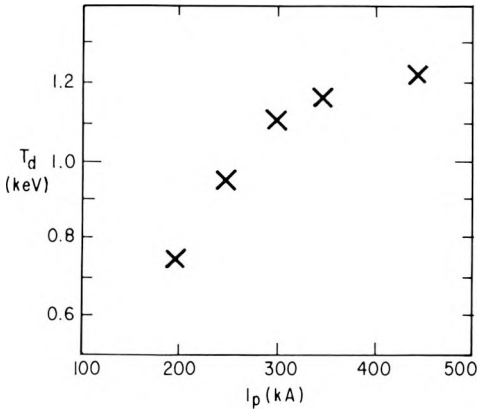

Figure 12. Peak deuteron temperature as a function of the plasma current. ^{3}He minority; P_{rf} = 150 kW; B_ϕ = 25 kG.

We have studied the neutral-beam-induced fusion reactions that occur with deuterium neutral beam injection ($D^\circ \rightarrow D^+$). The PLT studies of these "beam-target" fusion reactions provide a favorable prognosis for TFTR, since we find that the neutron emission rate, time evolution, radial profile, and energy spectra are consistent with d(d,n) ^{3}He reactions caused by energetic injected ions which are confined and slowed down in accordance with classical theory (Figs. 13 and 14). In Fig. 13 the variation over two orders of magnitude of the neutron emission rate exhibits the expected linear increase with beam current and the energy dependence of the cross-section when the beam voltage is varied; in Fig. 14 the emission decreases when the density is increased, because the beam penetration and beam slowing-down time decrease.

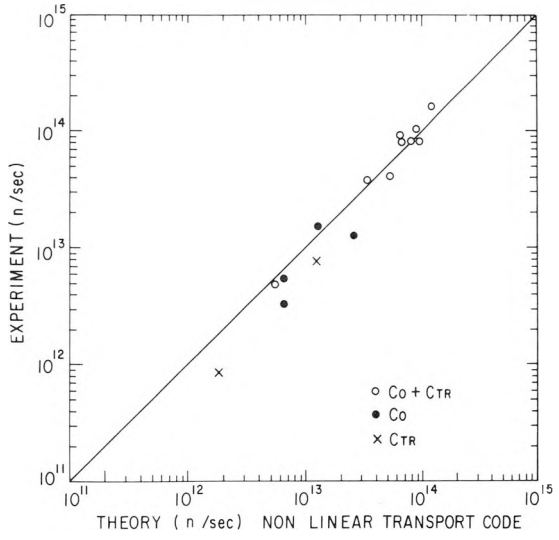

Figure 13. Comparison of the experimental neutron emission during neutral beam injection with that calculated theoretically. Beams injected parallel (co) and anti-parallel (counter) to the plasma current direction.

Neutron spectral measurements provide information on the thermonuclear origin of the neutrons. A 14,000 lb paraffin + Li_2CO_3 neutron collimator (Fig. 15) accepts neutrons emitted from the plasma in a direction parallel to the plasma current. A nonthermonuclear neutron emission due to a directed velocity of the reacting deuteron pairs shows up as a Doppler shift of the neutron energy. We found that with $D^\circ \rightarrow D^+$ injection, there was the Doppler shift (Fig. 16) expected from the beam-target d(d,n) ^{3}He fusion reactions. With $H^\circ \rightarrow D^+$ injection, there was no measurable Doppler shift, as is expected with a thermonuclear neutron emission originating in a beam-heated Maxwellian plasma.

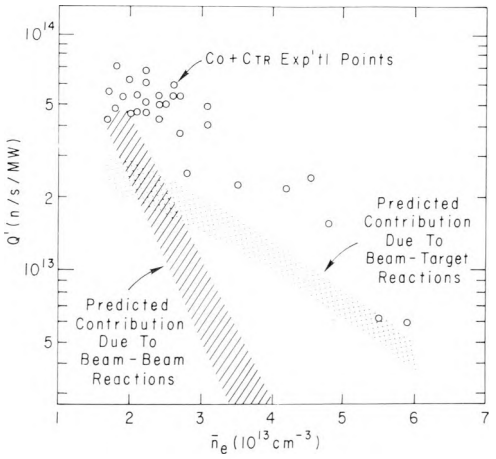

Figure 14. Experimental neutron emission rate per megawatt of injected beam power as a function of the line average density. The shaded regions indicate the calculated contributions of beam-beam and beam-target reactions.

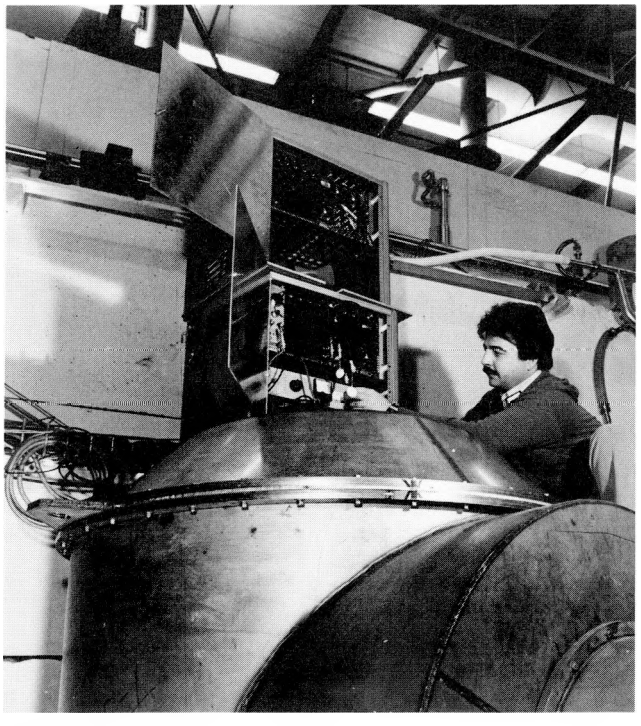

Figure 15. PLT neutron collimator.

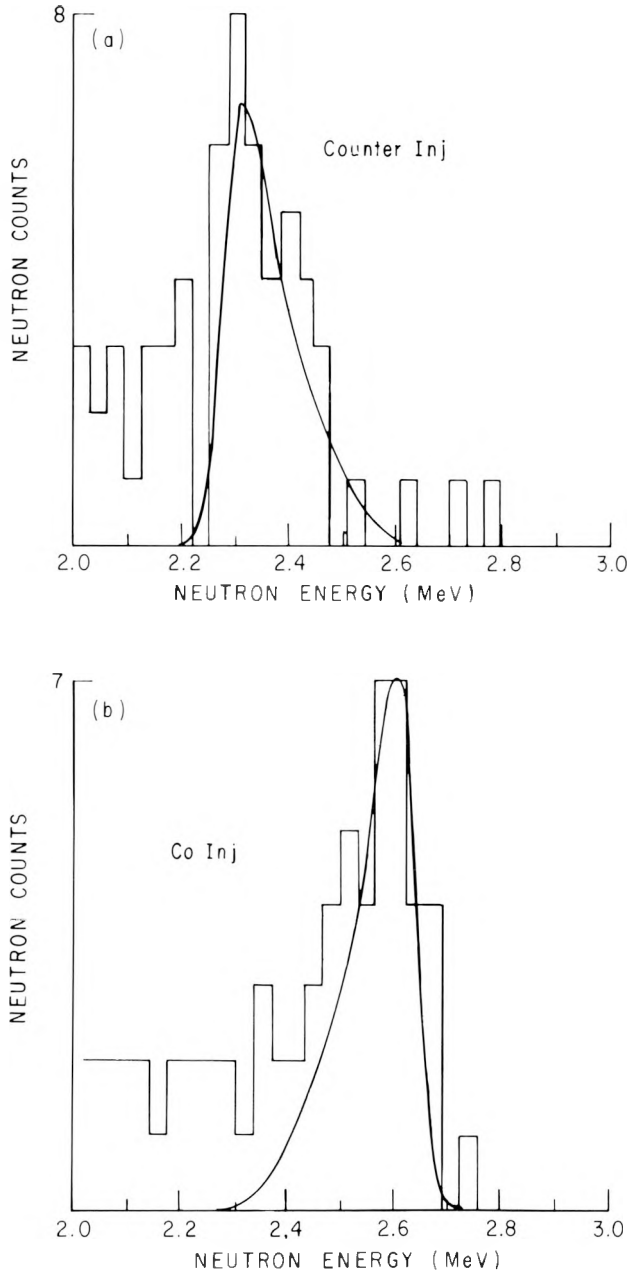

Figure 16. Collimated $D^o \rightarrow D^+$ neutron spectrum with the theoretically calculated spectrum for (a) 30 keV counter injection, and (b) 26 keV co injection.

The D-D fusion reaction occurs in two equal branches, the reaction d(d,n) ^{3}He, producing a 2.5 MeV neutron, and the d(d,p)t reaction producing a 1 MeV triton. If the triton is confined inside the plasma, then it slows down through the maximum of the D-T cross-section, with a large burnup probability (~1%) in the d(t,n)α reaction. On PLT, the 14 MeV D-T neutron emission level can be ~1% of the 2.5 MeV neutron level (Fig. 17), indicating that these fusion-produced tritons are confined in PLT for durations comparable to the triton slowing-down times (i.e., $\gtrsim$ 50 ms). Confinement of the charged fusion reaction products is a requirement for ignition and these PLT 14 MeV neutron measurements are the first indication that a tokamak can confine MeV ions.

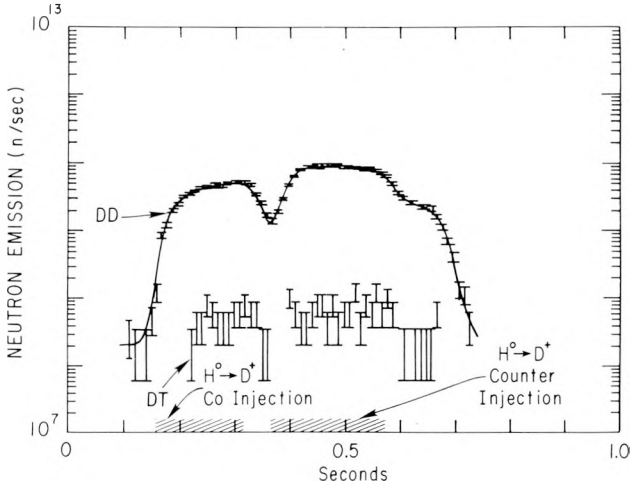

Figure 17. Time evolution of the PLT D-D (2.5 MeV) neutron emission and the D-T (14 MeV) neutron emission.

X-Ray Fluctuations and Magnetohydrodynamic Instabilities

Improved X-ray imaging systems were installed on PLT in an effort to provide enough views to analyze the intricate behavior of the magnetic topology during MHD fluctuations. Powerful analysis techniques comparable to those used in "brain scanning" have been applied in order to convert the raw chordally-integrated data to local X-ray emissivities.

A 75-chord system, capable of simultaneously measuring the line-integrated emissivity in three energy bands at 25 spatial positions each, views the plasma from the side at one toroidal position. Two 9-detector arrays image the plasma from above at displaced toroidal positions. This configuration should allow separation of the n = 1, m = 2 and n = 2, m = 3 modes, which are theoretically predicted to flatten profiles ad-

jacent to q = 2 and q = 1.5 in their initial stages and to enhance the transport between the surfaces by "braiding" in the stage where they "overlap."

Enhanced spatial resolution in the interior of the discharge, coupled with increased temporal resolution due to neutral-beam-induced plasma rotation, has revealed detailed images of the evolution of the plasma during internal disruption. In particular, the m = 1 oscillations can persist through and after the disruption (Fig. 18). This is in contrast to the theoretical prediction, in which an m = 1, n = 1 magnetic island overwhelms the central region of the discharge, effecting a flattening and consequent symmetrization of the X-ray emissivity profile.

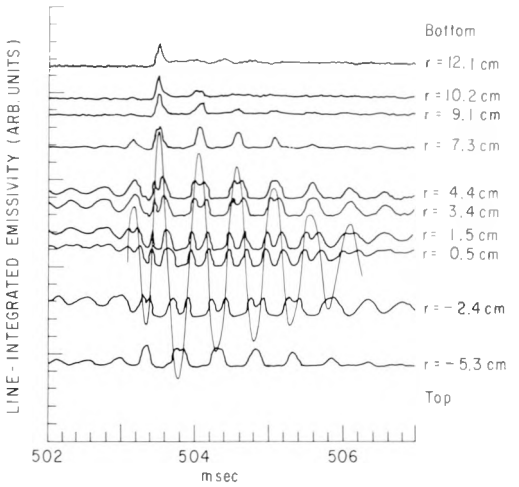

Figure 18. Signals from X-ray detectors viewing an internal disruption in the PLT. The X-ray emission along chords tangent at the listed radii exhibits a sinusoidal shape prior to the "sawtooth drop" at 503.4 ms; the central trace has a dominant double frequency component because it views the maximum emission twice per cycle, whereas external detectors view only motion along a gradient. After the disruption, the fluctuating emission is localized in a thin helical filament whose trajectory is indicated by the line superimposed on the data traces.

A computerized tomographic reconstruction technique, based on decomposition of the fluctuations into poloidal harmonics, has been applied to one-dimensional projection data of a minor external disruptive instability. At each rotation of the mode a reconstruction of the local source function is computed, assuming an m = 2 poloidal symmetry. Resultant evolutions of the emissivities are shown in Fig. 19. The progressive growth of a flat region in the vicinity of q = 2, followed by a sudden drop in central emissivity, and the subsequent slower recovery of the profile, are apparent.

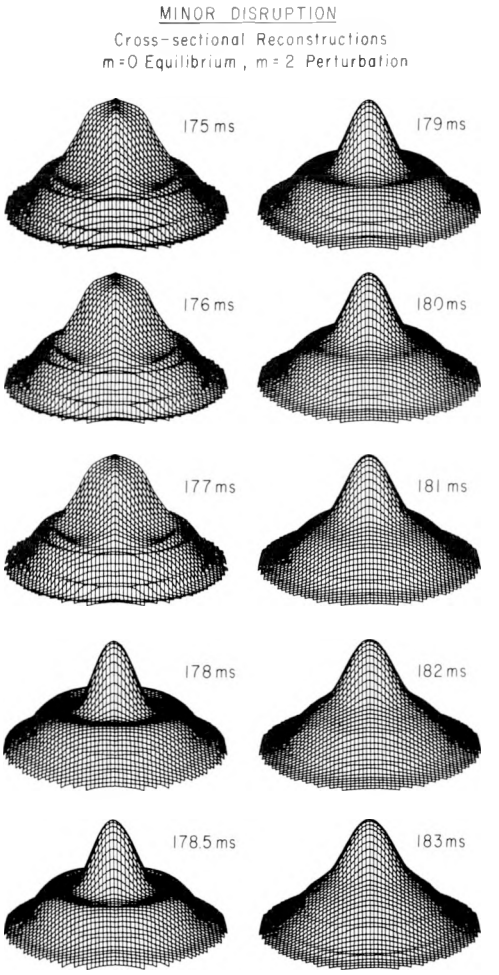

Figure 19. Reconstructed X-ray emission profiles in a cross-section at fixed toroidal angle throughout a minor disruptive instability. The previously symmetric profile develops an elliptical shape with the polarization of the ellipse reversing at roughly half the minor radius of the plasma; the mirroring of the ellipses about the q = 2 radius results in a flat region, corresponding to the m = 2 island. The extent of the leveling increases into the disruption at 178.5 ms, after which the profile relaxes to a symmetric, peaked equilibrium by 183 ms.

Atomic Physics and Plasma Spectroscopy

During 1979, our previous programs of quantitative radiation measurements were extended and further developed, with special emphasis on establishing localized measurements in the high-temperature interior of the plasma. Such measurements are likely to be of special interest in future high-temperature plasma diagnostics. Some highlights are listed below, with more details in the references.

Wavelengths of a number of highly-ionized atoms of titanium, chromium, iron, and nickel, with ionization potentials in the 1-2 keV range, either were measured for the first time, or the previously determined wavelengths were improved. These spectral lines fall into two categories: the electric dipole or allowed resonance lines, and the forbidden (magnetic dipole or spin-change intercombination) lines. The former account for most of the radiated power, and are also of particular interest for absolute ion-density measurements. The latter, because of their relatively long wavelengths, have special advantages for single-shot spatially and spectrally resolved measurements of ion temperatures and motions, local density fluctuations, etc. When a sufficient number of such wavelengths, belonging to a variety of ions with ionization potentials $E_i \sim T_e$, is established, it will be possible, in principle, to construct a spectrometer that will give, e.g., T_i (r,t) in a single discharge.

The newly-established spectral lines were used for determination of radial profiles of ion temperatures with both neutral beam and ICRF heating. Compared to neutron and charge-exchange neutral hydrogen temperature measurements, the spectroscopic T_i measurements are not sensitive to minor deviations from Maxwellian distributions, and measurements at locations other than the maximum are possible (Fig. 10). Similarly, the evolution of the toroidal rotation during unbalanced neutral beam injection was determined from Doppler shifts of various ion lines, as in Fig. 2. Such measurements are still in their infancy, both from the point of view of instrument development and the state of knowledge of the appropriate atomic parameters, as evidenced by the substantial gaps in the profiles.

During four-beam high-power neutral injection experiments in 1978, a large increase in the lithiumlike (Fe XXIV) and berylliumlike (Fe XXIII) iron radiation was observed. This radiation did not appear to be caused primarily by increase of ion concentration, and was tentatively ascribed to depression of ionization states from heliumlike iron by means of charge-exchange recombination with beam-injected hydrogen atoms. This interpretation has been substantially confirmed by simultaneous observation of Fe XXV, XXIV, XXII and Ti XX ion radiation (Fig. 20), including particularly the behavior of

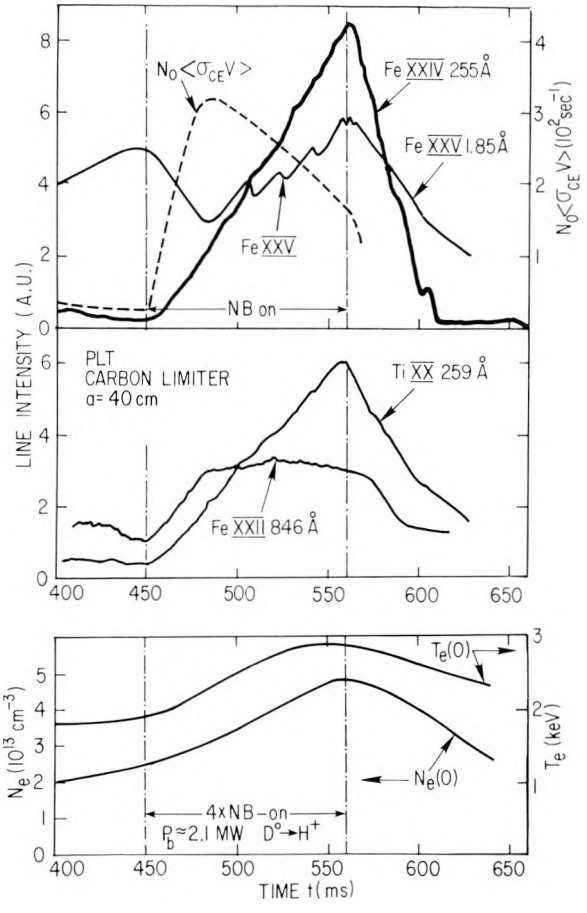

Figure 20. Behavior of various iron ion lines during high-power neutral beam heating; despite increasing $T_e(0)$ the heliumlike Fe XXV light drops, whereas the lithiumlike Fe XXIV and Ti XX light increases by a large factor. The boronlike Fe XXII (which has an ionization potential intermediate between Fe XXIV and Ti XX) increases only moderately. This behavior is ascribed primarily to shift of ionization levels from heliumlike to lithiumlike states by charge-exchange recombination.

radial profiles of the ions (e.g., Fe XXII and Ti XX) of similar ionization potential and ionization rates, and also comparison of neutral beam and ICRF heating. However, it has become evident that the charge-exchange recombination does not explain everything, and some plasma-dynamic effects must be involved.

The recombination phenomenon is likely to be important in large tokamaks relying on neutral-beam heating, because the probable density of neutral hydrogen atoms will prevent the atoms with $Z \sim 20$-30 from reaching the relatively radiationless heliumlike state. The acceptable density of such atoms in the discharge is therefore reduced by a substantial factor (~ 5).

Bragg Curved Crystal Spectrometer — X-Ray Spectroscopy

The X-ray line radiation from highly-ionized heavy impurity ions (Ti, Cr, Ni, Fe) can be used to measure plasma parameters in the inner core of tokamak discharge. Time-resolved measurements of the (1s-2p) K_α resonance line of heliumlike iron (Fe XXV) and its dielectronic satellites, which are due to transitions of the type $1s^2 n\ell - 1s2pn\ell$ with $n \geqslant 2$, have been performed on PLT with a high resolution ($\lambda/\Delta\lambda = 15000$ at $\lambda = 1.85$ Å) Bragg curved-crystal spectrometer. The observed spectra have permitted a detailed comparison with theory and were successfully used to measure central ion and electron temperature and to investigate the ionization equilibrium.

A typical spectrum is shown in Fig. 21. It contains the resonance line of heliumlike iron (w) as well as the resonance line of lithiumlike iron (q) and various satellites of the heliumlike charge state. Gabriel's notation (A. H. Gabriel, *Monthly Notices of the Royal Astronomical Society, 160* (1972) 99) has been used for line identification. The width of the spectral lines is determined by Doppler broadening and can be used for ion temperature measurements. The intensities of the resonance lines w and q are proportional to the abundances of Fe XXV and Fe XXIV, and are therefore a direct measure of the charge state distribution. The resonance line w is especially important for diagnosing the process of charge exchange recombination of Fe XXV during the injection of neutral hydrogen beams. In ohmically heated discharges the intensity ratio I_q/I_w determines the deviation of the relative abundance $n_{Fe\,XXIV}/n_{Fe\,XXV}$ from coronal equilibrium. This deviation is due to transport of Fe XXV out of the central core and can be used to measure the particle diffusion coefficient. The satellite line j originates from dielectronic recombination of heliumlike iron with electrons of 4.649 keV. The line w is collisionally excited by electrons with energies above 6.7 keV. The intensity ratio I_j/I_w can be used to obtain the electron temperature.

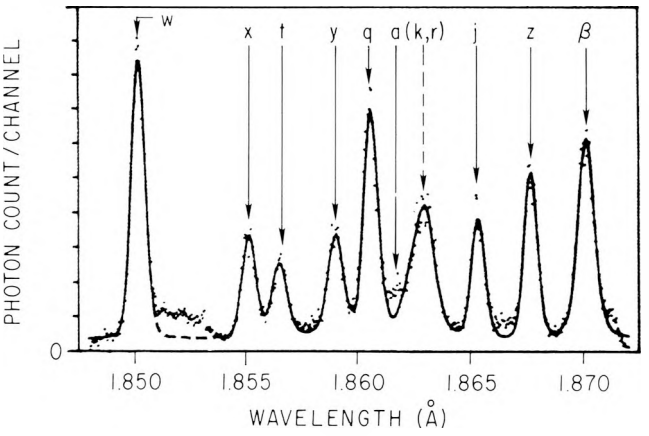

Figure 21. Dielectronic satellite spectrum of Fe XXV as recorded from PLT for a central electron temperature of 1.65 keV. Gabriel's notation is used for line identification. The resonance line of Fe XXV at 1.85 A is indicated by w.

Typical results are shown in Figs. 22 and 23. Fig. 22 presents the ion temperature results derived from Doppler broadening measurements (--I--) of the resonance line w, and for comparison those obtained from the neutral charge exchange diagnostics (Δ) for a PLT discharge with auxiliary neutral beam heating. Figs. 23a and b show the intensities of lines j and q relative to that of the resonance line w as a function of the central electron temperature measured by Thomson scattering. The data have been obtained from ohmically heated PLT discharges. The relative intensity of the dielectronic satellite j is found in good agreement with the theoretical predictions demonstrating that this line ratio can be used as an independent electron temperature diagnostic. On the other hand, the intensity ratio of the lithiumlike and heliumlike resonance lines, shown in Fig. 23b, deivates appreciably from the theoretical predictions for coronal equilibrium. These deviations are ascribed

to transport of Fe XXV. More recent measurements have shown that these deviations depend strongly on the plasma density in agreement with theoretical expectations.

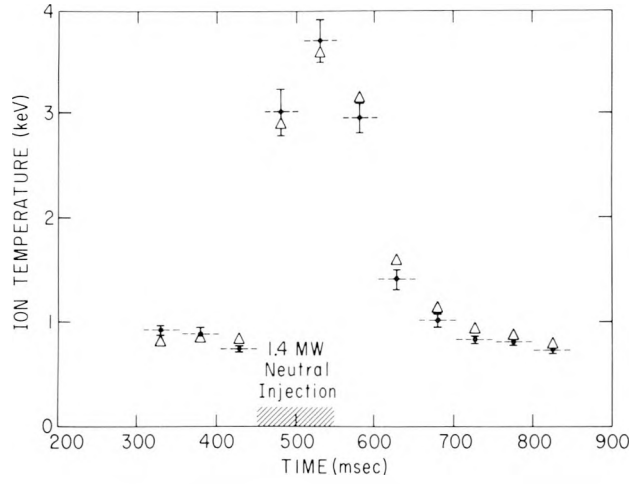

Figure 22. Comparison of ion temperature results from Doppler broadening measurements (---I---) with those obtained from charge exchange diagnostics (Δ). The data were obtained from a simultaneous observation of a deuterium plasma with auxiliary heating by injection of a 1.4 MW hydrogen beam. The dashed lines represent the time resolution of 50 ms for the spectral data.

Phenomena at the Plasma Edge

Experiments were performed to measure the energy distribution of hydrogen atoms and ions which leave the plasma edge and strike the walls and limiters of PLT. The aims of these measurements were to ascertain what impurity generation mechanisms were important and whether ion outflux or charge exchange neutral outflux was the more important energy and particle loss mechanism. To perform these experiments new diagnostics were developed.

To measure the energy of ions as they impact on surfaces in the plasma edge we extended the work of Erents et al. (S. K. Erents et al., *Journal of Physics D, 11* (1978), 227) and Staudenmaier et al. (G. Staudenmaier et al., *Nuclear Fusion 20* (1980) 96) on surface probes to include effects of broad energy distributions and non-zero Larmor radii. These experiments rely on interpreting the depth distributions, lateral spreading behind an aperture, and trapping behavior of deuterons implanted in carbon and

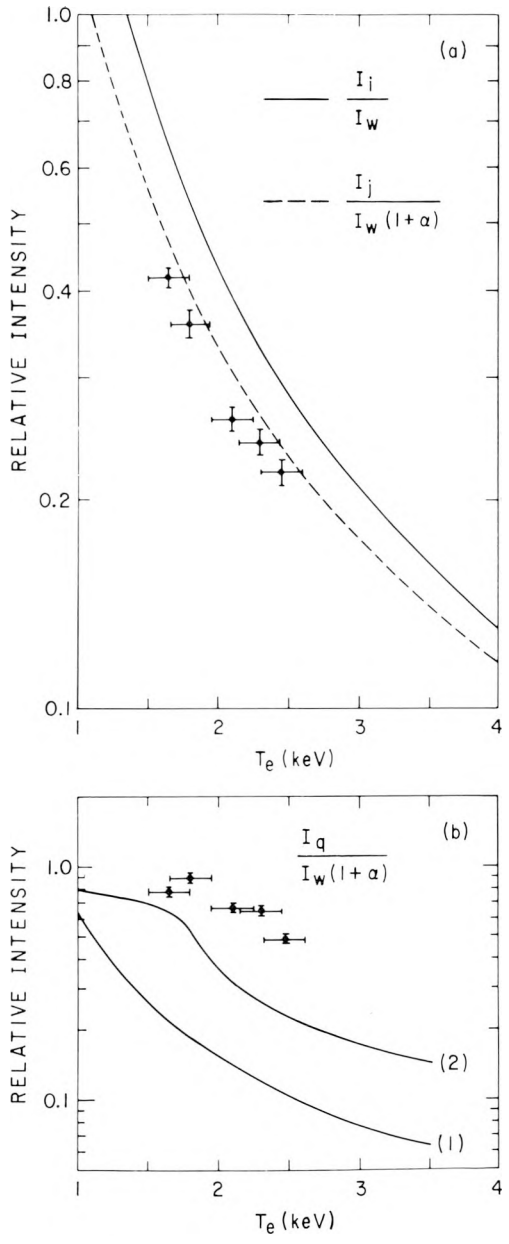

Figure 23. Line intensities relative to the intensity of resonance line of Fe XXV, as a function of the electron temperature T_e.

(a) Experimental results for the dielectronic satellite j and theoretical predictions.

(b) Relative intensity of the resonance line of Fe XXIV and predictions for coronal equilibrium by Jordon and Summers. The theoretical results differ due to the assumptions made with regard to the ionization and recombination rates.

silicon targets. Laboratory calibrations of the ranges of energetic D^+ implanted in Si were made. Calculations of trapping behavior and lateral spreading were performed for monoenergetic and Maxwellian energy distributions, impacting normally and with cos θ distribution. Measurements in low density, ohmically heated PLT discharges point to a high flux of 100-500 eV ions impacting on the "ion drift" side of the probe. The "electron drift" side of the probe experienced about half the flux at half the mean energy per particle. These energies are higher than those determined by Doppler broadening, but equal to those determined by charge exchange. Of the several explanations proposed for the discrepancy, none has been proven.

The radial dependence of the flux and energy to the ion side of the probe, determined from trapping behavior, is shown in Fig. 24. The depth profile and lateral broadening data are in agreement with the trapping data. Extrapolating to the limiter position and assuming poloidal symmetry we calculate that ion bombardment of the limiter causes power and particle losses of 50 kW and 8×10^{20} D^+ ions/sec. We also calculate that impurity generation by ion sputtering releases 1.6×10^{19} Fe atoms/sec and 1.2×10^{19} carbon atoms/sec from the stainless steel and carbon limiters. Thus ion impact on the limiters is important for power and particle losses as well as impurity generation in low density, ohmically heated plasmas.

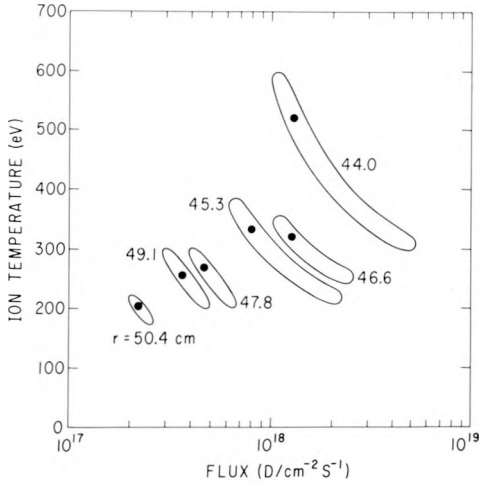

Figure 24. Radial dependence of the temperature and flux of ions hitting the ion side of the probe. The outside limiter was at 45 cm and the bottom limiter was at 40 cm.

A low energy neutral detector system (LENS), based on the time-of-flight principle, was designed to detect neutral particles, in the energy range 20 to 1000 eV, which leave the plasma. Overlap with the energy range accessible to stripping cell diagnostics allowed cross calibrations to be made. Absolute agreement within a factor of 3 for E = 500 eV was found between the LENS and the stripping cell detector adjacent to it.

For low density ($\bar{n}_e \sim$ 1-4 X 10^{13} cm^{-3}), ohmically heated deuterium plasmas, the energy distribution of the charge exchange outflux (Fig. 25) shows initial peaking at energies below

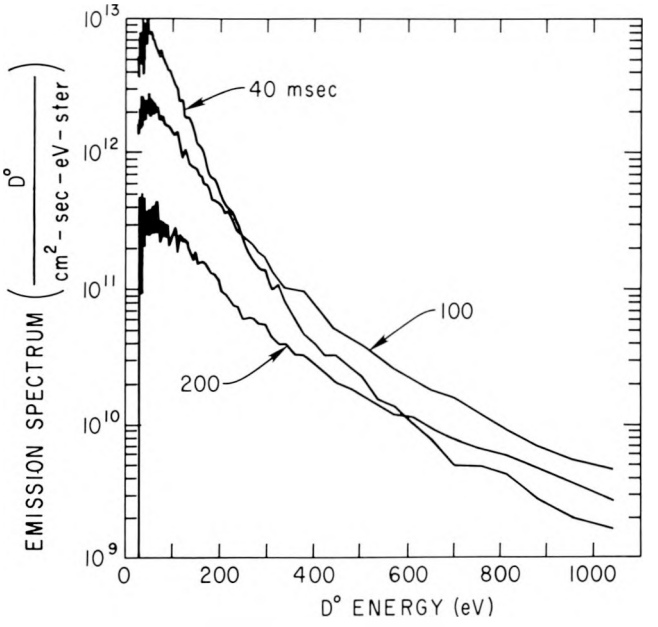

Figure 25. The differential flux emission function $d\Gamma/dEd\Omega$ plotted at t = 40, 100, and 200 ms.

100 eV. As the discharge evolves, the average neutral energy increases to a value of E ~ 200 eV and remains there during the flat top, steady state portion of the discharge. For the steady state portion of these discharges the central ion temperature was in the range 500-1000 eV. This indicates that most of the charge exchange outflux originates in the colder outer region of the plasma. The total outflux of particles in the energy ranges $28 < E < 1000$ eV and $200 < E < 1000$ eV is shown in Fig. 26. One again sees that the particles with $E < 200$ eV represent more of the particle outflux than those with $E > 200$

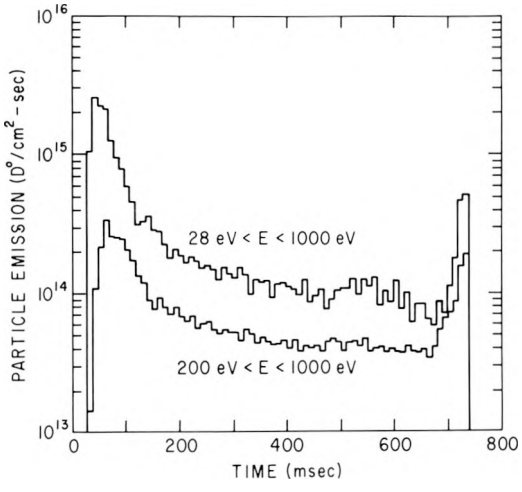

Figure 26. Time evolution of the flux plotted with 10 ms resolution for two energy windows. $T_{i\ axis}$ = 800 eV, $\bar{n}_e$ = 1.2 X 10^{13} cm^{-3}, and I_p = 450 kA for shot #24581 shown.

eV. A striking difference in intensity is evident between discharge initiation and steady state. At initiation, the neutral outflux, assuming cos θ emissivity of the plasma, is typically 3 X 10^{15} D^o cm^{-2} sec^{-1}. This falls by a factor of 30 in 400 ms. From these fluxes and published energy dependent sputtering yields (J. Bohdansky et al., *Symposium on Fusion Technology* Pergamon Press, New York, 1979, 80) we calculate that sputtering of the wall (away from the limiter) by charge exchange neutrals introduces 2 X 10^{13} Fe cm^{-2} sec^{-1} at discharge initiation, but only 2 X 10^{12} Fe cm^{-2} sec^{-1} during steady state. During steady state, the total power and particle outflux by neutrals is ~1 kW and 2 X 10^{19} D^o sec^{-1}. Thus during the steady state portion of low density ohmically heated discharges, charge exchange away from the limiter is a negligible cause of particle and power loss or impurity generation.

In addition to these studies of D^+ and D^o outflow, a major effort was made to install and diagnose glow discharge cleaning in PLT.

Electron Cyclotron Wave Studies

The recent development of powerful millimeter sources (i.e., gyrotrons) has stimulated interest in wave absorption near the electron cyclotron frequency, f_{ce}, since an understanding of the absorption process can describe the proper conditions for efficient application of electron-cyclotron resonance heating (ECRH) in tokamaks. For ECR heating of tokamaks, the attractive feature of the ordinary mode near the fundamental electron cyclotron frequency is that the wave can be launched from the low-magnetic field side of the torus. During FY79 direct measurements were made of the ordinary-mode wave absorption near the fundamental electron cyclotron frequency over the midplane of a hot tokamak plasma.

Since in tokamaks $B \propto R^{-1}$, the absorbing cyclotron layer can be placed at the desired R or r by choosing the appropriate central magnetic field level $B(R_o)$ for the fixed transmitter frequency, f = 71 GHz. Laser Thomson-scattering measurements give both the density, $n_e(r)$, and temperature, $T_e(r)$, profiles. Thus by changing $B(R_o)$ we can measure the optical depth τ (or absorptivity) as a function of r, or equivalently, as a function of pairs of values of n_e and T_e. In Table I we summarize ordinary-mode absorption results for two different experimental runs. The theoretical values of the optical depth, τ_{th}, have been obtained by use of measured values of n_e and T_e. The numbers in Table I are the mean values followed by the standard deviation in the measured values of density, temperature, and τ_{exp} for four successive reproducible plasma discharges. It is apparent from Table I that there is good agreement between theory and experiment for values of τ in the range $0.1 \lesssim \tau \lesssim 2$.

For low values of n_e ($f_{pe} < f_{ce} = f$), one finds $\tau \propto n_e T_e$. Thus the f_{ce} ordinary-mode propagation studies could be used to determine the local electron pressure, and therefore either n_e or T_e if one of the quantities is measured separately.

TABLE I. A COMPARISON OF THE MEASURED EXPERIMENTAL VALUES OF THE OPTICAL DEPTH, τ_{exp}, WITH THE CORRESPONDING THEORETICALLY CALCULATED VALUES, τ_{th}, FOR THE PROPAGATION OF ORDINARY MODE 71 GHz MICROWAVES. THE DATA WERE COLLECTED OVER TWO SEPARATE EXPERIMENTAL RUNS LISTED SEPARATELY IN THIS TABLE.

$B(R_o)$ (kG)	$T_e(r)$ (eV)	$n_e(r)$ (10^{13} cm^{-3})	τ_{th}	τ_{exp}
19.1	160 ± 88	0.384 ± 0.08	0.05 ± 0.03	0
20.2	293 ± 171	0.716 ± 0.246	0.21 ± 0.16	0.09 ± 0.03
21.5	240 ± 14	0.7 ± 0.14	0.14 ± 0.04	0.11 ± 0
23.8	647 ± 35	1.09 ± 0.11	0.57 ± 0.06	0.38 ± 0.05
24.9	900 ± 115	1.32 ± 0.087	0.98 ± 0.16	0.876 ± 0.06
21.5	270 ± 57	1.30 ± 0	0.29 ± 0.06	0.3 ± 0.028
22.6	416 ± 186	0.96 ± 0.23	0.35 ± 0.18	0.33 ± 0.07
24.2	760 ± 57	2.59 ± 0.41	1.43 ± 0.13	1.49 ± 0.15
25.0	850 ± 70	2.7 ± 0.42	1.65 ± 0.30	1.89 ± 0.0

Poloidal Divertor Experiment (PDX)

PDX is a large tokamak device equipped for poloidal divertor and field-shaping experiments. The goals are:

- Development and determination of the effectiveness of poloidal divertors, magnetic limiters, and other techniques for controlling impurities in large, high-temperature, collisionless tokamak plasmas; in particular, development of a shielding divertor for use with long-pulse reactors.
- Determination of the confinement scaling as a function of collisionality for the range of parameters from present-day plasmas to those of reactor-like plasmas; use of divertors to control the effective Z and of neutral beam heating to control the plasma temperature.
- Optimization of the plasma cross section under conditions of relatively "flat" current distributions which are produced in conjunction with effective divertor control of the density of neutral species and impurities.
- Determination of the maximum beta for a stable plasma confined in a tokamak under nearly optimum conditions of impurity control and cross-section shaping.
- Development of plasma refueling techniques that are compatible with impurity control in reactor-like plasmas.

MAJOR ACTIVITIES

Summary

Fabrication of the Poloidal Divertor Experiment was brought to a conclusion this year, and the first pink-glow discharges were made on November 29, 1978. This was followed by two months of power tests and diagnostic installation. Full-scale circular cross-section plasma operations started early in February, 1979. Extensive glow discharge cleaning, feedback con-

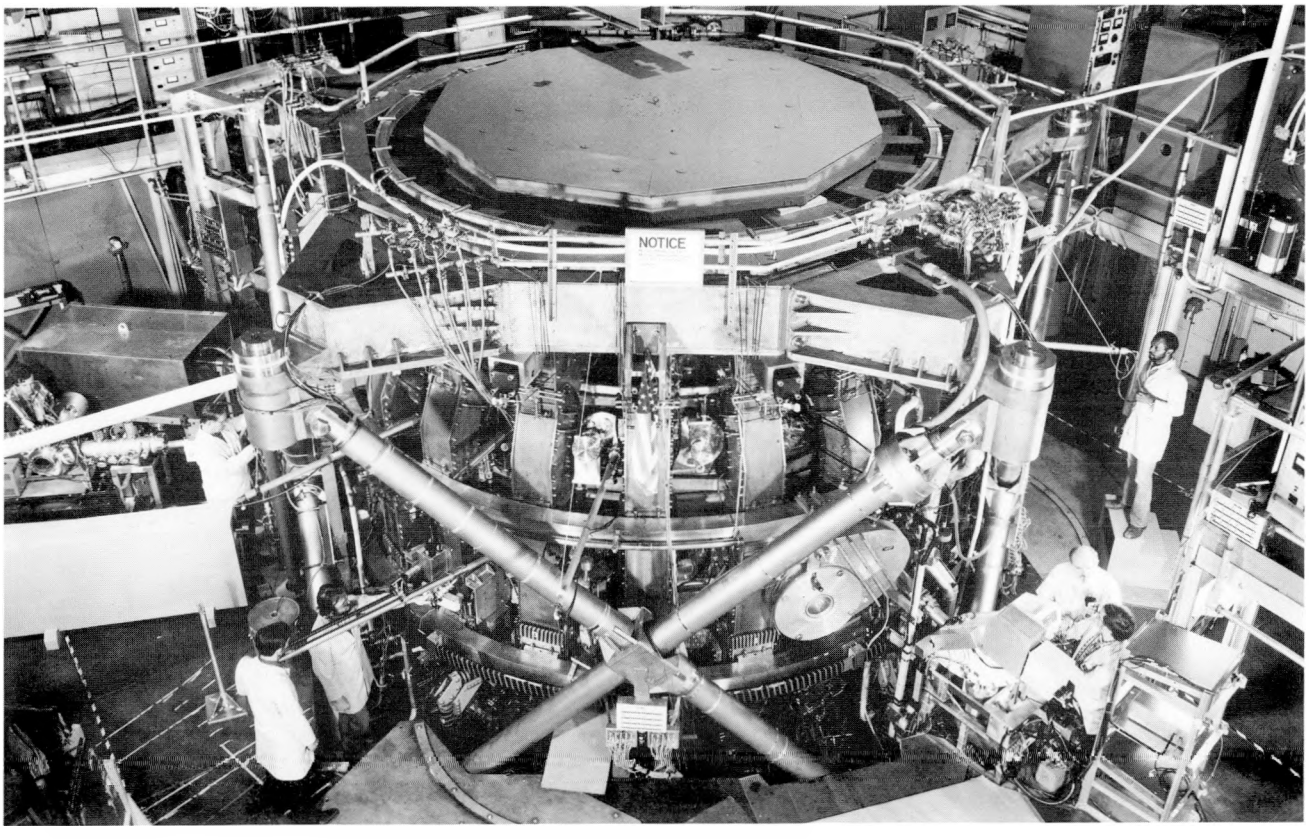

Figure 27. The PDX machine.

trol of plasma position and current, and the use of titanium limiters and gettering allowed PDX to produce low-q ($q \simeq 3$), low-Z ($Z \simeq 2$), and long-confinement-time ($\tau_E \simeq 35$ ms) plasmas after only two months of operation. (See Fig. 28.)

Early in April, 1979, PDX physics experiments were suspended. The next six months were spent in preparations for divertor operation. Throughout this time neutral-beam fabrication proceeded at the Oak Ridge National Laboratory with a target of installation in FY80.

Fabrication

Power testing, which began late in September, 1978, proceeded throughout the first quarter. The program included testing individual PF coils, followed by combined PF tests, individual TF and system tests, and combined TF and PF systems tests. Early in December, the TF system was tested to full power.

The installation of all major mechanical components was completed by November 21, 1978. This included raising of the center shaft into position and assembly together with the end caps and the upper and lower thrust hubs. Final details of the vacuum system, bus, water, and hydraulic systems were completed as the opportunity offered, before or after the initial experimental operations.

Final fabrication cost was $25,445,200.

Discharge Cleaning

Conventional low power Taylor-type discharge cleaning was initially applied for only 16 hours due to difficulties with discharge initiation at low fields in the presence of stray fields produced by induced currents in the divertor-coil vacuum jackets. This problem was solved by reconnecting poloidal coils to passively cancel the error fields and allow discharges to be started at steady-state 3 kG toroidal fields. Intensive conditioning was undertaken with a dc glow discharge in which H_2 at a pressure of 3×10^{-2} torr flowed through the vacuum chamber at 10 torr-ℓ/sec. One or two anodes located on the midplane provided a discharge current of 2-4 amps at 400-500 volts.

Impurity production was monitored with a differentially pumped residual gas analyzer and by in situ surface analysis. Impurities produced were mainly CH_4, C_2H_4, and CO. The initial gas phase removal rate of 1.5×10^{18} molecules/sec decreased inversely with time for 120 hours with a total removal of 15 gm or 120 monolayers of carbon. (See Fig. 29) Surface removal rate of

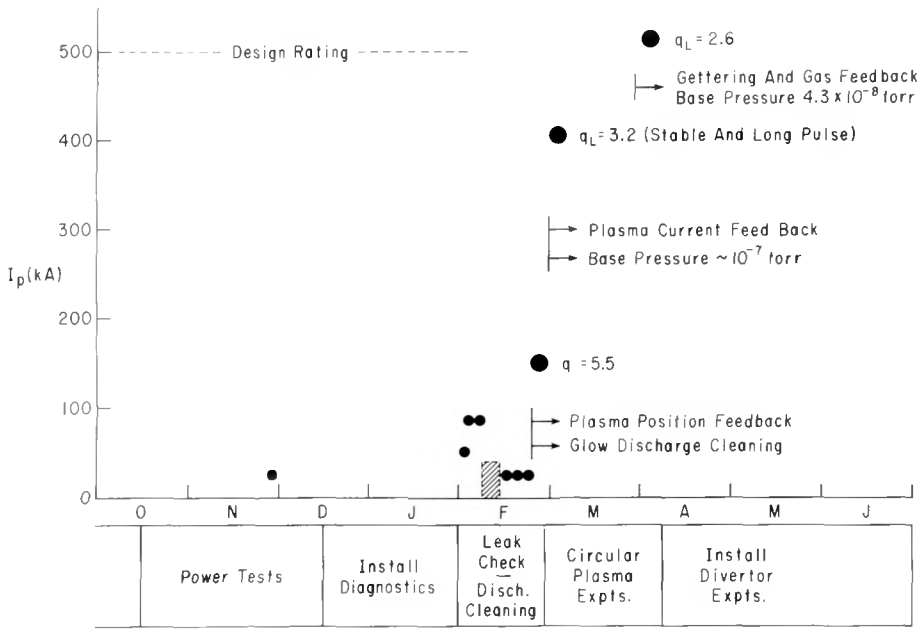

Figure 28. Progress toward operation at design rating of 500 kA.

carbon and oxygen at the surface analysis station was 6 X 10^{10} atoms cm^{-2} sec^{-1}.

Initial glow discharge cleaning was accompanied by frequent arcing, but this gradually decreased along with the impurity level and the discharge occupied an increasing portion of the vacuum vessel. The improving cleanliness of the tokamak discharges was indicated by the diminishing intensity of the soft x rays. The low level of oxygen and carbon ($Z_{eff} \simeq 2.0$) after a short period of operation, despite the large surface area exposed to the plasma, is attributed largely to the efficiency of glow discharge cleaning.

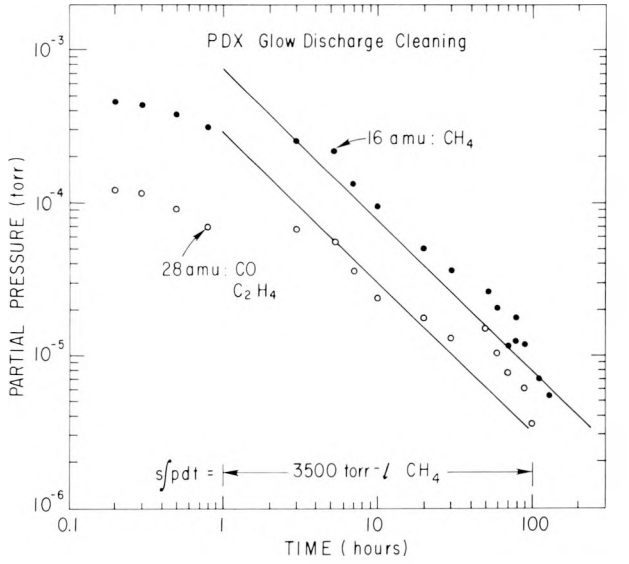

Figure 29. Vacuum vessel cleanup by glow discharge.

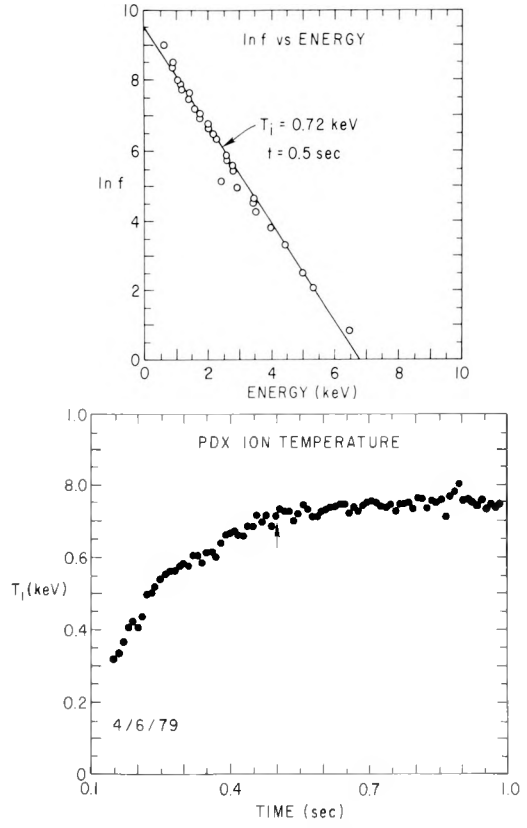

Figure 30. Ion temperature determination from charge exchange neutrals.

Gettering, Feedback Control, and Diagnostics

Internal vacuum vessel components that were exposed to the plasma (such as limiters, protective plates, and microwave horns) were fabricated from 99.9% pure titanium. Modest titanium gettering was done using one 3 gm/hr evaporator in the divertor burial chamber.

The vertical field power supply was feedback-controlled by use of an internal saddle coil detector and held the radial plasma position to ± 2-3 mm during the plasma current flattop. The vertical position of the plasma was also held to ± 2-3 mm. In addition, the ohmic heating power supply was feedback-controlled during the plasma flattop, which allowed the plasma current to be held constant to ± 3% during a pulse and from pulse to pulse.

Diagnostics included magnetic measurements of I_p, R_o, $\beta\theta + \ell_i/2$, δ B_p, a three channel 2 mm and 1 channel 119 μ interferometer for $\bar{n}_e$, a four-radial-channel soft x-ray system for $T_e(r)$ and impurity measurements, microwave radiation measurements of $T_e(r)$, hard x-ray measurements of energetic electrons, visible and vacuum ultraviolet measurement of impurities, charge exchange and neutron production measurements of ion temperature, bolometric measurements of radiation profiles, and surface analysis measurements of the "plasma-wall" interaction.

Circular Plasma Results

Typical plasma parameters for a circular deuterium plasma discharge with titanium gettering were: $V\ell$ = 1.2 V, I_p = 360 kA, $\bar{n}_e$ = 2 X 10^{13}

cm^{-3}. $T_e(0)$ = 1.2 keV, $T_i(0)$ = 0.58 keV, $\overline{Z}_m \simeq$ 2.2, $\tau_E \simeq$ 30 ms, and q_L = 3.2.

In the absence of a completed Thomson Scattering System, density and temperature profiles were based on microwave interferometer measurements and soft x ray pulse height analysis. Charge exchange analysis gave the central ion temperature (see Fig. 30), and the profile was estimated from a transport calculation. Energy confinement times tended to improve with density (see Fig. 31) and fall in the same range as those measured on PLT under similar conditions. The soft x-ray spectrum indicates the presence of Cl, Ti, and Cr impurities. (See Fig. 32.) $\overline{Z}_x$ was determined from the enhancement of the soft x-ray continuum and was in the range of 2 to 3.2 for this discharge. No evidence for spatial peaking or accumulation in time was found outside the relatively large error bars of $\Delta\overline{Z}_x \simeq \pm 0.5$. Vacuum ultraviolet measurements yielded estimates of oxygen and carbon impurity concentrations early in time and both UV and x rays give Ti densities in the middle of the pulse. The contributions to $\overline{Z}$ as indicated by UV spectroscopy were $\Delta\overline{Z}_s(C) \simeq 0.25$, $\Delta Z_s(O) \simeq 1$, and $\Delta\overline{Z}_s(Ti) \simeq 1$.

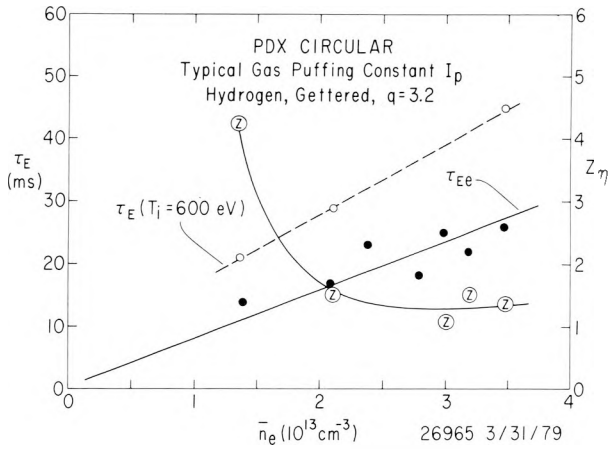

Figure 31. Preliminary energy confinement data for circular discharges.

Runaway electrons, observed by hard x-ray and neutron detectors, on occasion reached energies greater than 8 MeV and caused photoneutron production at the titanium limiters ~ 10^9 n/sec. Residual activation from Ti to nuclear reactions was observed predominantly on the outside limiter. The PDX runaway levels and photoneutron flux were considerably lower than those seen during the PLT shakedown.

Power radiated by the plasma was measured with a scanning bolometer at a position 100° azimuthally away from the limiter; for a typical case it was 240 kW out of a total of 430 kW. Spectroscopic estimates of the power radiated

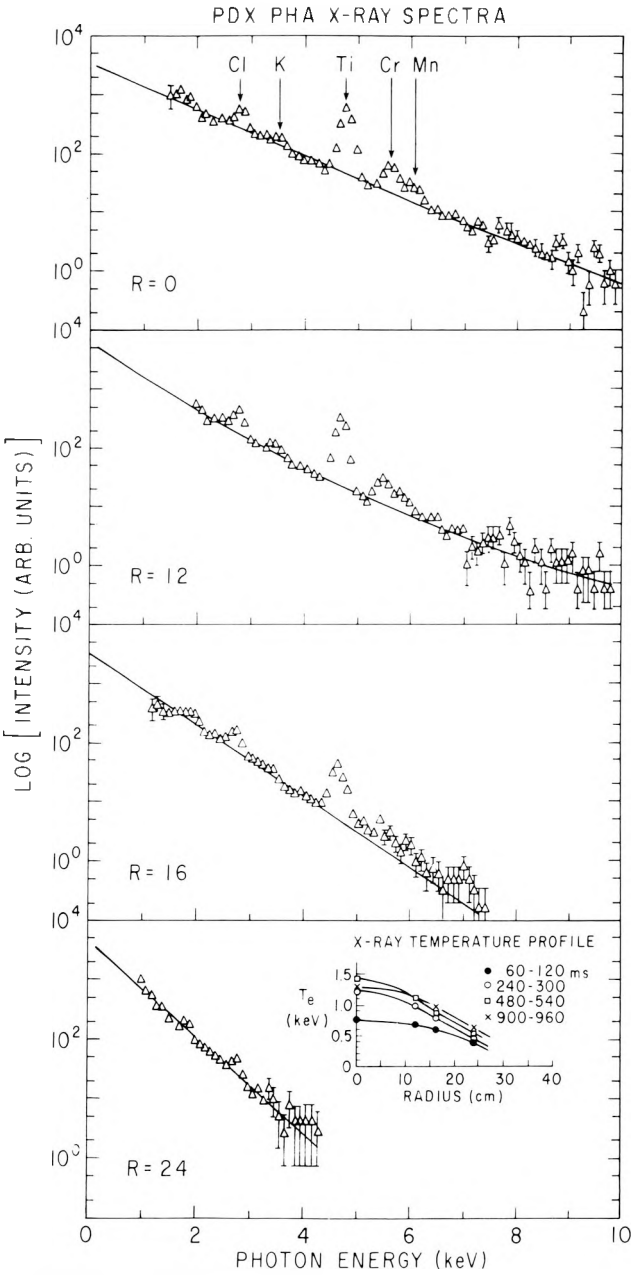

Figure 32. Soft x-ray spectra.

by the measured impurities gave P_R (C) $\simeq$ 5-20 kW, P_R (O) $\simeq$ 70 kW, and P_R (Ti) $\simeq$ 150-190 kW, giving a total power radiated of 225-290 kW (neglecting Cl radiation), in good agreement with the bolometric measurement. Surface physics measurements of impurities deposited on probes gave roughly the same ratio of O, Ti and Cl as the vacuum UV and soft x-ray measurements. The radial distribution of power radiated from the discharge was essentially flat, but with an ~50% peak at r = a/2 ($T_e \simeq 600$ eV) and a second peak near the plasma surface.

PDX was routinely run at $q_\ell = 3.1$; it may also be run at $q_\ell = 2.4$ (I_p = 520 kA) by use of a current waveform that increases in time from an initial value corresponding to $q_\ell = 3.5$ to a final value of $q_\ell = 2.4$. (See Fig. 33.)

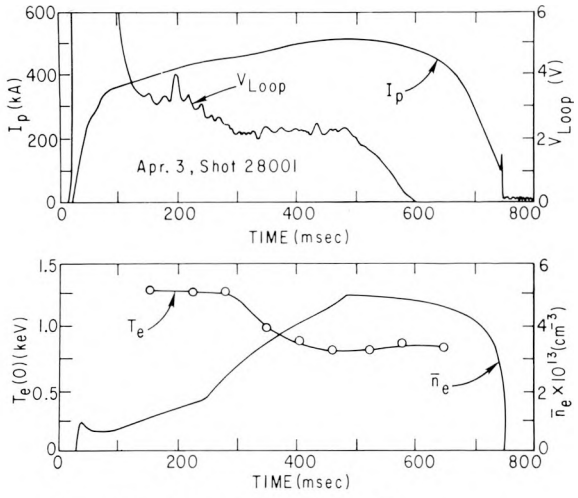

Figure 33. 500 kA discharge (q = 2.4).

PDX Neutral-Beam Fabrication

Neutral-beam heating of PDX plasmas will be necessary for operation in reactor-like regimes where the effectiveness of poloidal divertors can be tested and meaningful cross-section shaping experiments can establish MHD beta limits. The PDX 6-megawatt, 50 keV system is being fabricated as a joint project of Oak Ridge National Laboratory and Princeton. Four main beam-lines will be installed for injection nearly perpendicular to the magnetic axis of the PDX plasma. The sources are modeled after the PLT 60-ampere injectors, but will be upgraded to 100 amperes. At low electron densities of 2×10^{13} cm^{-3}, the ion temperature is projected to reach 10 keV, while at high densities, near 10^{14} cm^{-3}, the beta is maximized at ~ 5% with ion temperatures of 3 keV.

As of September 30, 1979, installation of the first beamline is scheduled to begin at the end of the calendar year.

PDX Modification

PDX Modification is a general upgrade of the PDX facility proposed for implementation in successive steps during the period 1980-82.

The high beta capability of PDX is extended into the 6-8 percent range by acquisition of a 15 kA EF power supply. The total auxiliary heating capability is extended to 10 MW by the transfer of the 45 MHz ICRF system from PLT to to PDX. The neutron shield provides personnel shielding during deuterium injection experiments in which 10^{15} neutrons/pulse are projected. The neutral beam long pulse upgrade extends the neutral beam line energy-handling capability and provides for the construction of neutral beam sources that will inject ~ 4 MW for 2-3 seconds.

The divertor long pulse hardware activity will upgrade the energy collection system to absorb ~ 5-fold increase in energy per pulse. A divertor system under investigation is the gaseous neutralizer.

The results obtained from these upgraded systems will provide design data for ETF and INTOR.

Smaller Devices

Supplementing the large-tokamak research programs at the Princeton Plasma Physics Laboratory is experimental work carried out on a family of flexible smaller devices — the linear machines L-3, QED-1, Q-1 and H-1, and the new small torus, ACT-1. These devices all produce steady-state magnetically confined plasmas and lend themselves to precision measurements of plasma-physics phenomena. In addition, their smaller size permits modification at minimum cost, giving PPPL several highly versatile test-beds for advanced ideas in toroidal magnetic fusion. Noteworthy this year has been the experimental confirmation on QED-1 of the gaseous divertor-collector concept. Showing that outflow of plasma can successfully plug the back-streaming of neutral atoms from a gas collector, this experiment opens the way for the replacement of the ultra-high heat dissipation metal collector plate in a reactor divertor by an undamageable cloud of low-pressure neutral gas.

Manufacture of the new small machine, Advanced Concepts Torus-1 (ACT-1) was completed this year and the device has already seen a few months of preliminary operation. A 100-kW, 200-MHz rf source (on loan from MIT) is being readied for use with ACT-1, to test the concept of steady-state current drive for tokamaks by radiofrequency means.

Other work from this group of smaller devices also pertained to radiofrequency applications of controlled fusion. Linear and nonlinear effects associated with rf plasma heating at the lower-hybrid frequency were studied both on the H-1 and the L-3 machines and whistler-wave propagation was diagnosed in precise detail on QED-1. The Q-1 machine achieved quantitative experimental confirmation of the toroidal-fusion-relevant, impurity-driven drift-wave instability.

MAJOR ACTIVITIES

The ACT-1/L-3 Program

ACT-1 CONSTRUCTION

ACT-1 (Advanced Concepts Torus-1) is a steady-state toroidal device built primarily for studies of radiofrequency heating and current generation. The machine produces a toroidal plasma with minor and major diameters of 20 cm and 118 cm respectively. It consists of 26 sets of toroidal field coils and 26 identical toroidal-section chambers with large ports offering broad access to the plasma. The chambers are made of aluminum with water cooling capable of handling 50 kW steady-state heat load. The vacuum system uses Viton seals, turbomolecular pumps, and titanium gettering. A 600-kW motor-generator set provides steady-state power to the water-cooled field coils which can produce 5.6 kG magnetic field on axis. ACT-1 was designed in FY78, and the construction was completed in August 1979. The first plasma was produced on August 9, 1979. The machine is shown in Fig. 34.

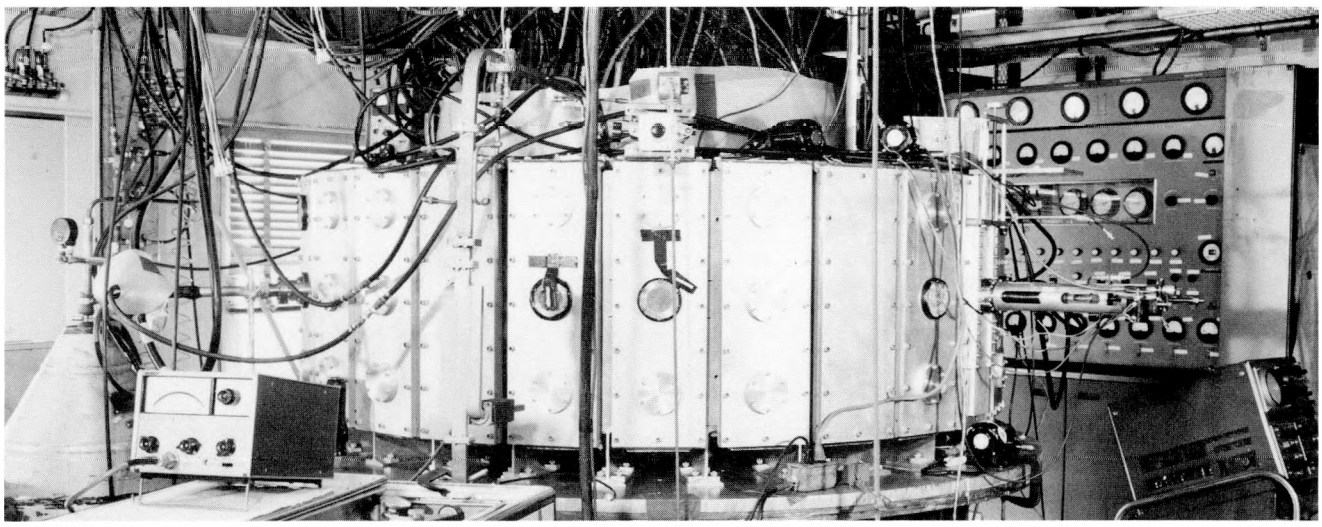

Figure 34. General view of the Advanced Concepts Torus (ACT-1). The 100-kW rf transmitter may be seen at right rear.

During late FY79 ACT-1 operated typically with a simple zero-transform toroidal magnetic field, with plasma equilibrium maintained by vertical plasma current flowing to the limiter to prevent electric field buildup due to gradient-B drift. Plasma could be produced by electron cyclotron resonance heating and also by a tungsten-filament source. This latter method creates a relatively uniform low-noise plasma with $n_e \lesssim 2 \times 10^{12}$ cm^{-3}, $T_e \lesssim 10$ eV and $T_i \lesssim 1$ eV.

RF CURRENT GENERATION IN ACT-1

The absence of Ohmic current makes ACT-1 an ideal test-bed for rf current generation studies. A 100-kW transmitter (150-200 MHz) on loan to PPL from the Alcator group at M.I.T. will be used to launch unidirectional lower-hybrid waves to impart momentum to the plasma electrons. A 100-kW dc power supply has been constructed for this transmitter and a 90°-phased power divider, together with a water-cooled electrostatic antenna, has been built for high-power steady-state operation. In addition to the ring antenna, a dielectric-filled waveguide has been designed. This experiment will come into operation in FY80.

PONDEROMOTIVE-FORCE EXPERIMENTS IN L-3

It has long been recognized that lower-hybrid wave energy propagates along localized resonance-cone trajectories. However, at high power levels the strong localized electric fields of the wave can modify the plasma density through the ponderomotive force, which leads in turn to an alteration of the resonance-cone trajectory. This behavior was investigated experimentally in the linear L-3 device and the results are in good agreement with theory as shown in Fig. 35. When the high-power, lower-hybrid driver, is modulated, the resulting density oscillation couples to electrostatic ion cyclotron waves ($\omega^2 = \omega_{ci}^2 + k_\perp^2 c_s^2$). The frequency of the latter is determined by the modulating frequency. The wavelengths of the propagating electrostatic ion-cyclotron waves were measured at various frequencies and the wave dispersion was verified for plasmas with several ion-species (He^+, Ne^+, Ar^+, Kr^+). Moreover, with a non-sinusoidal shape for the modulation envelope and, in the detection apparatus, a notch filter set at the second harmonic of the modulation frequency, it was possible to make interferograms for this component as well.

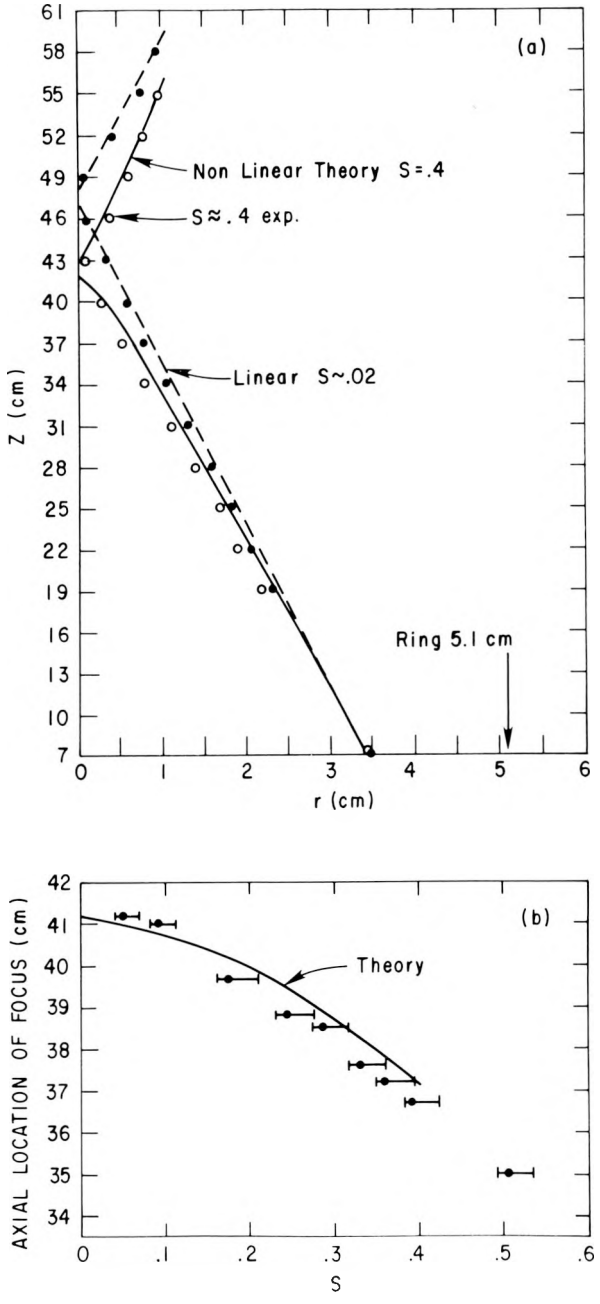

Figure 35. Resonance cone modification by ponderomotive effects. (a) Location of the peak electric field in the r-z plane for linear ($S \equiv E^2/8\pi nT \sim 0.02$) and nonlinear ($S \equiv E^2/8\pi nT \sim 0.4$) power levels. (b) Axial location of the peak electric field vs. S.

PLASMA HEATING WITH A WIDE $K_{||}$-SPECTRUM WAVEGUIDE SYSTEM OPERATING IN THE ION CYCLOTRON RANGE OF FREQUENCIES.

Ion Bernstein waves launched from an external waveguide rf coupler operating in its TE_{10} mode may offer an attractive means for heating a reactor plasma. The proposed system would operate in the ion cyclotron range of frequencies, i.e., 50-200 MHz, and the waveguide aperture of 15-50 cm width and 100-300 cm height, would be quite compatible with reactor sizes. (Fig. 36) Large waveguide openings help to minimize voltage breakdown problems and it is anticipated that the rf power (~ 100 megawatts) could be provided with present-day-technology and at relatively low cost.

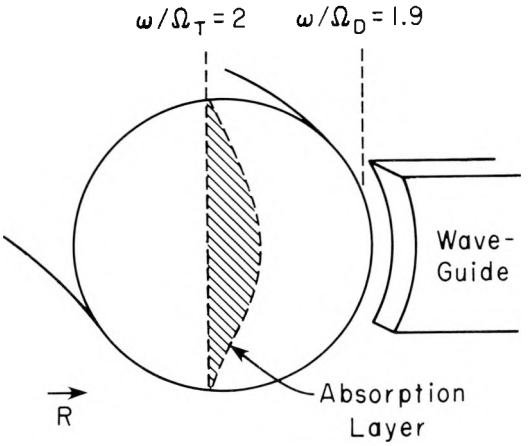

Figure 36. Launching scheme for a toroidal plasma, showing absorption layer at $\omega = 2\Omega_T$.

In a reactor plasma, the ion Bernstein wave may be expected to transform into a high-density ion Bernstein wave, Fig. 37. This high-density mode is no longer rigorously an electrostatic wave but instead satisfies $E_{||}/E_{\perp} << K_{||}/K_{\perp} << 1$. Electron Landau damping is thus greatly reduced — by as much as several orders of magnitude — compared to the original ion Bernstein wave. Because of this reduced damping, an externally launched ion Bernstein wave with $n_{||} \leq 6$ is expected to penetrate to and deposit most of its wave power in the core of even a reactor plasma. A relatively large window in $n_{||}$ implies only mild technical constraints on the design of the waveguide array.

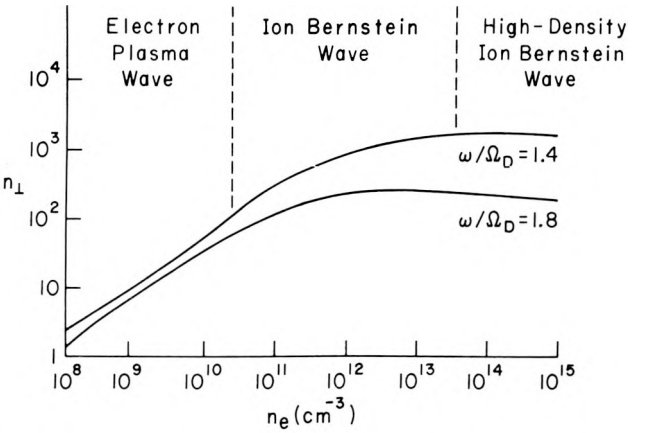

Figure 37. $n_{\perp} \equiv k_{\perp}\, c/\omega$ as a function of n_e for $\omega = 1.8\ \Omega_D$ and $\omega = 1.4\ \Omega_D$, $n_{||} = 3$.

The H-1 Program

A NEW LOWER-HYBRID WAVE LAUNCHER

A major advantage associated with plasma heating by lower-hybrid radiofrequency means is the ability to launch the heating wave from a waveguide array. Linear wave studies on the H-1 device have led this year to the invention of a new type of waveguide grill, one in which the periodic boundary conditions necessary for generating a slow plasma wave are enforced not by electrically phasing rf power in adjacent waveguides but by providing passive reflecting elements on each side of the active elements, as shown in Fig. 38.

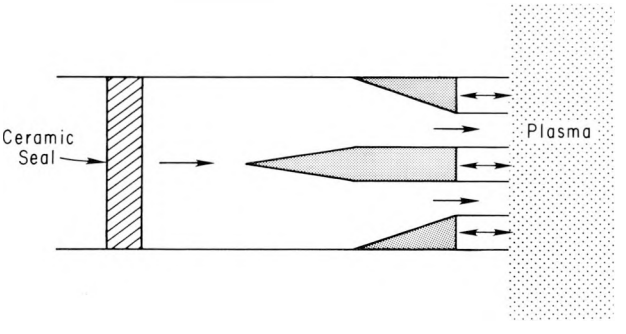

Figure 38. Top view of wave guide grill showing fixed grill structures. The single arrows indicate channels of active rf power flow; the double arrows, two-way flow in the passive elements. Spacing of the active and passive channels enhances the spectrum at the desired wavelength parallel to the magnetic field.

In this grill the wavelength parallel to the field is determined by the spacing between elements. Spacing of shorted passive elements is designed to enhance the spectrum at the desired wavelength.

This concept was first tested with a simple 2-element array which verified that such a system can be tuned for low reflectivity and enhanced radiation into the resonance cone. The more advanced systems under study on H-1 minimize the mechanical and electrical problems associated with phased waveguide arrays such as multiple transmission feed lines, custom-built ceramic windows, and crosstalk between guide elements. For lower-hybrid heating of large toroidal systems, these new grills will offer substantial reduction in cost and complexity.

PLASMA CONVECTION INDUCED BY RF HEATING

Studies on H-1 of nonlinear effects associated with lower-hybrid heating have led to an understanding of the increase in the reflectivity of waveguide arrays at moderate power levels ($\sim$ 80 W/cm^2). Probe measurements near the mouth of a twin waveguide show that within $\sim$ 20 μs after rf initiation the plasma near the mouth of the waveguide is vertically distorted. The plasma above the midplane drifts into the guide, while that below the midplane moves away (Fig. 39). This displacement was found to be part of a vortex motion of plasma with its center a few millimeters outside the mouth of the guide (Fig. 40). Probe measurements show that the vortex is driven by an electric field set up by asymmetric heating of the electrons.

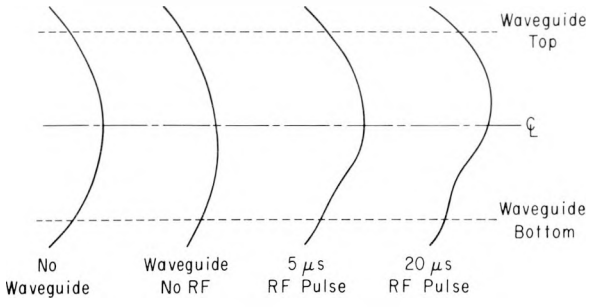

Figure 39. Cross section of the plasma surface (a) without waveguide, (b) with waveguide positioned to right, as in Fig. 40, but no rf, (c) 5 μsec after rf is turned on, (d) 20 μsec after rf is turned on.

The vortex rotation leads to a moderate increase in reflectivity from $\sim$ 5 to 12% at 1 kW. The basic reason for this change is that the plasma below the midplane pulls away from the guide by $\sim$ 5 mm, diminishing the effective waveguide cross-section for efficient coupling of slow waves.

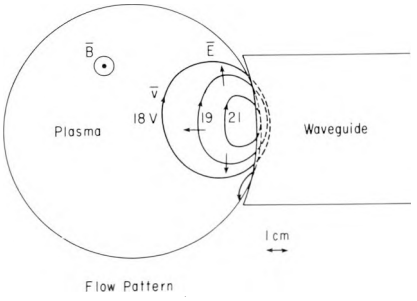

Figure 40. Flow pattern of convective eddies near the waveguide after a 10 μsec, 1 kW, rf pulse. The distortion represented in Fig. 39 is not shown. The straight arrows on the 19 V contour indicate the direction of the electric field.

The QED-1/Q-1 Program

EXPERIMENTAL SIMULATION OF A GAS DIVERTOR-COLLECTOR (QED-1)

Dissipation of the enormous heat carried by particles diffusing away from the main plasma of a fusion reactor has always posed a major technical problem. A possible solution was proposed some years ago by F. H. Tenney, namely, to use neutral gas (rather than a metal plate) as the collector into which the escaping plasma is diverted. The interaction between plasma and neutral gas has now been studied in the QED-1 device. Plasma flows, at about the ion acoustic speed, from the QED-1 plasma chamber, through a 2-cm diameter tube, into the gas-filled collector chamber, thereby simulating the operation of a tokamak divertor.

Simple theory predicts that the plasma pressure can withstand the back-pressure of neutrals in the collector chamber, resulting in a plugging phenomenon, and the QED-1 experiment verifies that a plasma with $n_e \simeq 10^{14}$ cm^{-3} and $T_e \simeq 5$ eV can indeed hold back neutral gas at pressures > 0.1 torr. As the neutral gas pressure, P_2, in the collector chamber is increased (by increasing the gas feed rate into this chamber), a critical value is reached at which the plugging effect of the plasma breaks down and the total gas pressure, P_1, in the plasma chamber rises sharply. The pressure ratio P_2/P_1 just before the critical point is two orders magnitude greater

than the value of this ratio which obtains when, as the feed rate is increased, plasma plugging has broken down (Fig. 41).

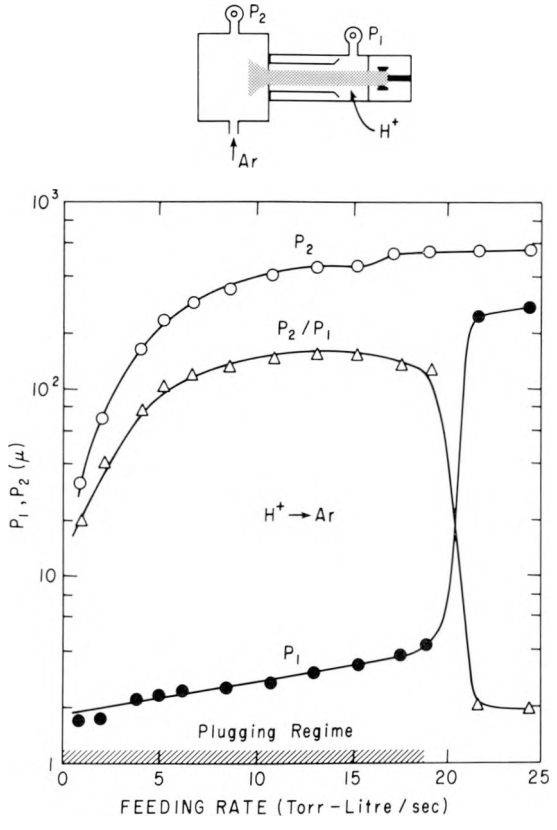

Figure 41. Neutral gas pressure P_1 in plasma chamber and P_2 in collector chamber versus argon feeding rate into collector chamber. As the argon feed rate is increased to 20 torr-ℓ/sec, the plugging breaks down due to high back-pressure of Ar (P_2) with respect to the plasma pressure.

The phenomenon of gas plugging appears to arise from the ionization of the divertor neutrals by plasma electrons, which greatly increases the viscous drag due to the plasma flow. To study viscous drag, a modest amount of krypton was bled into the plasma, midway along the tube. Small holes in the tube wall allowed spectroscopic observation of the plasma at positions evenly spaced upstream and downstream from the gas inlet. Fig. 42 shows the spatial distribution of a spectral line of the Kr^+ ion, at each of three values of T_e. Clearly seen in the higher-T_e plots is the downstream shift due to drag of the Kr^+ ions by the flowing plasma.

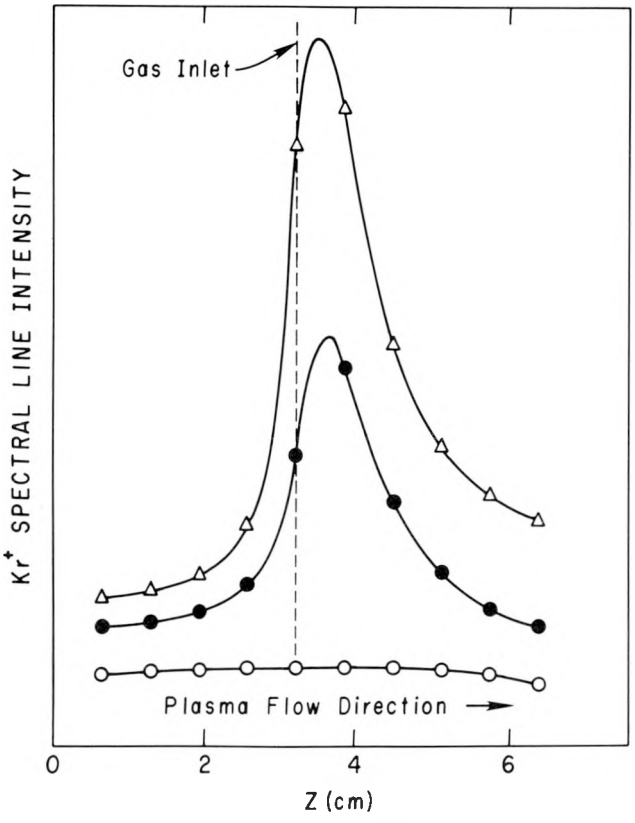

Figure 42. Intensity of Kr II (4846.6 Å) line as a function of axial distance. The three curves (o, ●, ▲) correspond to different plasma temperatures in the range 0.5 to 2 eV, with $T_{eo} < T_{e\bullet} < T_{e\blacktriangle}$. Plasma flow is from left to right.

WHISTLER WAVES IN A COLLISIONAL PLASMA COLUMN (QED-1)

The study of whistler waves in the QED device ($n \sim 5 \times 10^{12}$ cm^{-3}, B ~ 200 G and T_e between 0.4 and 1.5 eV) has continued. There is excellent agreement between experiment and fluid theory for both dispersion and spatial damping at the lowest electron temperatures, as can be seen in Figs. 43 (a) and (b). As T_e is increased from 0.4 to 1.5 eV, however, there appears a growing discrepancy between the observed damping and that computed for classical values of the electron-ion collision frequency. The discrepancy, visible in Fig. 43 (c), probably arises from the increase in plasma turbulence which occurs as T_e is increased.

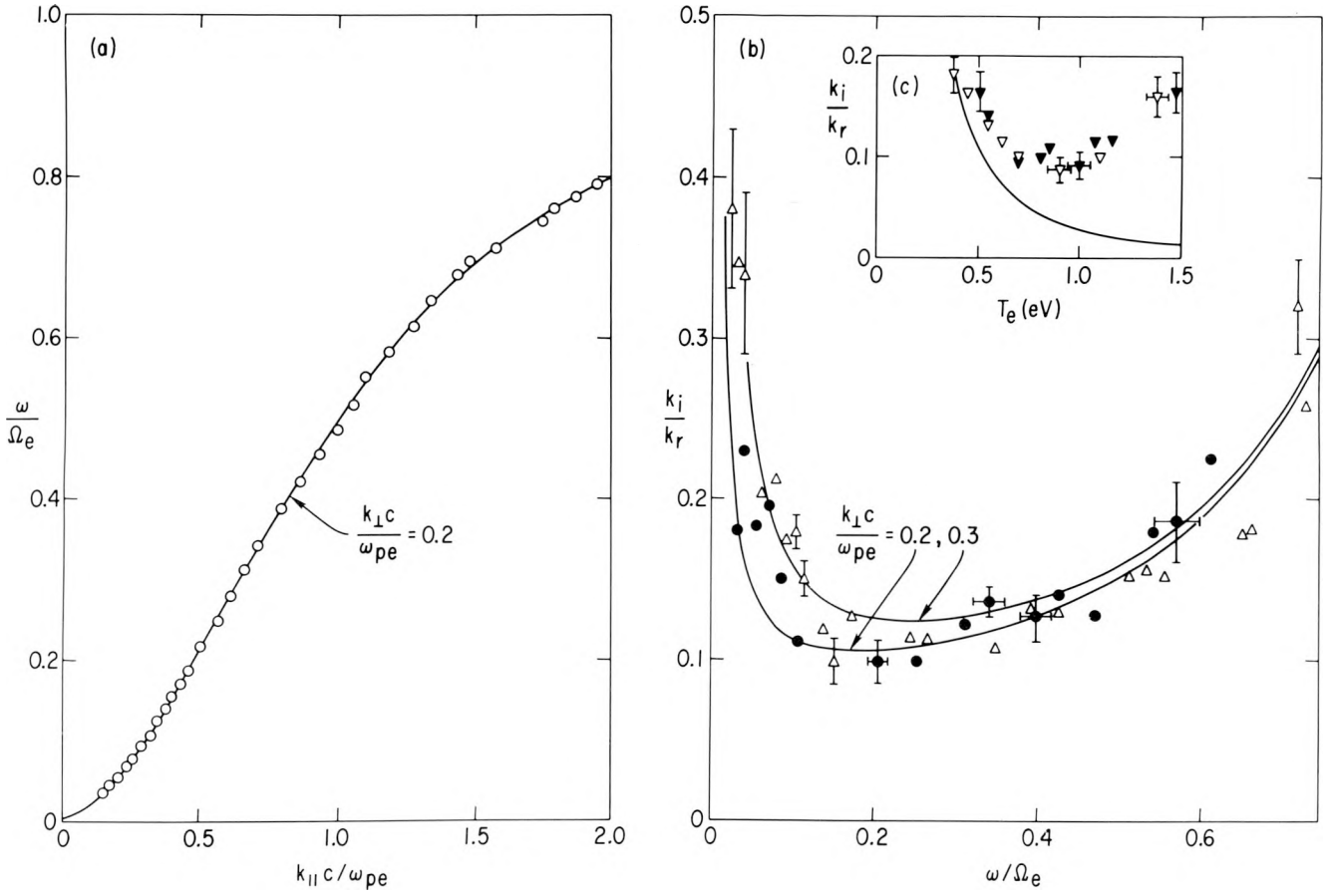

Figure 43 (a). Dispersion data. B = 220 G, n = 4 X 10^{12} cm^{-3}, plasma radius R = 3.0 cm, ω_{pe}/Ω_e = 30. Theoretical curve is drawn for $k_\perp c/\Omega_{pe}$ = 0.2.

(b) Spatial damping rate versus frequency for two sets of plasma conditions. Triangles B = 155 G, n = 3.5 X 10^{12} cm^{-3}, R = 3.4 cm; circles: B = 250 G, n = 5.5 X 10^{12} cm^{-3}, R = 2.7 cm.

(c) Spatial damping rate versus electron temperature. Open triangles: B = 170 G, ω/Ω_e = 0.27, gas flow to arc source varying from 15 to 10 torr ℓ/sec; Filled in triangles: B = 400 G, ω/Ω_e = 0.29, gas flow 10 torr ℓ/sec; electron drift current varying from 0 to 17.5 A. Theoretical solid curve is based on Spitzer collision frequency.

IMPURITY-DRIVEN DRIFT WAVE

Theoretical studies have predicted the existence of impurity-driven drift-wave instabilities driven by the free energy of the density gradients of the main and impurity ions, leading to anomalous diffusion of both species. Such an instability has been identified and studied on the Q-1 machine. Impurity (cesium) ions are injected (parallel to $\vec{B}$) through an annular mesh-covered aperture into a potassium plasma (see Fig. 44) so that the radial density gradients of the potassium (K) and cesium (Cs) are of opposite sign (negative and positive, respectively) just inside the aperture. The drift wave ($\tilde{n}/n \lesssim 15\%$) is observed in this region when the impurity fraction (n_{Cs}/n_K) exceeds 10%. The wave propagates opposite to the K^+ diamagnetic drift direction with azimuthal mode numbers from m = 1 to m ~ 10.

The experimental dependence of ω and γ on n_{Cs}/n_K and magnetic field agrees qualitatively with the results of a linear kinetic theory in slab geometry. This theory has been extended into a

radially non-local analysis which accounts for the radial structure of the mode and the localization of the impurities.

When the Cs ions are pulsed in for a finite length of time, the linear growth rate and nonlinear development can be observed. It is found that the mode which persists in the steady-state is preceded by two faster growing modes which decay back to the noise level as the steady-state wave grows. Apparently, wave energy is being transferred among the modes and the expected frequency sum rule for such a process is observed.

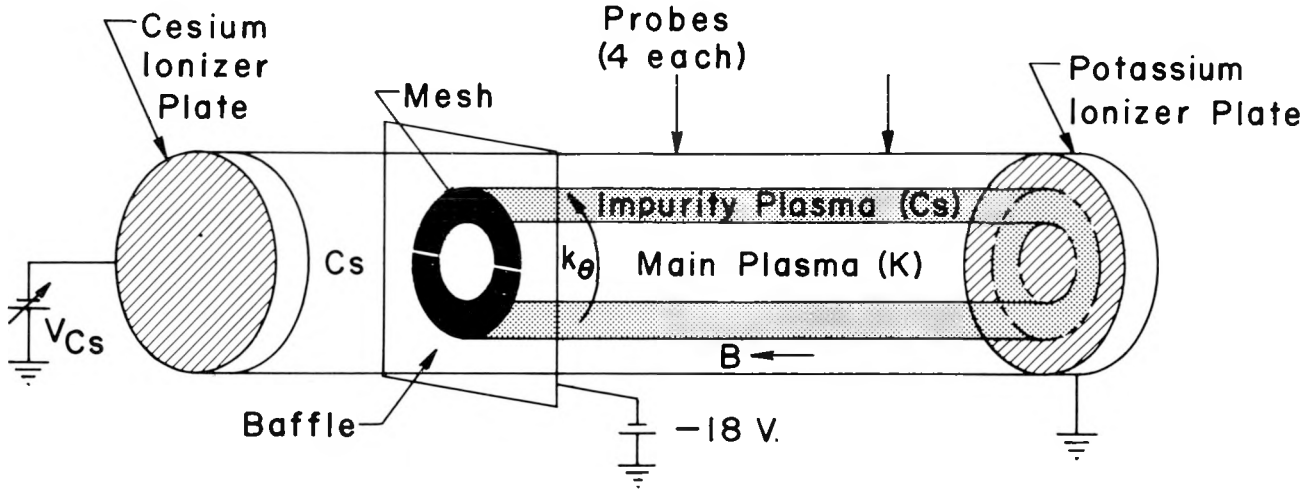

Figure 44. Schematic of experimental arrangement for impurity-driven drift wave in Q-1.

Tokamak Fusion Test Reactor (TFTR)

The Tokamak Fusion Test Reactor (TFTR), shown in the artist's rendition in Fig. 45, is scheduled to begin operation in the latter part of 1981. The TFTR is the first magnetic confinement device capable of demonstrating the fusion of deuterium and tritium at reactor-level power densities.

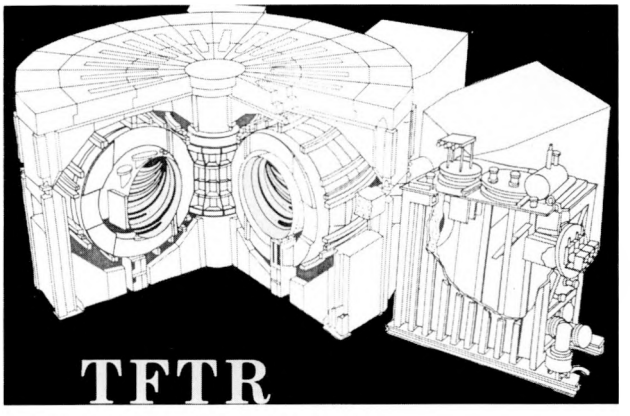

Figure 45. Artist's view of TFTR.

On the path to producing fusion energy under reactor-like conditions, the TFTR experimental program will realize many experimental goals that will impact the overall fusion program. The TFTR experimental program is being laid out to provide information necessary for the planning of next-generation reactor experiments (i.e., ETF).

TFTR will demonstrate the capability of handling plasmas under reactor plasma conditions. This will include the test of advanced limiter systems with the potential for avoiding the need for complicated divertors on future machines. In addition, TFTR will experience plasma current disruptions with a severity comparable to those in reactors. Methods to avoid these disruptions and systems to withstand the disruptions will be tested during the initial TFTR experimental program. The next stage in the experimental program will be devoted to the detailed study of plasma stability and transport in a regime not accessible in present devices (i.e., at mean values of electron temperature about 5-10 times higher). These studies will help to define the details and hopefully confirm the general features of our projections for tokamak operation at near-ignition conditions.

The high-powered neutral injection capability of TFTR will facilitate the study of a new regime of plasma heating. These studies will focus on aspects of beam heating of potential benefit or detriment to the next stage of fusion research devices. These studies will include injection-induced plasma rotation, beam-driven currents and heating-induced impurity contamination.

TFTR represents an essential link between the present hydrogen machines and the first engineering test reactor, not only in its capability to produce fusion power, but as importantly in its capability to produce and study plasmas at near-ignition conditions.

MAJOR ACTIVITIES

The technical design activity was essentially completed in FY79. The construction efforts progressed satisfactorily.

The Tokamak Flexibility Modification (TFM) project was initiated as a scaled-down version of the Tokamak Improvement Project (TIP). Tests were started at Lawrence Berkeley Laboratory (LBL) which indicated that at least one-second operation is feasible.

In TFTR Research and Development, major prototypes such as the Neutral Beam Power Supply and the Ohmic Heating Interrupter were completed. The M-3 mock-up was delivered by Grumman Aircraft Corporation.

The Neutral Beam program made important advances in FY79. Prototype components such as the power supply and the absolute valve were fabricated and are undergoing tests. The prototype beam line was completed by LBL.

Construction

In FY79 the TFTR site construction by Terminal Construction Corporation, under contract to the Princeton Office of the DOE, progressed from the excavation stage to the completion of almost all the underground work in the Experimental Complex. Substantial progress was made towards closing in the Motor Generator Building, the Cooling Towers and Pump House, the Maintenance and Utility Building, and the Field Coil Power Conversion Building.

Figure 46 shows the completed structures of the Pump House and Cooling Towers in the right foreground, and behind them the Motor Generator Building. Closure of these buildings is important for schedules, since it will permit

Figure 46. TFTR experimental complex, September 1979.

the installation of systems within them during the winter of 1979/1980. For example, by the end of FY79, the installation of the two Motor Generator units manufactured by General Electric Company and being assembled by Belding Corporation, was already 12% complete.

To the left of the Motor Generator Building is the structure of the two-story "L" shaped Field Coil Power Conversion Building.

To the left background, the Test Cell area is shown with most of the steel in place for the grade level floor. Concrete for this floor has already been cast in some sections to the left.

To the right of the Test Cell the concrete floor of the Neutral Beam Power Conversion Building may be seen. Beneath this floor is a large basement which will serve as the Pump Room for the Tokamak Cooling Water Systems.

At the end of FY79, construction of the Experimental Complex had reached 50% completion.

Figure 47 shows the Office and Laboratory Building with the auditorium in the front center. This building is part of the TFTR Project, and is being built by J. F. O'Healy Construction Corporation under contract to the Princeton Office of the Department of Energy. The East Wing (upper left) has a basement which will house the TFTR Control and Data Acquisition Computer Rooms, and will be connected to the Experimental Complex by a tunnel. The computers will be put in place by October of FY80.

Figure 47. Aerial view of the Office and Laboratory Building, September 1979.

Remote Handling

The M3 mockup, which is a full size replica of a section of TFTR (Figs. 48-50), was designed and manufactured by Grumman Aerospace Corporation and delivered to Princeton at the end of FY79. Some additional machining work has yet to be done on the stainless steel vacuum vessel before assembly can be completed.

This mockup will be used for checking the feasibility of initial assembly procedures, and for developing remote handling techniques. Throughout FY80, diagnostics, metallic vacuum vessel seals, actuators, adjustable limiters, and other components will be fitted and tested so that any operational difficulties can be corrected.

Remote maintenance techniques, essential when TFTR becomes radioactive during tritium

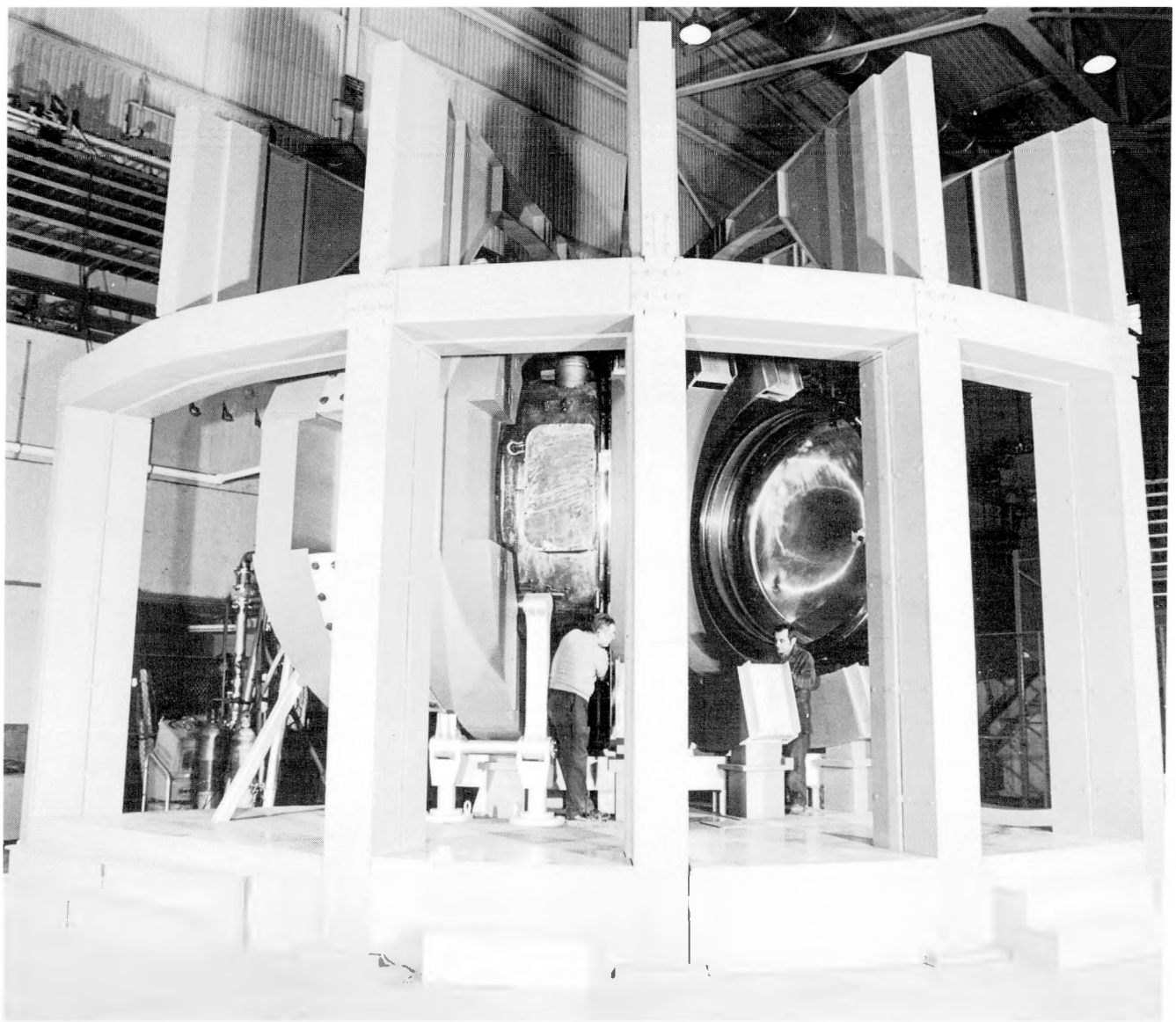

Figure 48. M-3 mockup of TFTR.

operation, are being developed in parallel with the assembly procedures. Priority is being given to the remote handling equipment which can be used for initial hands-on assembly. Two servo-operated manipulating arms are on order for attachment to a mobile in-vessel vehicle. They will be used to repair, replace, or modify components within the vacuum vessel. A large bridge-mounted manipulator fitted to an overhead crane is necessary for passing the in-vessel manipulator and the servo-operated arms through the access port in the vacuum vessel.

In FY79 work was started at Idaho National Engineering Laboratory on a remote welder. It is expected to be finished in FY80.

Neutral Beam Development

Activities in the Neutral Beam Line and Neutral Beam Power Supply centered around proto-

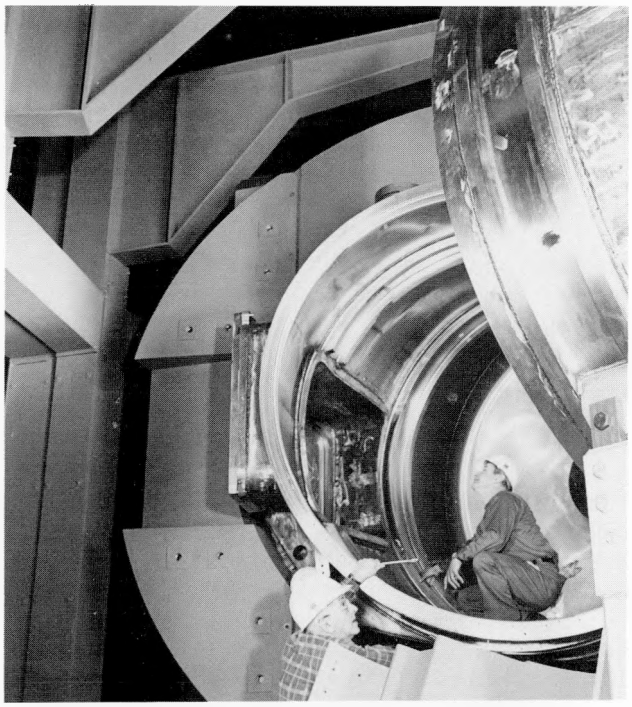

Figure 49. A view inside the vacuum vessel of the M-3 Mockup.

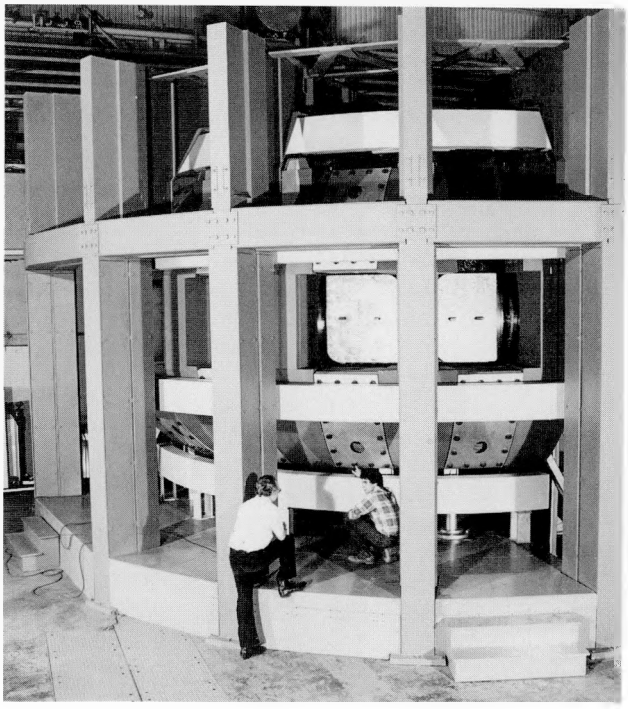

Figure 50. PF coils in position on M-3 Mockup.

type completion and the start-up of production units. The prototype beamline was completed by Lawrence Berkeley Laboratory during the summer and intensive testing was performed for three months. McDonnell Douglas Corp., an industrial subcontractor, completed the prototype neutral beam ion source. This source, a critical part of the plasma heating system, is one of three per neutral beam injector. The completion of this prototype marks an important milestone in the overall development of the heating system.

The prototype absolute valve, used for the isolation of the torus vacuum system from the neutral beam injector system, was fabricated by Leybold-Heraeus and is ready for final assembly and testing. In September, the first support structure for the neutral beam vacuum enclosure was delivered to Princeton.

Procurement of Neutral Beam Power Supplies (NBPS) from Transrex has progressed to the point where the prototype is now undergoing acceptance tests. These acceptance tests should be complete during the first quarter of FY80.

The development program with RCA for the HV Switch Tube was completed at the end of FY79. Production of these tubes has started and three tubes have already been shipped to Aydin, a subcontractor to Transrex, to be installed in the Modulator/Regulator subsystem of the NBPS. In addition, two tubes have been supplied to the LLL HV testing stand.

The Ion Source protection equipment development program is continuing with Argonne National Laboratory. A prototype design has been completed and constructed.

The HV Transmission Line development program is continuing into FY80. A sample line has been constructed and successfully held off test voltages of up to 275 kV and has passed the "worst cases" thermal tests.

A temporary Neutral Beam Test Facility, to accommodate the delivery of the prototype NBPS as well as the first NB ion source, is being established. The facility should be complete at the beginning of next year, in time to install the power system and begin dummy load testing.

Research and Development

To accomplish the wide variety of research and development efforts associated with the

design and construction of TFTR, the Princeton Plasma Physics Laboratory has established both an in-house R&D program and a contractual program with a number of highly specialized technology corporations and national laboratories.

Accomplishments during this period include: design and fabrication of a prototype neutral beam power supply (Transrex); design and fabrication of a prototype ohmic heating interrupter (Westinghouse); and fabrication and testing of the prototype inner support structure (Rockwell). Westinghouse also completed the R&D sample program for Toroidal Field Coil production.

Other R&D this fiscal year included selection of the silver-coated Cefilac Helicoflex seal for the large number of circular and non-circular vacuum ports on the TFTR vacuum vessel; successful welding of the vacuum vessel bellows, and successful brazing of large diameter (39 inches) ceramic insulating rings to metallic elements which can be welded into vacuum ducts.

The TFTR R&D program will continue at a lower funding level in FY80 with the major efforts concentrated on neutral beam component development and remote handling and maintenance.

TFTR Experimental Research

The TFTR experimental research effort supports the fabrication, testing, and eventual operation of the TFTR. The development of the CICADA control system in general, and plasma position control in particular, are ongoing segments of the experimental research program. The TFTR Flexibility Modification (TFM) Project was approved during the past year. Results from transport modeling studies of the TFM discharges were used to support the proposal and to provide the basis for the system requirements.

To realize the full operating potential of TFM, it is necessary to control plasma impurities as well as the recycling of deuterium and tritium. These problems are particularly difficult, however, due to the large particle and energy fluxes which will be incident upon material surfaces in the TFM mode. Consequently, an extensive impurity control R & D program has been initiated within the TFM project. One phase of this program is the selection and testing of materials for possible use as limiters or protective plates. Small samples are subjected to simulated and actual tokamak plasma bombardment to determine bulk thermal response, surface properties, and hydrogenic retention characteristics. In addition, a full size limiter has been fabricated for testing in PDX and is shown in Fig. 51. The material, TiC coated POCO graphite, has exhibited favorable behavior in the sample tests. The limiter, which is approximately 25 cm long, will be inserted into the PDX discharge by an actuator mechanism as shown.

The other major aspect of the impurity control program is the development of a surface pumping system compatible with the limitations on stored tritium. Ti sublimation gettering has been effective in a number of other tokamaks. Work is underway at the Sandia Laboratories in Livermore, California to determine the decomposition characteristics for hydrogenic species which have been pumped by Ti films. Fig. 52 shows the measured decomposition at 250°C of a 1000Å Ti film fully loaded with deuterium. The rate is initially very high at large deuterium concentrations, then falls to a plateau level and finally approaches zero at zero deuterium concentration. From these data, it has been concluded that tritium can be removed from Ti films at 250°C in reasonable times.

Central Instrumentation, Control, and Data Acquisition (CICADA)

During the past year CICADA took delivery of all thirteen SEL computers and successfully demonstrated control and monitoring applications. Three prototype operating consoles were active and three CAMAC links.

A test system comprised of a SEL computer and a CAMAC link was installed on the PLT x-ray experiment and is performing satisfactorily. It is used on-line during runs to collect, process, and display experimental data.

A stand-alone, microprocessor-controlled CAMAC test station was supplied to Transrex for testing the neutral beam power supply; another stand-alone system, to the Mound Facility for testing the tritium gas system. Clock and timing system hardware was provided to both Lawrence Berkeley Laboratory and General Atomic.

At the end of September, the computer manufacturer's new MPX/networking operating system was installed in our computers. Effort is now directed toward integrating the PPL software into this system.

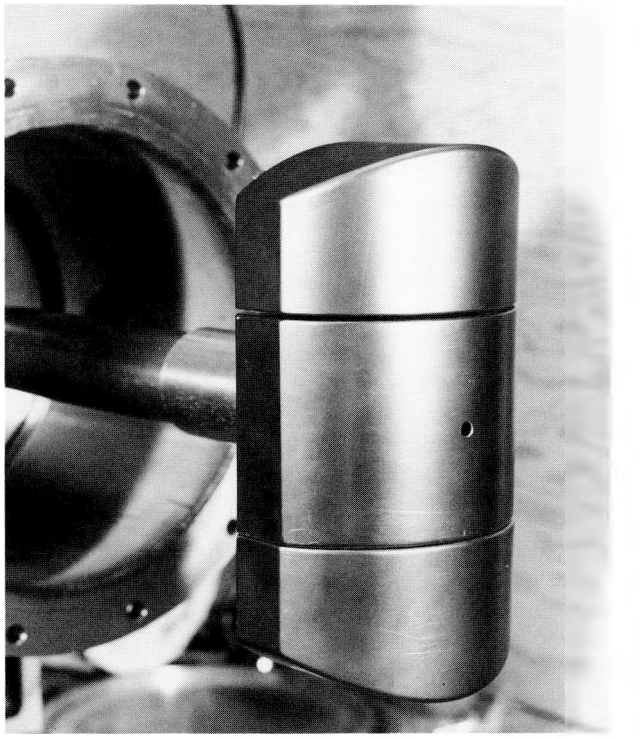

Figure 51. TFTR/TFM test limiter for experiments in PDX. The material is TiC coated POCO graphite and it will be inserted into the PDX discharge to determine the effects of plasma bombardment.

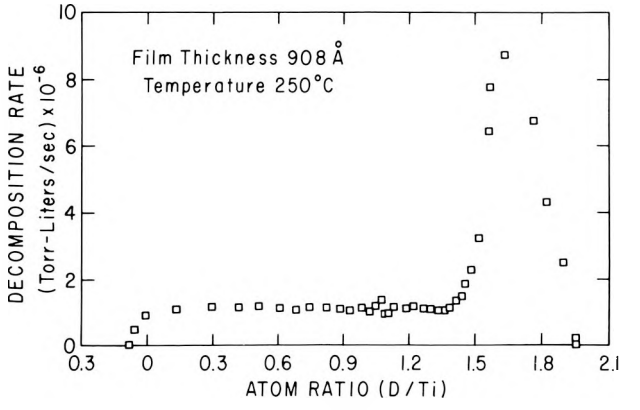

Figure 52. Measured decomposition rate of a deuterided 908 Å Ti film at 250°C as a function of the deuterium concentration.

Flexibility Modification

The TFM (TFTR Flexibility Modification) Project is a scaled-down version of the original T.I.P. (TFTR Improvement Project). The main emphasis is still on making improvements to TFTR to permit extended plasma performance. At present the scope includes adding a fourth neutral beam to the tokamak, with all beams having approximately 1.5 sec pulse length, improving the capability of the vacuum vessel to withstand higher plasma loads, and increasing the maximum beta.

Development tests were initiated at LBL to provide information on the long-pulse capabilities of the TFTR ion sources, and initial results indicate that at least one-second operation is feasible.

Development was initiated on new materials for protective surfaces to be installed in the vacuum vessel.

Engineering work was concentrated on the design of a gettering system to control plasma density and impurity influx. Experiments on a number of tokamaks have demonstrated that such gettering over an appreciable surface area ($\geqslant 10\%$) of the vacuum vessel is an effective method of meeting both of these objectives. The preliminary design of two candidate surface pumping systems that provide the gettering function was completed. One system uses the proved (PLT, ISX) concept of titanium sublimation gettering, while the other system uses zirconium/aluminum gettering, to be tested in a plasma environment within PDX next year.

Work was started on determining the plasma disruption loads in the TFTR-TFM system. Experience on the Princeton Large Torus (PLT) and Poloidal Divertor Experiment (PDX) has shown that loads induced on conducting elements within the vacuum vessel during plasma disruption can be large enough to cause major failures. Since there are many such elements in TFM, including the protective plates and surface pumping panels, computer programs have been developed to determine eddy currents induced in conducting elements located within the vacuum vessel and for the determination of loads arising from these currents interacting with local magnetic fields. These programs can be used to determine similar loadings in other reactors.

Diagnostics

Significant progress was made this year on a wide variety of diagnostics in readiness for entry into the predominantly fabrication period of TFTR diagnostics. The understanding of the effects of the radiation environment, the selection and evaluation of detectors and the development of new diagnostic techniques have all progressed satisfactorily. Lateness of definition of protective plates in the TFTR vacuum vessel, shortages of manpower and difficulty in placing contracts in the second half of the year have all contributed to some delays relative to the schedules.

During the year a neutron source for calibration and carrying out noise measurements in diagnostic components was commissioned, and radiation studies were also done at the medical reactor at Brookhaven. A thin platinum bolometer was developed and has been shown to be relatively insensitive to radiation and will shortly be tested on PLT. The tritium sensitivity of channel electron multipliers and radiation sensitivity of windows and 'O' ring materials for vacuum gate valves have also been studied.

Concurrent with these problems introduced by the TFTR radiation environment, development of a 1-mm interferometer, a far-infrared CH_3OH interferometer (the prototype operated successfully on PDX), a CO_2 laser forward scattering system for ion temperature measurement and advanced charge exchange systems have been carried out to cater to the larger size of the TFTR plasma. Interfacing these and many other diagnostics, evolving from their PLT and PDX predecessors, to the TFTR tokamak with its special bakeout, remote handling, radiation shielding and tritium containment requirements has continued through the year. A good start of the integration of the diagnostics with the CICADA computer system has been made by installing one of the TFTR computers for the operation of the PLT X-ray wave system. All these programs will move forward, together with a much larger effort on definition and fabrication of the diagnostic instruments to be used on TFTR.

Procurement

Fiscal year 1979 saw the successful negotiation and placement of major subcontracts (over $500K) for the following TFTR components:

- TF coil case assembly
- Tritium cleanup systems
- PF coils under 12 ft.
- TF coil case ancillary structural components – plate
- Metal enclosed dc equipment
- Capacitor charge and discharge system
- Vacuum vessel inboard/outboard supports
- Power diode assemblies
- NB vacuum enclosures

Additional funding for accelerating delivery schedules of certain major components has been successfully applied to the following subcontracts:

- TF coils assembly and installation in TF case – Westinghouse Electric Corp.
- PF coils under 12 ft in diameter – Brown Boveri Corp.
- TF coil case assemblies – Allis-Chalmers

A decision as to what methods will be utilized in accelerating delivery of the vacuum vessel (supplied by Chicago Bridge and Iron Co.) will be reached by mid December, 1979.

The successful placement of the following major procurement (over $500K) is nearing completion and should be accomplished early in FY80:

- Cryogenic piping system
- H/C system piping/vacuum system foreline piping
- Non tritium gas delivery system

Delivery to the TFTR site of the following major components took place during FY79:

- 13.8 kV switchgear
- 13.8 kV mainleads
- Machine area cooling water tanks
- Energy conversion system transformers (partial)
- Energy storage capacitor bank (partial)
- DC reactors (partial)
- 2500 MVA circuit breakers
- MG flywheel set
- Master-Slave manipulator
- 13.8 KV current limiting reactors
- Component cooling water chiller

TFTR Blanket Module Experiments*

The utilization of fusion energy based on the D-T cycle requires that the reacting plasma be surrounded by a blanket to capture the fusion neutrons. The captured neutrons breed tritium from lithium in order to replenish the burned fuel, while the heat deposited by the thermalizing neutrons can be converted to electricity. In 1979 the Electric Power Research Institute (EPRI) sponsored a study under PPPL direction to assess the feasibility of applying blanket modules to the TFTR in order to conduct engineering-oriented fusion blanket experiments. This investigation included an analysis of the engineering data that could be obtained to aid in the design of future fusion reactor blankets, as well as the operational experience that would be gained for the first time in important areas of fusion blanket systems. Conceptual designs were carried out for an Engineering Test Station intended to provide modular blanket capability, and for a blanket module that would be used for tritium breeding experiments.

MAJOR ACTIVITIES

Objectives and Engineering Benefits of TFTR Blanket Module Experiments

Table II lists the areas where important experiments can be carried out using TFTR fusion neutrons. In the base of a tritium breeding blanket, the information to be obtained includes integral neutronics data and tritium breeding rate profiles, using the TFTR toroidal neutron source and spectrum, as well as power deposition profiles (although blanket heating will normally be exceedingly small).

Of all the intense neutron generators that will be available in the 1980s, only the TFTR provides the following features: (1) a geometrically extended D-T fusion-neutron source; (2) a neutron spectrum (including backscattered neutrons) that is characteristic of a practical toroidal fusion reactor; (3) sufficient test volume for a representative reactor blanket module.

In addition to obtaining specific engineering data, operational experience would be gained for the first time in certain important areas of blanket technology: (1) fabrication of breeding elements; (2) blanket dosimetry and thermometry in a fusion reactor environment; (3) electromagnetic isolation of the blanket modules from the tokamak plasma; (4) remote handling of blanket modules; (5) neutron shielding effects.

*Sponsored by EPRI Contract TPS 79-705.

TFTR Engineering Test Station

The basic requirement of the Engineering Test Station (ETS) is to provide structural support and utilities/instrumentation interfaces for blanket module experiments adjacent to the TFTR vacuum vessel. The ETS would be located in one bay of the TFTR, between adjacent toroidal field coils.

The ETS would support blanket modules with dimensions up to 78 cm in width, 85 cm in height, and 100 cm in depth, and with a weight up to 4000 kg. Access to electricity, water, air, gas, and pneumatic rabbit tubes will be made by means of a shield plug mounted on the same pallet as the blanket module. Fig. 53 depicts a blanket module installed on the ETS.

Global Tritium Breeding Ratio

A toroidal fusion reactor cannot exhibit a global TBR (Tritium Breeding Ratio) as large as the ideal TBR because of incomplete blanket coverage. For a given distribution of blanket modules, uncertainties (in addition to nuclear cross-section uncertainties) in predicting the global TBR arise from difficulties in (1) modeling a heterogeneous blanket with finite width and height, (2) modeling the neutron source geometry, and (3) determining the neutron flux and spectrum incident on a specific blanket region, taking into account neutron backscattering around the torus, degradation, and absorption. For a given total fusion-neutron production rate, the uncertainty in breeding rate in a local blanket region is estimated to be about $\pm 40\%$.

The fusion-neutron source geometry in the TFTR as well as the fusion-neutron flux incident on representative regions around the torus will be measured. This information together with the integral neutronics data and direct measurements of tritium generation in a blanket module would form sets of reference data used to calibrate design codes for toroidal reactors. The result is expected to be a significant reduction in the uncertainty in estimating the minimum

TABLE II. POTENTIAL FUSION BLANKET EXPERIMENTS ON THE TFTR

TRITIUM BREEDING

- Relate measured tritium production and neutron transport to fusion-neutron source characteristics and reactor geometry.

CHEMICAL FUELS

- Determine neutronics characteristics, power deposition profiles, and activation levels in relevant assemblies.

HOT BLANKET EXPERIMENTS

- Obtain engineering data on spatial power deposition, temperature transients, and thermal cycling.

BLANKET INSTRUMENTATION

- Obtain operational experience with practical neutron and gamma-ray dosimetry and thermometry for fusion reactor blankets.

ELECTROMAGNETIC INTERACTIONS

- Verify techniques for electromagnetic isolation of blanket modules from the pulsed tokamak fields.

SHIELDING

- Obtain data on neutron shielding with special duct configurations.

RADIATION DAMAGE

- Compare radiation damage to organic insulators with results from other irradiation programs.

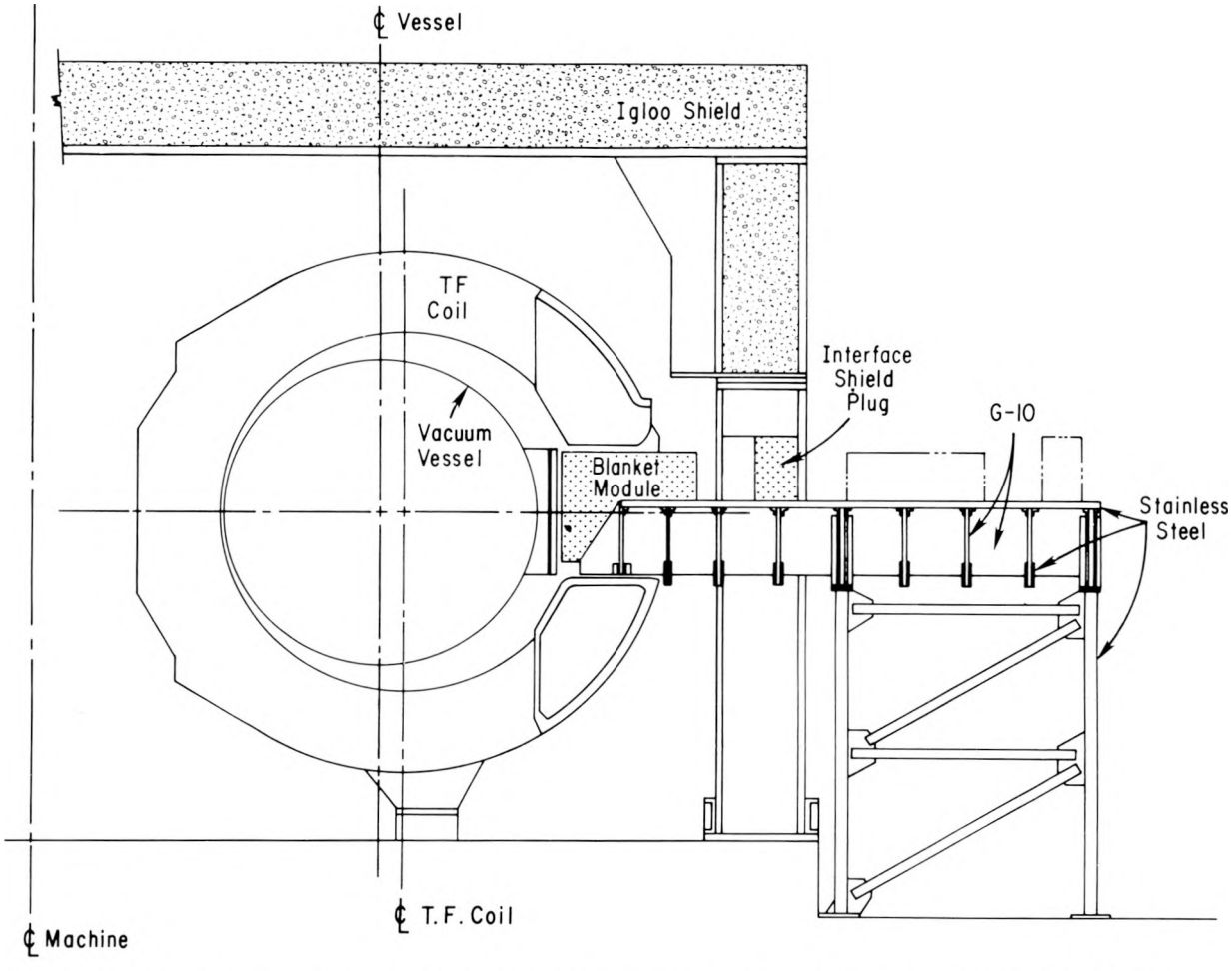

Figure 53. Elevation view of the TFTR showing a blanket module installed on the Engineering Test Station.

blanket coverage and required distribution of breeding modules for obtaining tritium self-sufficiency in future fusion reactors.

Lithium Blanket Module

There are a great many conceivable types of blankets for tritium breeding, and it is necessary to establish a priority ranking among them in scoping the TFTR fusion blanket program. In the 1979 conceptual design carried out with the Babcock & Wilcox Lynchburg Research Center, a gas-cooled, Zircaloy-clad, lithium oxide (Li_2O) lattice was selected for the most detailed analysis.

The spatially averaged specific activity of the central Li_2O rods due to tritium beta decay will be on the order of 1 nCi/g after a single moderate-level pulse in TFTR yielding a typical first-wall fluence of 1.5×10^{12} n/cm^2. After a single D-T run in Mode II of no more than 10 shots, the quantity of tritium bred can be measured absolutely with an uncertainty of ±10%. Combining this uncertainty with that of the incident neutron fluence on the front face (±8%) yields an expected uncertainty in the measured TBR of less than ±15%.

Engineering

The Engineering Division is a service-oriented group of over 250 personnel. It provides the Laboratory with the technical support required for experimental physics devices and programs.

During FY79 a large portion of the Division underwent a major reorganization in order to avoid disadvantages intrinsic to operation with large multifunctional sections. The resulting functional sections are unified under three branches; the Power Branch, the Computer Branch, and the Diagnostics Branch.

Power Branch

Composed of three functional groups—the AC Power Section, the Rectifier Section, and the Neutral Beam Power Section—this branch handles ac and dc power and energy requirements for the laboratory and associated experimental devices. Engineering services provided include the maintenance of adequate and reliable line power to the Forrestal Campus, the design and fabrication of high energy electrical storage systems, power converters, and high voltage direct current power supplies for the neutral beam sources used in experimental programs.

Computer Branch

The Applications Programming Section, Data Systems Programming and Operations Section, and Controls Section of this branch provide computer and control-related functions for experimental programs. Examples of these services include on-line computer reduction of experimental data, systems and scientific computer programming, hardware for acquisition and display, and device-related supervisory and annunciation controls.

Diagnostics Branch

This branch is composed of four sections: Electronics, Electro-Optics, Instrumentation, and Mechanical Engineering. A wide variety of electronic circuitry in devices for special applications is provided by the branch, exemplified by such items as low level signal processors, digital and analog control systems, fiber-optic isolation for control and data transmission, and XUV image sensors. Also included are the design and fabrication of specialized microwave and laser devices for plasma diagnostics. In addition, the branch has responsibility for all mechanical aspects of diagnostics equipment relating to vacuum penetrations, port coordination, peripheral support structures, high power rf accessories, and the laboratory deionized water systems.

Division Administration

This group is responsible for the primary functions of management and leadership. It provides information, data and support for budgeting and monitoring, and guidelines for effective engineering procedures. It is a service group for engineers, and is their liaison with other PPPL administrative offices.

The following groups are not associated with any of the branches.

RADIO FREQUENCY SECTION

The group is responsible for the design, development, and fabrication of high power rf generators and neutral beam tube-type modulators used for plasma heating with ICRF, LHR, and NBI methods.

TFTR DIAGNOSTICS SECTION

Unique in the Engineering Division, this group is organized as a project, and is responsible for diagnostic devices to be used on the TFTR. Working closely with both TFTR physics and engineering groups, this section, together with the resources and expertise of the entire Engineering Division, is engaged in the definition and design of some forty diagnostics experiments.

MAJOR ACCOMPLISHMENTS

Power Branch

AC POWER SECTION

The largest project completed by the Section for the year was the engineering, field supervision, and checkout of the neutral beam supply autotransformers. The work was completed, the units were energized, and have operated satisfactorily.

A 4160 volt power line feed was installed for use on the PLT 55 MHz ICRH dc supply. Line power for a LHRH system is also tapped from this source.

Section involvement with DOE activities relating to TFTR construction increased steadily during the fiscal year. Considerable effort was given to integrating proposed additions and modifications of existing systems due to TFTR requirements.

Section activities for the year also included support to the Facilities Planning Group by the design of electrical aspects of Substation 18 and by starting design work on Substation 19.

RECTIFIER SECTION

Initial operation on PDX subjected the EF (Equilibrium Field) and OH (Ohmic Heating) rectifiers to heavier loads than had been encountered in PLT operation. As a result, certain previously noted latent defects were identified. Preliminary proposals for correction were made, and the proposed programs undertaken. Included were circuit renovation of both EF and OH rectifiers, strengthening some weak members, adding additional protective circuitry and instrumentation for rapid troubleshooting, and a new regulator circuit design for the OH rectifier that was fabricated using etched circuits. Hand wired logic circuit cards were also redone as etched circuits and installed on a step-by-step basis. Both rectifiers were simulated on a hybrid computer to obtain a better understanding of the circuit behavior, especially of the feedback control properties.

The hybrid computer also was used to simulate a TFTR power conversion circuit to aid in evaluating a firing module developed by Grumman. Similar simulations were carried out on a digital computer to investigate feasibility of a feedback control scheme for plasma positioning using the TFTR EF.

The Section completed fabrication and initial operation of the PDX pulse discharge cleaning power supply. This supply is used for high power cleaning of PDX when the OH rectifier, normally used for this application, is in use on PLT.

NEUTRAL BEAM POWER SECTION

PLT engineering by this Section during the year consisted of refurbishing the beam high voltage accel and decel supplies.

Accel supplies were augmented by enclosing and air-conditioning the rectifiers for more reliable operation. The accel supply firing boards were replaced, using more highly rated components. Decel circuitry was changed to enable an increase in momentary output current from 16 to 25 amps.

The fabrication of the PDX ion temperature and FIDE power supplies and controls was completed, while fabrication, installation, and testing of the beam heating power supplies was 90% complete. Work on the beam supplies involved substantial modifications of the PLT accel rectifiers to enable switching over to PDX at twice the previous power.

Section activities for TFTR consisted mainly of supplying aid in correctly locating equipment in buildings, and, to a lesser degree, advising on the procurement of power supplies. The FIDE diagnostic equipment for TFTR was in a preliminary definition stage at the end of the period.

Computer Branch

APPLICATIONS PROGRAMMING SECTION

Activities were concentrated on diagnostics programming software for PLT and PDX plus information displays for the experimental physicists of these machines. Some of the more significant examples are:

Bolometers: Smoothing in the radial direction was added to the array analysis, as was the capability to write out data at certain time slices. These data were processed with an experimental version of the smoothing and inversion procedure.

Microwave Scattering: A program to perform the Fourier analysis of microwave scattering data was written. The data are recorded using a LeCroy type 8210 waveform digitizer and type 8100 programmable amplifiers. This system is used to provide better time resolution of the microwave spectra than was possible with the previous spectrum analyzers.

PDX Charge Exchange: New equations and constants were added to compute voltage, current, energy, and mass for analyzer No. 3 in the PDP-11 monitor and control program. In addition, an option for direct user input of current and voltage was installed. Using this program, analyzers 1 and 3 were calibrated and calibration factors were added to the program. The real time and off-line analysis programs were rewritten to include the computations, constants, and calibration factors. The temperature versus time plot was added, as in the PLT programs.

Machine Diagnostics Programs-General: The routines were updated and modified to add new

features. An interactive plot control program for a plot parameter file was set up. This file contains all information necessary to create a plot of data taken during a machine event. Using this technique, real-time displays can be changed without reloading programs, thus simplifying the display process.

DATA SYSTEMS PROGRAMMING AND OPERATIONS SECTION

The most significant activity of this section during the fiscal year was the initial operation of the PDX machine data handling system. The DAS had been prepared to acquire day-one data from diagnostics that were installed and functioning. These data were collected using transient digitizers interfaced through CAMAC to a PDP-11 computer running RSX. This computer, in turn, wrote the data to files on the PDP-10 that returned plots of data to the user. This was the first live test of the complete network developed to allow the DAS to expand sufficiently to meet the PDX load. Throughout the year many more diagnostics for PLT and PDX have been added to the system load.

During the month of January the DEC System-10 CPU was upgraded from a KI-10 processor to a KL-10. After some hardware difficulties, the new processor has become as reliable as the earlier KI-10. The KL-10 provides a dramatic increase in speed due to cache memory and the fact that the core memory is four-way interleaved.

Several more computers were added to the DAS network. Included was the VAX 11/780 that communicates with a PDP-11, which in turn communicates with the PDP-10. The Neutral Beam diagnostic computer and the Diagnostic Control computer were attached, using the PPPL parallel Data Channel, allowing neutral beam data to be archived with other diagnostic data, and users on the PDP-10 to pass positioning information for various diagnostics on the machine.

A significant effort went into the development of programs to control and communicate with a wide variety of CAMAC modules. There are now routines to service approximately twenty different modules.

CONTROLS SECTION

Modifications to PLT operating controls were developed to facilitate safe usage of the HTA (Hard Tube Amplifier) employed for 200 Hz discharge cleaning. Modifications also were made to the ICRF controls for the same reason. The controls for both systems are now integrated with other machine operations.

Automatic conditioning of neutral beam sources and archiving of neutral beam diagnostic data using the neutral beam diagnostic computer were developed and applied to PLT.

The Section expended considerable effort on the "shakedown" start-up phases of PDX operation, where last minute changes in subsystem operational status frequently required temporary control changes.

The Section also provided PDX with vacuum controls, remote controls for limiter positioning and biasing, and for monochromator, bolometer, array detector, IR Laser, FIDE, Thomson Scattering, and the Fast Wave Experiment.

Diagnostics Branch

ELECTRONICS SECTION

An extensive plasma loop voltage measurement system was designed and built for PDX (Fig. 54). Accurate determination of this voltage is very important, as it indicates and/or confirms plasma conditions resulting from various experimental operations.

Loop voltages encountered range from millivolts to several kilovolts, and a dynamic range of 10,000/1 had to be accommodated. Unwanted noise and pickup coupled from machine accessories (720 Hz ripple from the OH systems, for example) also were problems requiring solution.

The final design solved these problems through the use of user-selectable amplitude ratios and low pass filters. The processor accurately conditions and transmits the signals through analog safety breaks to the control room. Circuitry for four separate loop voltage inputs has been provided.

The processor has operated accurately and reliably since installation in June, 1979.

A system to control gas injection into the PDX machine, and for monitoring and displaying gas pressure at a number of points was designed and installed. This system enables extremely flexible control of gas flow before and during a machine pulse. Modes available include steady flow, pulsed flow, both with or without feedback, and an external shaped flow option that permits arbitrary flow during a machine event.

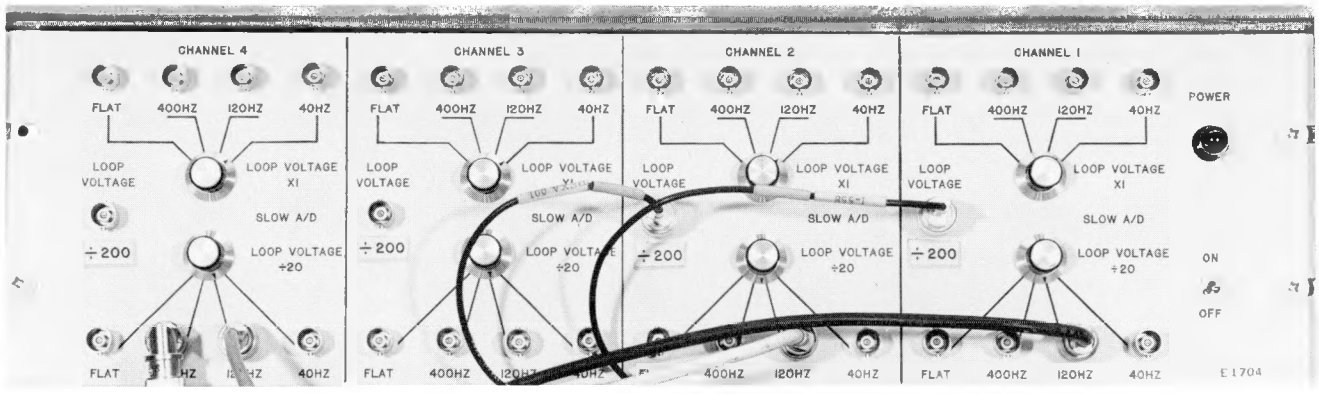

Figure 54. PDX plasma loop voltage processor control room output panel.

Several subsystems are used: the gas programmer, the gas feedback unit, the gas valve driver, a dc ion gauge controller, a preamplifier, and a metering system.

Electronic equipment to support the PDX Neutral Beam project was designed and fabricated during the period. Included were four 25 channel timers capable of operating alone or synchronized from the PDX master timer, data transmission systems with 50 kV isolation via light-pipes, and interface units from the timers providing various output levels for compatibility with a variety of equipment. Gas valve driver control units also were provided.

Other pieces of equipment produced for PDX by this section during the year were: a) a control system for the Surface Analysis Station using both manual and computer control via CAMAC and b) equipment for the FIDE and Charge Exchange Ion Temperature experiments, including timers of unique design, fiber optic isolated solenoid gas valve drivers, analog data transmission systems, also using fibers optic isolation, and specialized analog amplifiers with switching logic to combine the outputs.

ELECTRO-OPTICS SECTION

A windowless intensified CCD detector system for use with a vacuum monochromator was installed for Laboratory use in March of the fiscal year.

A commercially available Reticon Camera system with a processor-controller for use on PDX in making soft x-ray measurements was evaluated by the section. This equipment is now in lab use here.

An engineering CCD test camera was designed and fabricated for the Thomson Scattering Experiment. The camera is being used to evaluate CCD's for that diagnostic.

A periscope study to relay a near infrared image to a CCD camera was submitted by a commercial source, results being approved by all PPL users. This was used as a guide in the preparation of a periscope purchase specifications document.

A bolometer test set was constructed in order to evaluate platinum resistors as possible sensors. Irradiation tests were performed at Brookhaven.

Other section activities included fabrication of a prototype Faraday rotator solenoid, a grating polychromator amplifier, and general support to the Thomson Scattering Experiment at PDX. Camera design studies for neutral beam calorimetry, plasma TV, and the TFTR x-ray camera were undertaken during the latter part of the fiscal year.

INSTRUMENTATION SECTION

An ultralow noise amplifier (Fig. 55) was developed and installed for use with the PDX far infrared laser interferometer system for plasma density measurements. Features include a noise density of 1 nV/root Hz, 72 db gain over a range of 25 kHz to 3.5 MHz at the 3 db points, and an output of 0.8 volts rms into 50 ohms. Two units are employed, one receiving a reference signal, the other a signal phase-shifted in accordance with plasma density, both signals produced from Schottky barrier diode detectors. Both units drive phase detecting circuitry. In order to protect the rather fragile detectors, a relay is included in each amplifier to shunt the input with 50 ohms when power fails or is turned off.

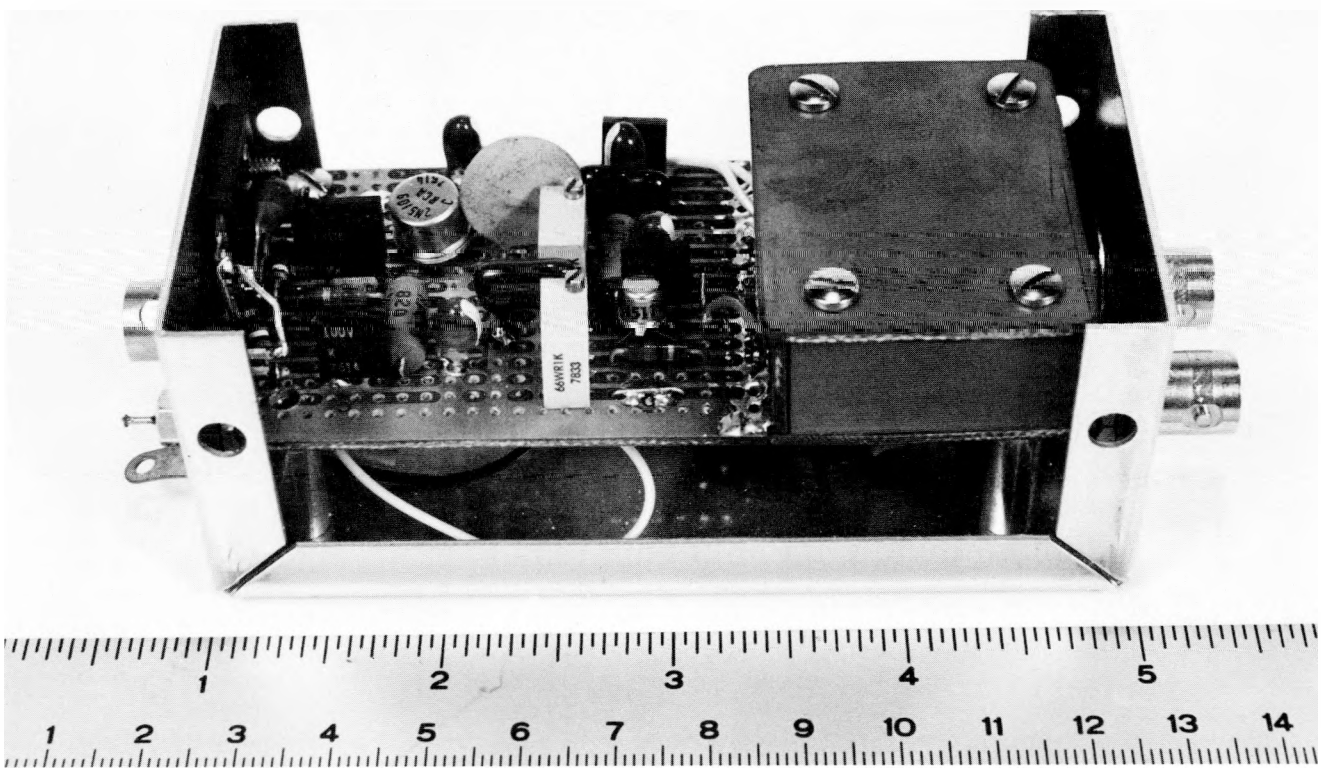

Figure 55. Ultralow noise amplifier.

Considerable effort by this Section was devoted to the support of PDX start-up operations. A digital safety break system with medium and high speed channels was installed along with accessories to assure system coordination.

A large number of devices were designed, built, and/or procured for both PLT and PDX in support of diagnostics and data acquisition. In addition, studies began for a number of TFTR diagnostics, and a one millimeter microwave interferometer.

MECHANICAL ENGINEERING SECTION

Fabrication and installation of the PLT ICRF antenna load assembly was completed and successfully tested. The assembly consists of four half-turn head coils with ceramic covers, Faraday shields, high voltage feed-throughs, and coaxial line lengths.

Blades and remotely driven positioning mechanisms for the upper, (See Fig. 56) lower, and outside limiters were completed and installed on

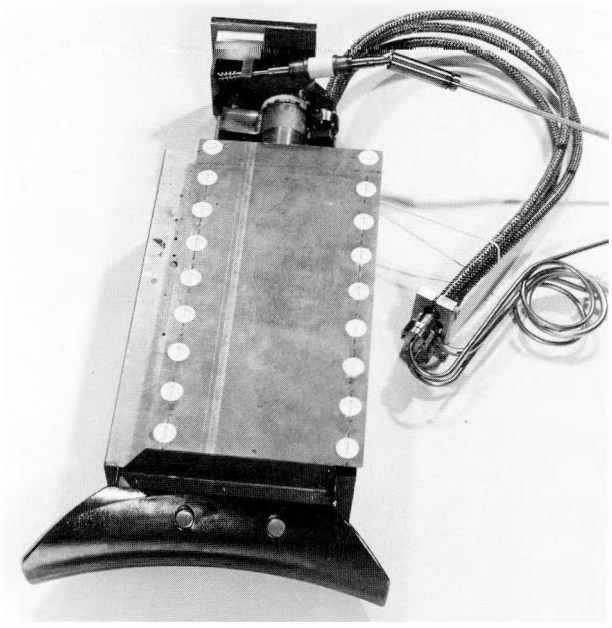

Figure 56. PDX limiter blade and positioning mechanism.

PDX. The blades were designed for cooling with helium or nitrogen and are adjustable over sufficient ranges to allow changes in plasma shape. Mirnov coils were mounted on the back of the blades, as well as in other locations inside the vacuum vessel.

The forward scattering experimental apparatus was completed and installed on PDX. This equipment is used in conjunction with a laser beam directed downward through the plasma. The resulting photon scatters at 10 degrees from the beam are collected for analysis by scannable viewing optics in the assembly. The optical train includes an image rotator, a discriminator (prefilter), and an invertible grating to diffract the light to the appropriate polychromator. The train also can collect input from the Single Point Scannable Thomson Scattering System.

Supply of deionized cooling water to the PLT high power ICRF generator tubes necessitated an addition to the CS water system, design and installation being completed during the year. The system also was augmented to provide water to the PDX neutral beam lines. Another water system activity was design completion of the piping alterations, valving, and control changes required to allow parallel operation of the main system chillers, a change-over to take place in FY80.

Independent Sections

RADIO FREQUENCY SECTION

This Section was occupied with the design and construction of several major radio frequency plasma heating devices and accessory components for neutral beam heating. Modifications of existing equipment to meet new requirements also were accomplished. The remainder of activities included insuring that all high power RF equipment at the Laboratory operated correctly, as well as liaison to insure successful operation of the RF equipment lent to M.I.T.

The PLT ICRF program was a two faceted effort, one to modify the existing 25 MHz system for semi-long pulse (100 ms duration with minimal droop) operation; the other to complete and test the first 55 MHz generator.

At the end of the fiscal year the 25 MHz project was complete and the generator has produced the required power of 500 KW with 100 msec pulses into the PLT load system. Operation at still longer pulse durations was requested, this work being in progress at the year end.

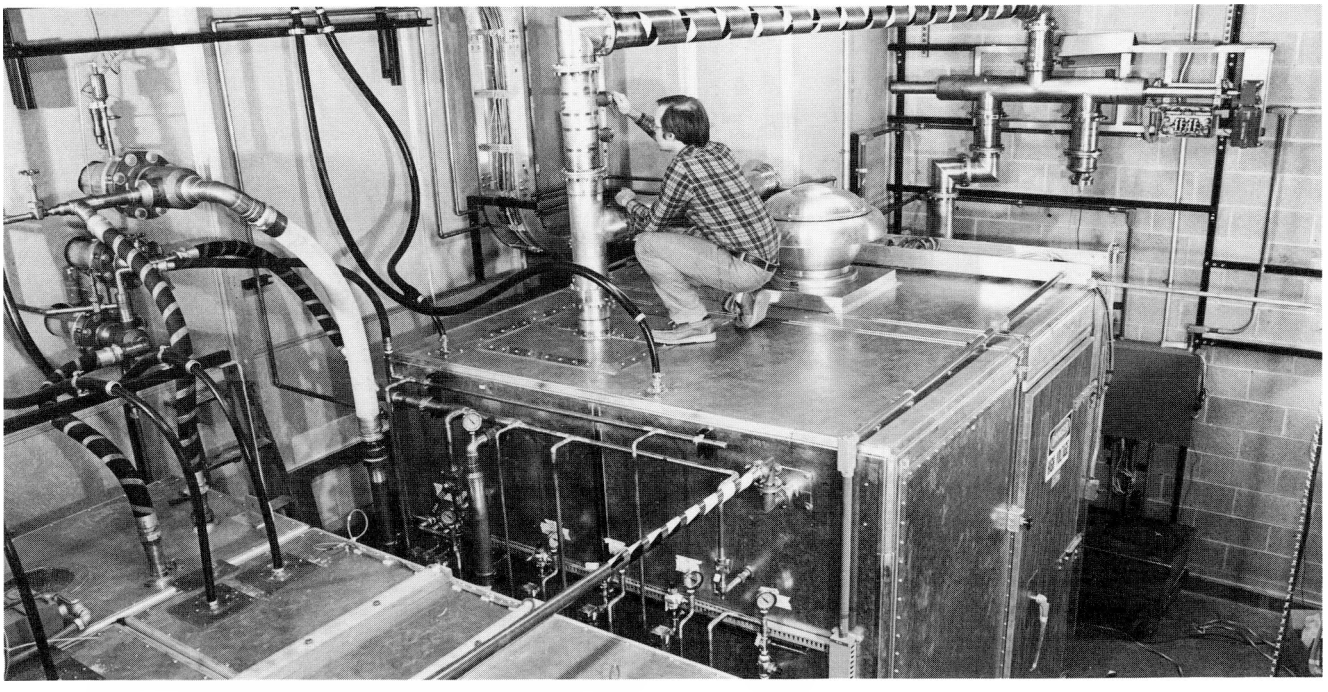

Figure 57. PLT high power ICRF equipment under contruction.

Construction of the 55 MHz generator (Fig. 57) was completed, and testing to in-excess-of 1 MW output had been realized, when notice was given to change the operating frequency to 42 MHz. The testing phase was halted to permit redesign for operation at the new frequency, this work also being in progress at the end of the year.

Design and construction of a 1.2 MW, 900 MHz LHRF generator system for PLT was started, and half the system hardware had been emplaced by September 30. Six type VA955 klystrons are used to feed a six-guide phased array at the machine. Major tasks in this program included design of a movable coupler, a six-guide vacuum window, an improved phase monitoring system, and a long pulse, high voltage power conversion system.

Two neutral beam diagnostics modulators were constructed and tested for use on PDX, one for ion temperature diagnostics, the other for FIDE on that machine. The FIDE modulator was designed to provide fast rise and fall pulses. A typical FIDE signal, for example, might be a 10 ms burst of square wave with 200 μs period. The older ATC neutral beam modulators were used as the basis for this equipment. Each was updated, using improved fiber optics, faster electronic circuitry, and a fault blanking circuit on the high voltage deck.

TFTR DIAGNOSTICS SECTION

A survey made of TFTR data handling requirements provided information to generate preliminary estimates of local memory, sample rates, and types of digital conversion modules. The objective is to provide a few standard modules to cover all diagnostic data requirements and thus simplify procurement, servicing, and spares provisioning.

Two design reviews were held on the conceptual design of the diagnostic neutral beam system. The mechanical design of the beamline was well under way by the Vacuum Systems Section of the FOM (Fabrication, Operations, Maintenance) Division. This Division will manage detailed design and fabrication of the beamlines as an in-house effort. Procurement documents for bids on the source were being generated in September.

Purchase of the beam power supply has been deferred indefinitely. It was agreed that a spare heating beam supply could be used for the diagnostic beam to effect at least an interim cost reduction. Possible technical problems with this approach were under study by the Neutral Beam Power Section. This Section is to be responsible for the management and coordination of engineering work on the diagnostic beam project.

A system level review of the charge exchange analyzer requirements was completed. Various electronic approaches were evaluated for performance and cost effectiveness. An electronic pulse counting technique for each channel appears to be the best choice in this application. A detailed cost estimate and program plan was produced using this approach.

As an aid in the charge exchange vacuum system design, the PPPL computer group converted a Grumman-developed vacuum code for use on PPPL computers. Another code was developed specifically for the magnetic design by the Field Design Section of the FOM Division.

The grounding study was completed and formally documented. Detailed recommendations were made to control the design of the cable raceways and installation of the diagnostics.

Machine Design and Fabrication

The Machine Design and Fabrication Division is an engineering activity responsible for design and fabrication of experimental devices at PPL. This work is in direct support of the Research Department.

Resources of the MD&F Division are divided among six sections. A general description of each section's activities is given below together with details of specific accomplishments during the report period.

In the last month of FY79 the MD&F Division was reorganized into the Fabrication, Operations and Maintenance Division. The primary design function of MD&F was transferred to the Advanced Projects Design and Analysis Division. The next annual report will reflect this change in responsibilities.

MAJOR ACTIVITIES

Division Administration

Administrative matters for the MD&F Division are handled in this section. Included are budgetary and personnel issues as well as technical supervision of the Division's work.

A PERT-type computer system is used for planning and management. Cost and schedule data are run for all the Division's work, and resources versus time are generated in tabular and graphic form. Cost and schedule progress is monitored with these data.

Time reports and other personnel records are kept in this section. In addition, maintenance and trouble reports as well as spare parts authorization and spare parts inventory replacement approval are also a function of this section.

Under the reorganization noted above, the FOM Division has five branches, Administrative, Coil, Vacuum and Cryogenics, Installation and Maintenance, and Energy Systems. There are also 18 sections. The major personnel changes are in the Field Design Group and Mechanical Drafting Group which were transferred to APDAD.

Coil Design and Fabrication Section

During the first quarter of the year a major portion of the Section's effort was in support of the successful power test program carried out on the PDX device.

During the balance of the year the major activity was the preparation of the shop and necessary tooling required to fabricate the large coils for the TFTR device.

The former "meson" area, located at PPA and adjacent to our present shop, was cleaned out and set up to perform initial operations on the copper conductors. Arrival of the first shipment of 55-foot copper bars is shown in Fig. 58. The bars

Figure 58. Receiving first bars for Large Coil Program.

Figure 59. Copper inspection bench—Large Coil Program.

Figure 60. 5-Head automatic taping machine—Large Coil Program.

are inspected (Fiq. 59), cleaned sandblasted, primed and taped (Fig. 60). The conductors are then moved into our main shop. Here the "small" winder (Fig. 61) will wind coils to 18 and 20-ft diameters, and the large winder (Fig. 62) will find coils to 28 to 32-ft diameters, weighing up to 12 tons. Two tension lines are set up to feed these winders, and each has the required equipment to cut off conductors (Fig. 63), braze (Fig. 64) and blast clean (Fig. 65) as one length of copper is added to the next. The total shop is shown in Fig. 66. An electrical test facility (Figs. 67 and 68) was set up to provide the capability of dc and ac hi-pot and impulse testing of the coils to maximum levels of 300 kV.

Other tasks performed included:

- Fabrication of replacement coils for the resistor breakers in the MG room.
- PDX bus changes and maintenance activities.
- Four neutral beam bending magnet assemblies were completed (See Annual Report for FY78.).
- Fabrication of test samples for the TFTR Program.
- Fabrication of a "thermal image" for the PDX TF system.

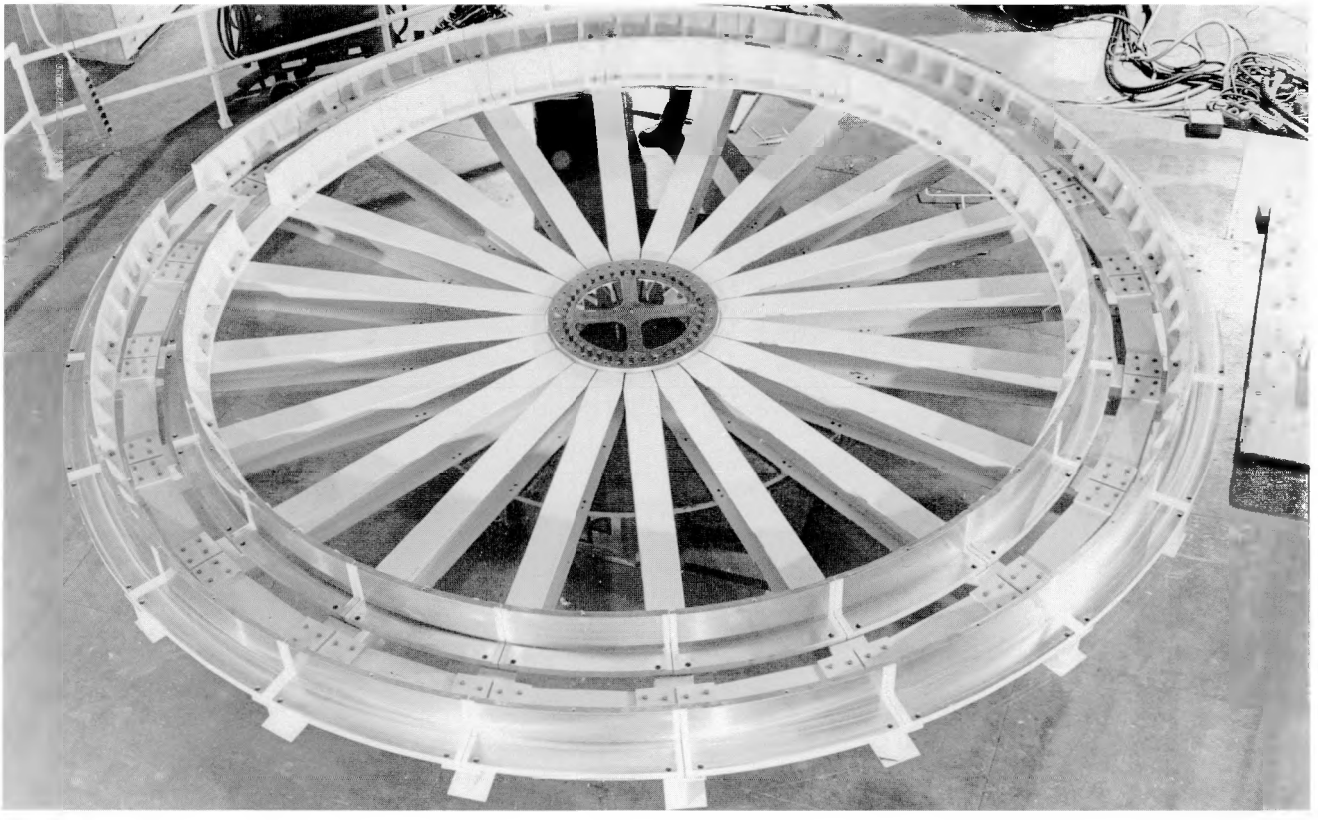

Figure 61. "Small" winding station—Large Coil Program.

Figure 62. Large winding station—Large Coil Program.

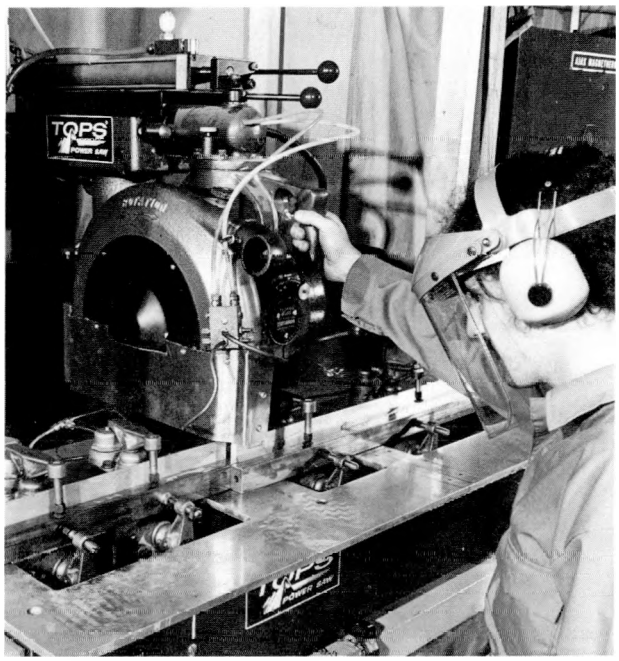

Figure 63. In-line cut-off saw—Large Coil Program.

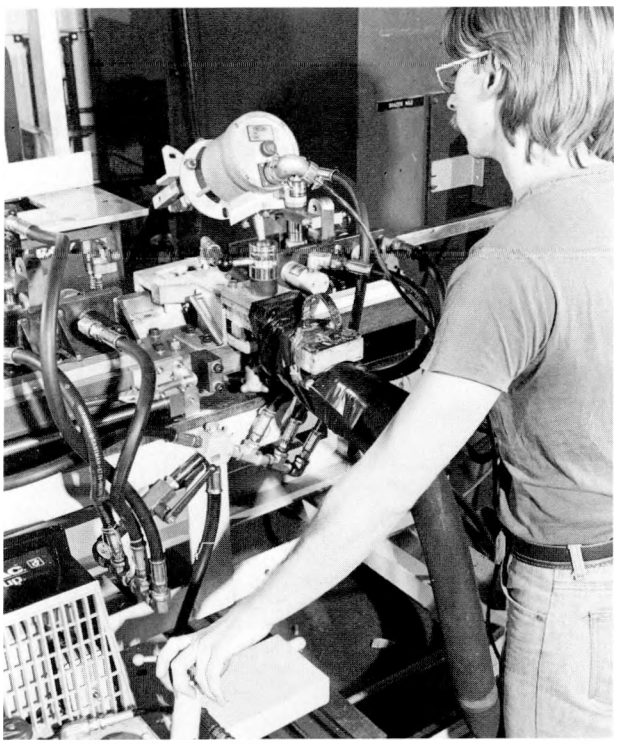

Figure 64. In-line induction brazing station—Large Coil Program.

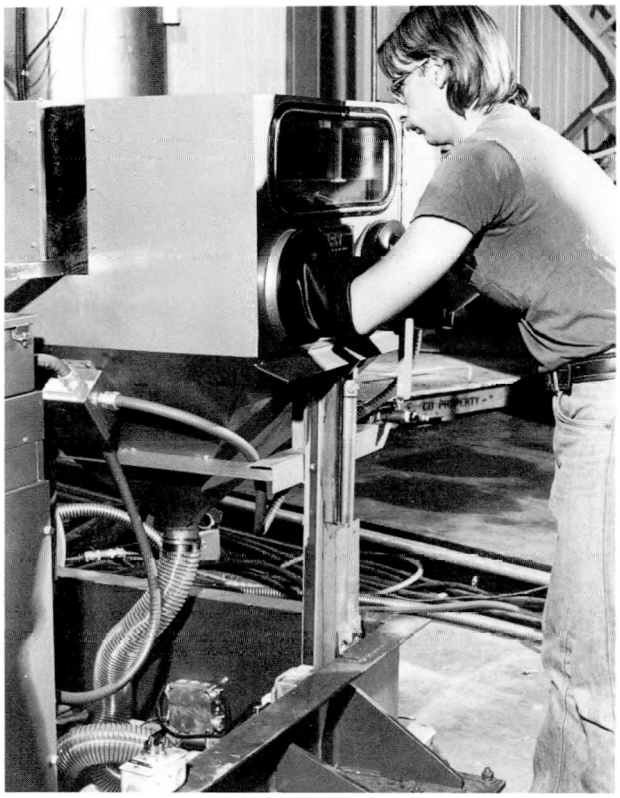

Figure 65. In-line sand blast station—Large Coil Program.

- Engineering support of the PLT stellarator design proposal.
- Engineering support of the Spheromak design proposal.

Engineering Services Section

This Section provides tradesmen for the various experimental activities at PPL. In addition, operators and maintenance people are assigned to operate the large MG sets. Trades available include carpenters, electricians, metalsmiths, plumbers, welders, millwrights, and general technician service.

Roughly the first half of FY79 was spent in final assembly and early operation of PDX. After initial start-up, Engineering Services support was available to remedy the many little problems associated with a new machine. Following this first run period, a substantial effort was again applied by Engineering Services to modify plumbing and structural aspects to accommodate the

full divertor operation mode. This work continued to the end of the fiscal year.

Work on TFTR projects increased substantially during FY79. The primary deionized water system for that machine was pre-assembled in the shop. It is now ready for final installation at the site.

A major support effort was also expended in set-up of the Coil Shop facility for fabrication of the TFTR large PF coils. That production line is now complete.

Support continued during the fiscal year for the TFTR Mockup effort. Work was done on the M-1, M-2, and M-3 mockups in the 1-H building area. This is an ongoing activity that will be continued next year.

MG operators provided their services for three shifts during a majority of this period.

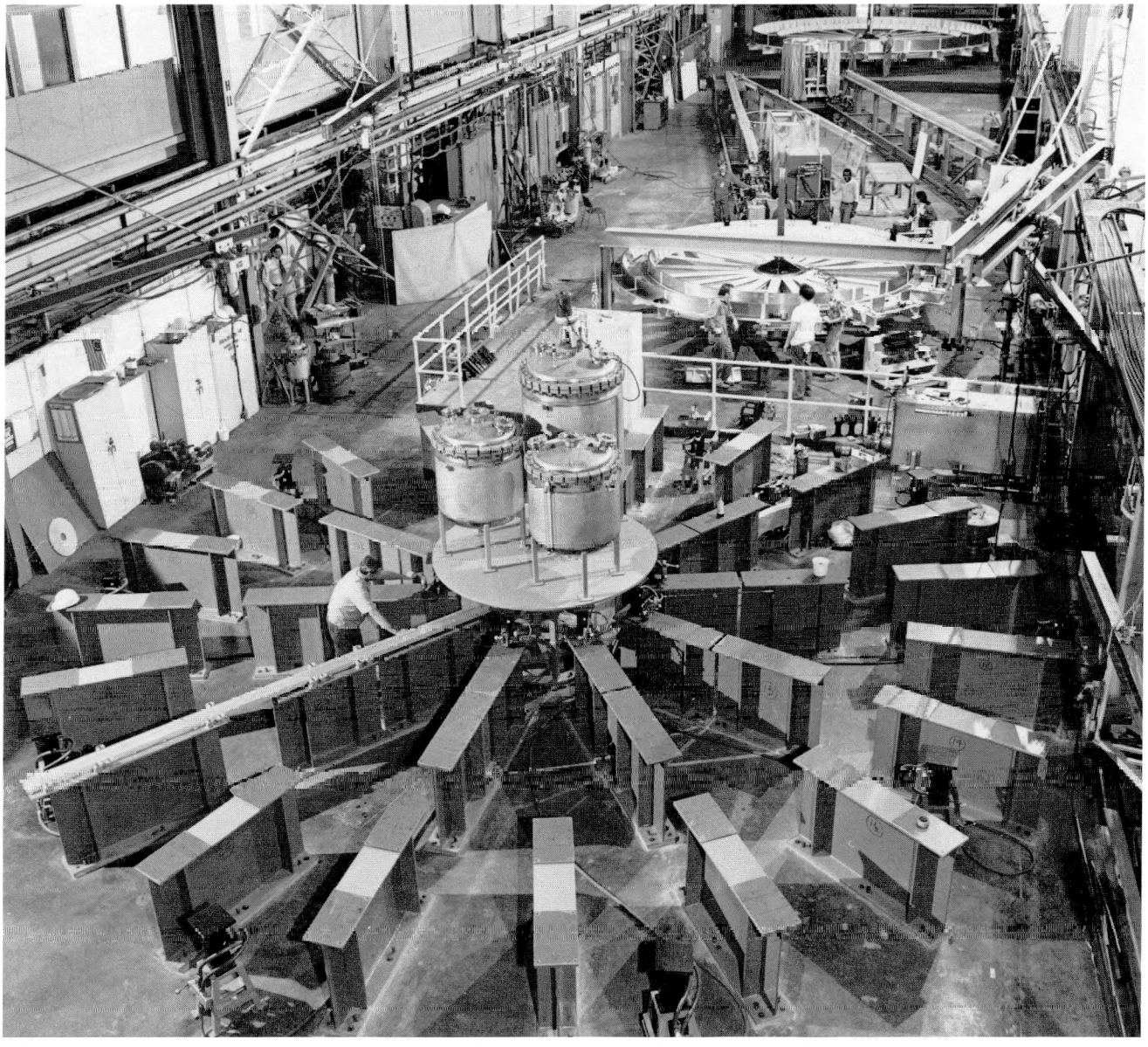

Figure 66. View of main shop—Large Coil Program.

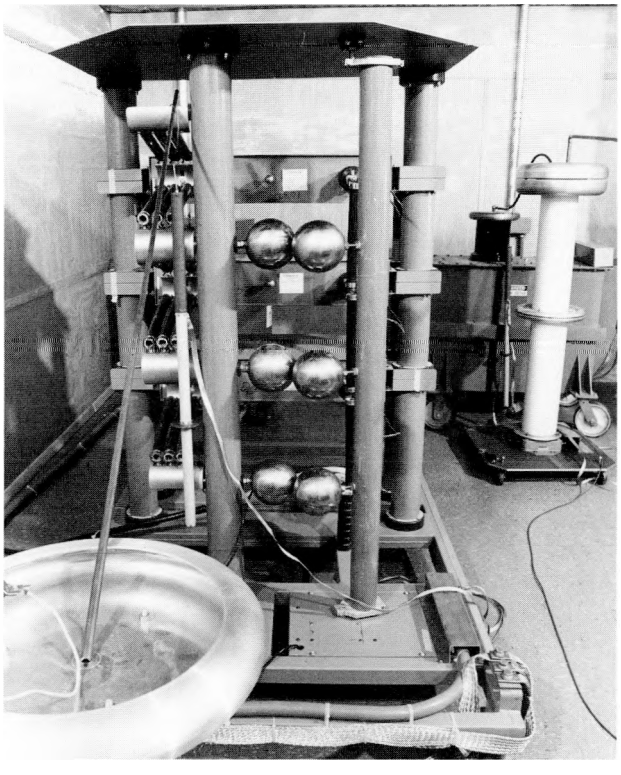

Figure 67. Coil Shop Electrical Test Facility—300 kV impulse tester and 100 kV corona detector.

Field Design Section

The following tasks were accomplished during the report period.

- The magnetic field analysis for the PLT stellarator scoping study was completed.
- A program was written to calculate the magnetics of a twisted TF stellarator.
- A three-dimensional iron code for the TFTR charge exchange analyzer was developed.
- Continued support was given to the TRTR Diagnostics Group by supplying additional eddy current calculations.
- Additional work was done for the Grumman force study on the PDX TF coils.
- PDX Upgrade (STRETCH) studies were continued into FY79. Current and voltage profiles were computed for application to a revised power supply system.
- INTOR studies produced shaping field, ohmic heating, and poloidal divertor coil parameters, etc. TF coil studies followed.
- Several PDX voltage suppression schemes were provided for the purpose of optimizing the method of reducing voltages across the PDX vacuum vessel break.
- Circuit models were devised to try to understand the low resistance conditions in the PLT TF system.

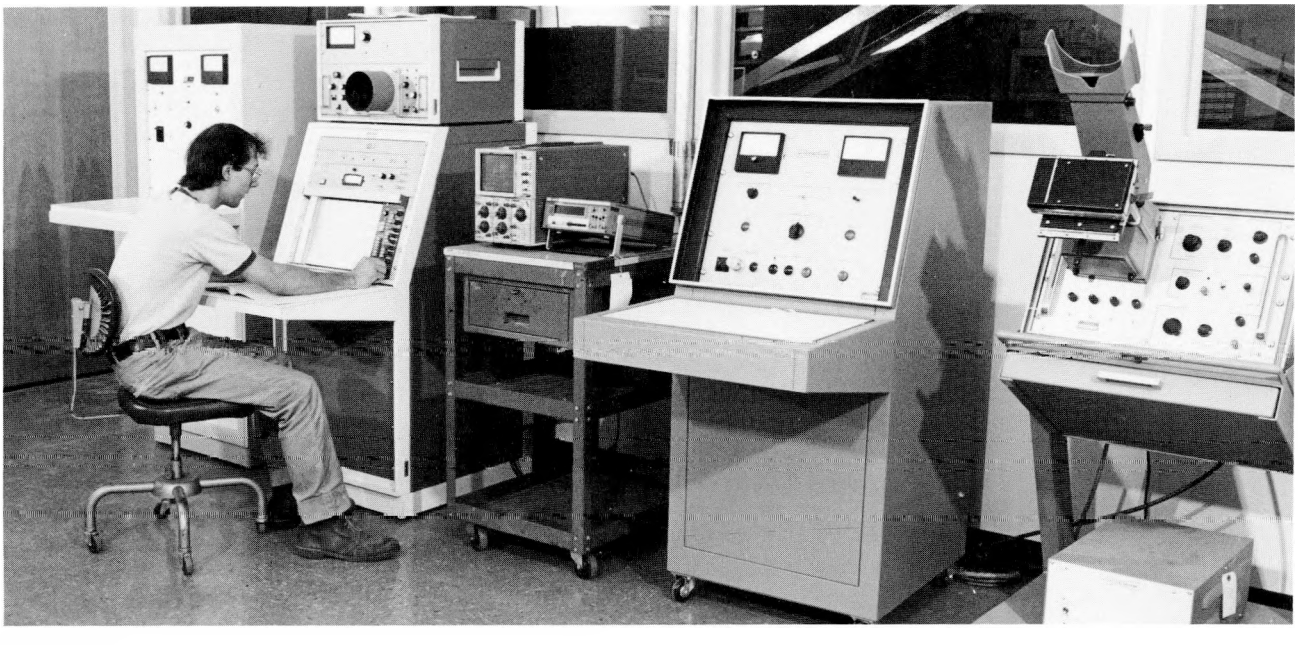

Figure 68. Coil Shop high voltage test facility—control room.

Structural Design and Fabrication Section

This Section was responsible for the following accomplishments during FY79.

PDX

The assembly and power testing of the PDX device continued as one of the major efforts of the section during the early months of the fiscal year. The final stages of the assembly included the completion of the center column assembly and conclusion of bus work and the water cooling systems. A first plasma was achieved during the power tests on November 29, 1978; however assembly tests continued into January 1979 in parallel with power tests.

MATERIALS TEST LABORATORY

Prior to and during the PDX power tests, the Materials Test Laboratory provided instrumentation, installation, setup, and calibration services together with the operation of the data acquisition system. After the power tests reduction and analysis of the data were performed and a comprehensive report was prepared.

In collaboration with the Electronics Section, a CAMAC compatible data acquisition and instrumentation protection system was designed, fabricated, and installed on PDX.

The PLT 3-Coil Test was instrumented and operated at full design load and current.

A number of routine tests (tension, compression, shear and metallographic) were performed, and fixtures and instrumentation for special purpose tests were developed.

STRUCTURAL DESIGN FINITE ELEMENTS METHODS

Finite Element Methods (FEM) were utilized in the following stress analysis studies.

- PLT Stellarator Scoping Study, completion or extended FEM model and study of stress on TF coil #4.
- TFTR PF coil analysis and torque tube teeth analysis.
- PDX liaison with Grumman Aerospace Corporation on the FEM study of the PDX machine completed during FY79.
- TEXTOR vacuum vessel analysis completed (device to be fabricated at Jülich, West Germany)
- SLPX sub-structuring analysis completed (proposed Superconducting Long-Pulse Experiment).

PLT - STELLARATOR SCOPING STUDY

The structural design of the helical coil support system for the proposed PLT-Stellarator was completed. Finite element methods were used in investigating a number of design alternatives and configurations. This work was completed in August 1979. A more detailed report can be found in PPPL-TM-328.

TFTR REMOTE MAINTENANCE

Engineering support for the development of remote maintenance equipment and techniques for TFTR continues. A crew of technicians fabricated tooling to remove the lower oval port flange from the vacuum vessel. Work continued on remote handling and initial assembly of the shear panels. A model of the vacuum pump duct including insulation was fabricated and used in removal rehearsals.

DESIGN SUPPORT FOR TFTR NEUTRAL BEAM

The fabrication of the four neutral beam support systems is 75% complete and on schedule. The first of the four units was received in September 1979. The neutral beam calorimeter prototype design was reviewed and updated. The drawings for the production units have been completed. The fabrication of the calorimeters is underway. The design of the neutral beam duct support system has been completed and fabrication drawings released. Fabrication of the four duct support systems will take place at PPL.

Vacuum Design and Fabrication Section

The Vacuum Section continued in its responsibility for the design, fabrication, and installation of vacuum and cryogenic systems. It also remains responsible for initial startup and checkout of

such systems. General support for maintaining and upgrading operating laboratory systems is also provided.

An engineering staff does design work, and a group of approximately 30 technicians fabricate and install vacuum system components. A well equipped shop including facilities for machining and welding provides fabrication and maintenance capabilities.

ACCOMPLISHMENTS

- PDX Fabrication and assembly of divertor parts for diverted plasma operation was completed. Operation of titanium evaporators and cryogenic panels reduced the background pressure in the vacuum vessel to 4×10^{-8} torr.
- PLT Support was provided for gas injection and gas purification.
- TFTR A high throughput gas injection valve was developed and tested. A facility was established for assembly of the TFTR neutral beam system. Consulting on cryogenic and vacuum problems continued.

Advanced Projects Design and Analysis Division

The Advanced Projects Design and Analysis Division was formed in August 1979 as a more effective organization for providing engineering support to advanced concepts for magnetic confinement type fusion machines. Although continuing to provide technical support to TFTR as a top priority, the Division has been actively involved in conceptual studies of advanced projects.

Work was in progress supporting Tokamak Flexibility Modification (TFM) for TFTR improvements, the electrical systems branch of the Engineering Test Facility (ETF) Design Center at Oak Ridge, and the INTOR Poloidal Divertor Studies.

Other activities included the preparation of a proposal to design and build the S-1 Spheromak, a modest-sized device intended to demonstrate formation of up to 500 kA spheromak plasma configurations on a 100-μsec time scale.

Design Studies for New Devices

During FY78, PPPL began to participate actively in the national reactor design effort in support of the Engineering Test Facility (ETF). An approach very similar to the ETF has been taken by the International Tokamak Reactor (INTOR) study group in preparing plans for an experimental tokamak reactor under the auspices of the International Atomic Energy Agency (IAEA). PPPL members have also been active in the INTOR design group, and have organized the supporting physics effort in the U.S. fusion community.

In view of the favorable prospects for implementation of a tokamak ETF/INTOR reactor facility, further design work on a short-pulse ignition experiment at PPPL [the Princeton Ignition Test Reactor (PITR)] has been held in abeyance. Design studies on a long-pulse superconducting hydrogen device will proceed in parallel with the ETF/INTOR effort, with a view to developing advanced tokamak design features, to improve the attractiveness of a future commercial tokamak reactor.

In the area of advanced concepts, PPPL has undertaken fabrication of the S-1 Spheromak, which basically resembles a tokamak but does away with the need for external toroidal field coils.

MAJOR ACTIVITIES

ETF/INTOR Studies

Studies of the requirements of reaching ignition in ETF/INTOR have been carried out at PPPL using transport codes that model the particle and energy balance in a tokamak. The plasma performance specifications have been that the burn should last at least 100 seconds, at a plasma pressure high enough to provide a neutron wall loading of at least 1.3 MW/m^2. Some results of computations employing an empirical model for electron thermal transport are shown in Fig. 69, for the case where a pure D-T plasma is heated to ignition by 150-200 keV deuterium beams injected nearly perpendicular to the main magnetic field. The physics aspects of ETF/INTOR are more fully discussed below in the section on Theory.

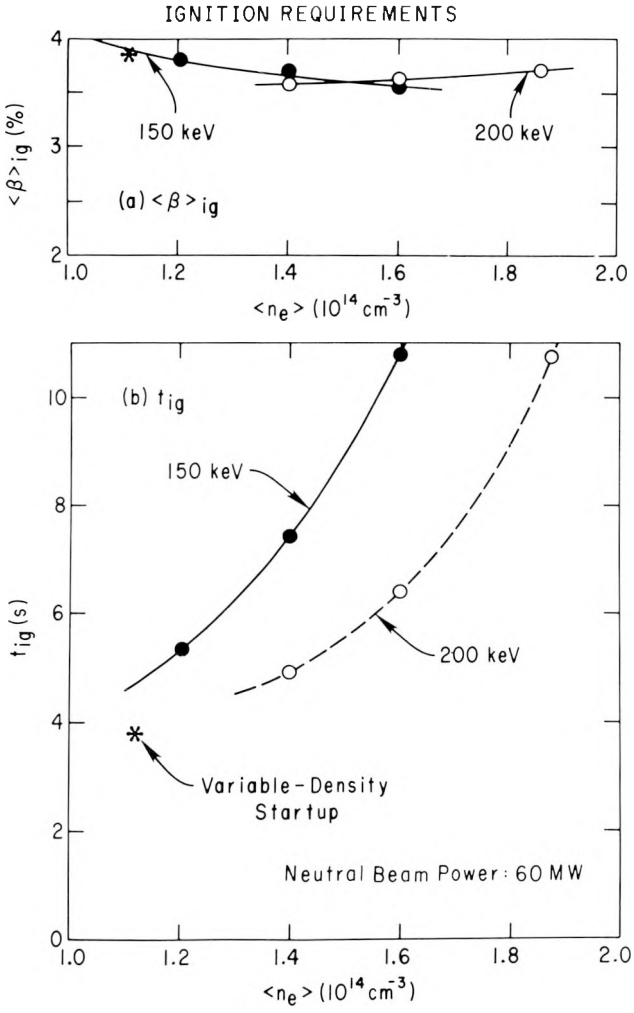

Figure 69. Computation of required ignition temperature and beta for ETF/INTOR in the case of 150-200 keV deuterium injection nearly perpendicular to the main field.

On the engineering side, PPPL has assumed responsibility for the electrical-system design of the ETF, and has moved personnel to ORNL to accomplish this task, including the supervision of industrial engineers at ORNL. The Design and Analysis Division directly supports this effort and a number of other activities, on assignment from ETF. In addition, the TFTR Division personnel, along with members of the Ebasco/Grumman TFTR industrial partnership, played key roles in the assessment of R & D needs for ETF/INTOR.

The S-1 Spheromak

The spheromak concept envisages a toroidal plasma with interior toroidal and poloidal fields, which is confined by purely poloidal external fields, based on a simple set of axisymmetric coils, as in a mirror machine. The stability of such a configuration was investigated theoretically at PPPL during FY78, and was found to be promising. Initial experimental results at the University of Maryland have tended to support our theoretical expectations.

In early FY80, PPPL proposed and received approval for the fabrication of the S-1 device (Fig. 70) which is intended to produce spheromak plasmas of sufficient size and lifetime so that questions of fine-scale stability and energy-confinement can be addressed. The plasma-formation technique of the S-1 (Figs. 71 and 72) is designed to avoid all dynamic (fast-time-scale) phenomena, so as to permit future scale-up to moderate-voltage power supplies in reactor size.

An initial poloidal field is generated by a winding inside a ring-shaped insulating shell. This field is weakened on the small-major-radius side of the ring by superposition of an externally generated vertical field.

The ring also contains a toroidal solenoid. When this solenoid is energized, it induces a poloidal current in a sleeve-shaped plasma which is formed at this time surrounding the ring. The toroidal field associated with this poloidal plasma current distends the poloidal field, stretching it in the direction of the central axis. Meanwhile, the decay of current in the poloidal field winding induces a toroidal plasma current.

Next, the pinch coils are energized, producing a separated spheromak configuration and further increasing the toroidal plasma current.

The S-1 is scheduled for initial experimentation operation in FY82. Meanwhile extensive computational studies are continuing, and small-scale models will be tested experimentally.

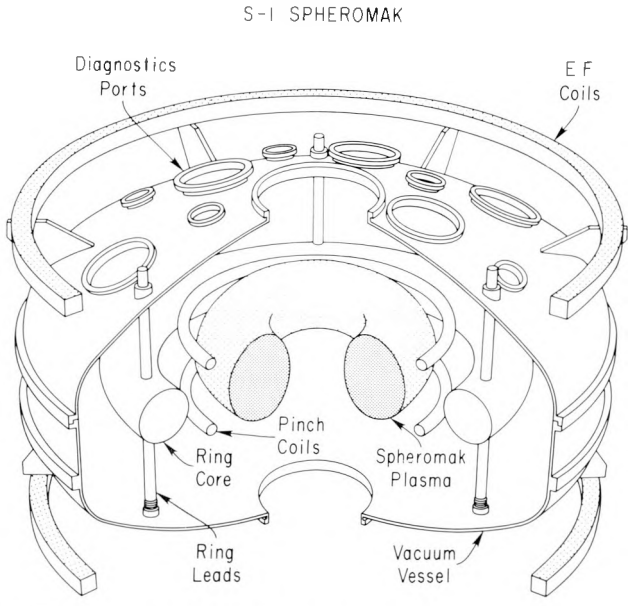

Figure 70. The S-1 Spheromak.

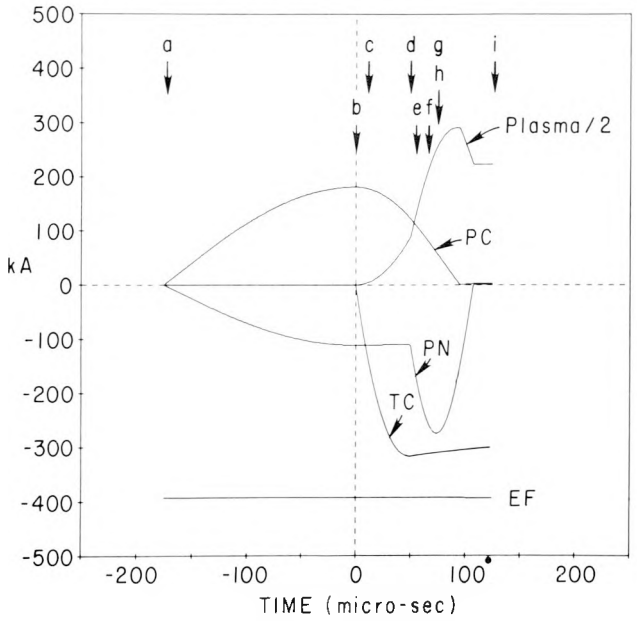

Figure 71. Time variation of the currents in the plasma and in the EF, TC, PN, and PC coils based on calculations of the circuit model.

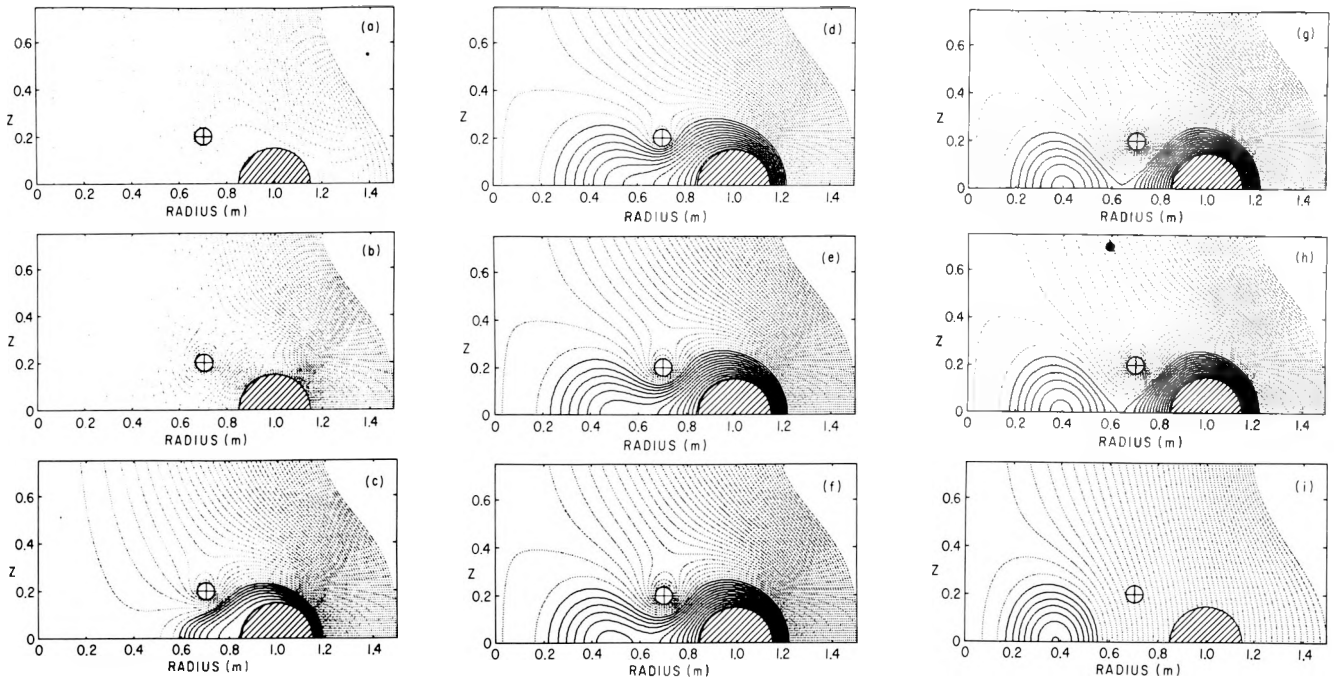

Figure 72. Evolution of Spheromak magnetic configuration.

Theory

The research of the Theoretical Division encompasses a wide range from fundamental work in continuum physics to design studies for tokamak reactors and applications to astrophysical plasmas. The Plasma Physics Laboratory is fortunate to have a large enough theoretical group to address these issues in a meaningful way, leading to immediate cross-fertilization between basic scientific investigations and applications.

MAJOR ACTIVITIES

Summary

This section describes some of the research highlights of FY79.

Both experiments and linear stability theory have shown that fine-scale turbulence will develop in tokamak and other toroidal magnetic confinement devices. Hence it has been a continuing goal of theoretical fusion research to understand in a quantitative manner how this turbulence affects confinement. Theoretical methods to deal with turbulent states were first developed in fluid mechanics. An important part of our research program consists of modifying a key approximation scheme of fluid mechanics—the direct interaction approximation—to address the more complicated problems of plasma turbulence.

Advances in computers and computational techniques now permit direct simulations of plasma turbulence which serve as "computational experiments" to both validate and guide our analytic efforts. The Theory Division has devoted a significant effort to improving the sophistication and accuracy of these computer experiments.

Although linear stability analyses have long been a major object of theoretical plasma investigation, new and significant understanding regarding the effects of toroidal geometry on drift waves and ballooning modes was achieved in 1979. Drift waves, which are thought to provide the anomalous heat conduction in low-β tokamaks, are always observed experimentally. We now understand how toroidal geometry effects negate the magnetic shear stabilization of these modes predicted by simplified slab-geometry analyses. Ballooning modes had been expected to occur in tokamaks as the plasma pressure increased, but analytic work in simplified geometrics predicted that these modes would become stabilized as the plasma pressure was raised still higher. Numerical work with realistic equilibrium states supported this prediction.

The presence of stochastic magnetic fields (small scale magnetic field fluctuations which destroy the magnetic surfaces) is expected to alter the large-scale stability properties of plasmas. A first attempt to model the effect of small scale fluctuations via an enhanced electron viscosity on the well-known tearing mode shows that micromagnetic turbulence leads to an even stronger instability. Evidentally the interplay between small- and large-scale instabilities must become an important topic in fusion research.

Applications—both fusion and astrophysical—are essential elements in the Theoretical Division program. These examples are given: trapping of cosmic rays, the modeling of an edge region of a tokamak, and the physics aspects of reactor design as identified by the International Atomic Energy Agency INTOR reactor study project.

Toward a Systematic, Quantitative, Analytic Theory of Turbulence

We are developing an analytic theory of microturbulence which has the following important characteristics: (1) it is *systematic* — i.e., neglected terms are small in some parameter; (2) it is *quantitative* — i.e., it can accurately predict numerical coefficients.

A formalism which satisfies criteria (1) and (2) is the Direct Interaction Approximation (DIA). The DIA emerges as the lowest order expansion in the skewness parameter, or degree of non-Gaussianity. The skewness is generally less than 1; it is very small in the limit of short autocorrelation time and when correlated structures can be neglected. The DIA is exact for certain model problems. It reduces correctly to weak turbulence theory, conserves energy, and handles in a reasonable fashion the wavelength dependence of the diffusion coefficient. Our program is to explore, both analytically and numerically, the consequences of the DIA for the nonlinear theories of drift and tearing instabilities.

As a first application, we have re-examined the Dupree-Tetreault prediction for the rate at which resonance broadening on the ions damps drift waves. We find this rate to be incorrect. We can show that the nonlinear growth rate is the renormalized version of induced scattering and that energy flows to long wavelengths. These results imply the existence of a strong mode-coupling process which seems to be generally ignored.

Presently, we are deriving the nonlinear dispersion relation for drift waves in sheared geometry, including the correct wavelength dependence of D in an energetically consistent fashion. This study should give the first consistent predictions for the nonlinear stability of drift waves.

Particle Simulations of Low-Frequency Microinstabilities in a Sheared Slab

Using 2-1/2-D particle simulation codes, we have carried out the investigation on (1) ion-temperature-gradient-driven modes and (2) shear Alfvén and drift-Alfvén modes for a collisionless plasma in a sheared slab geometry. The primary objective of the investigation is to test the existing linear theories and to study the associated anomalous transport.

Ion-temperature-gradient-driven instabilities have been investigated using an electrostatic code. Since the thermal fluctuations associated with the electron motion may destroy the coherence of the weak ion drift waves, we have incorporated into the code the Debye shielding effects which are induced by the adiabatic electrons in response to the ion density fluctuations. The measured frequency, growth rate, and mode structure for the linear stage of the instability are found to agree well with the predictions from a linear theory which takes into account the detailed kinetic response of the ions. During the nonlinear phase, large ion energy transport caused by the unstable modes has been observed which is primarily responsible for the nonlinear saturation. For a system where only marginally stable modes exist, we have also observed enhanced fluctuations with frequencies and spatial structures which match closely the theoretical values. We believe that they are caused by the re-distribution of the equilibrium fluctuation energy due to the presence of the eigenmodes. In addition, we have detected oscillations corresponding to the highly damped eigenmodes of the electron drift branch.

Shear Alfvén and drift-Alfvén eigenmodes have been studied using a finite-β, 2-1/2-D particle code based on the Darwin model. The code makes use of guiding center electrons while pushing the ions exactly. The sheared magnetic field is produced by the self-consistent electron current. According to the linear stability theory, weakly damped eigenmodes exist in a sheared slab. The modes are localized near the rational surface due to finite Larmor radius effects as well as ion Landau damping. As the plasma β increases, they are found to be less stable. Simulation results have confirmed the presence of these eigenmodes in terms of the measured frequencies and mode structures. Furthermore, enhanced fluctuations associated with the eigenmodes have also been observed. Again, they are the result of the re-distribution of equilibrium fluctuation energy due to the presence of the eigenmodes. Consequently, a second-order y-dependent eddy current has been induced, which widens the shear-free region near the rational surface and causes the formation of magnetic islands, resulting in large electron energy transport.

Unstable Drift Waves in Toroidal Plasmas

In slab geometry, both the collisionless and collisional electrostatic drift eigenmodes are found to be shear stabilized. The shear damping of drift waves is associated with the anti-well structure (Figure 73(A)) in which energy convects away from the mode rational surface. However, the mode rational surfaces are closely packed for drift waves. Due to toroidal coupling effects, such as ion magnetic curvature drifts, the eigenmodes of each poloidal harmonic are affected by the wave energy which is convected away from the neighboring mode rational surfaces. Recently, we have studied the shear damping effects for two-dimensional drift wave eigenmodes in a toroidal plasma using the ballooning -mode formalism. We have found that two types of eigenmode exist. One is the slab-like branch which represents the extension of the Pearlstein

-Berk slab eigenmodes. The other type of eigenmode is the toroidicity-induced branch which has no counterpart in slab geometry. It is characterized by potential structures with local potential wells as shown in Figures 73(b) and (c), which inhibit convection of wave energy, and experience negligible shear damping through tunneling leakages. These two branches may exist simultaneously. Employing the ballooning mode formalism, we have performed analytical as well as numerical studies on the two-dimensional collisional (resistive) and collisionless (universal) drift instabilities which are directly related to the new toroidicity-induced eigenmodes. Figure 74 shows the results. These results clearly demonstrate that, while in slab geometry, the eigenmodes are always stable, the two-dimensional toroidicity-induced eigenmodes become unstable for $\hat{s} < 1.2$, and the slab-like eigenmode experiences enhanced damping due to finite toroidicity compared with the slab results. The agreement between the analytical theory and the numerical results for the toroidicity-induced eigenmode is reasonably good.

Finally, we remark that the existence of the toroidicity induced eigenmodes clearly indicates that, contrary to conventional thinking, toroidal coupling effects cannot be simply regarded as perturbations to the slab eigenmode branch.

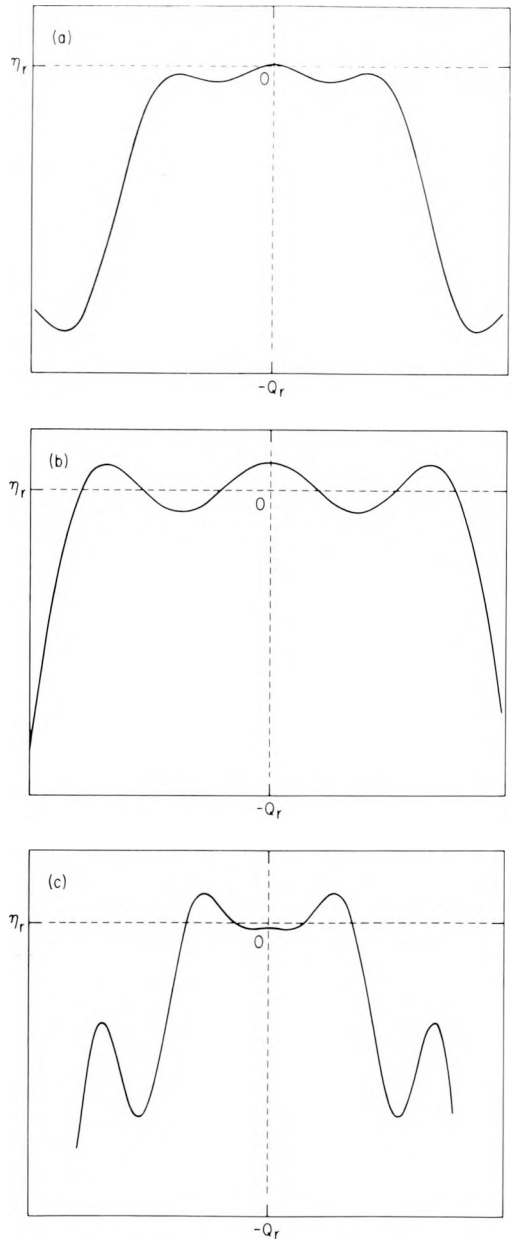

Figure 73. Typical potential structures $Q(\eta)$ for (a) the slablike, (b) weak, and (c) strong toroidicity induced eigenmodes.

High-β Stabilization of Ballooning Modes

Previous work has shown the beta in tokamaks to be limited to a critical value, of order β

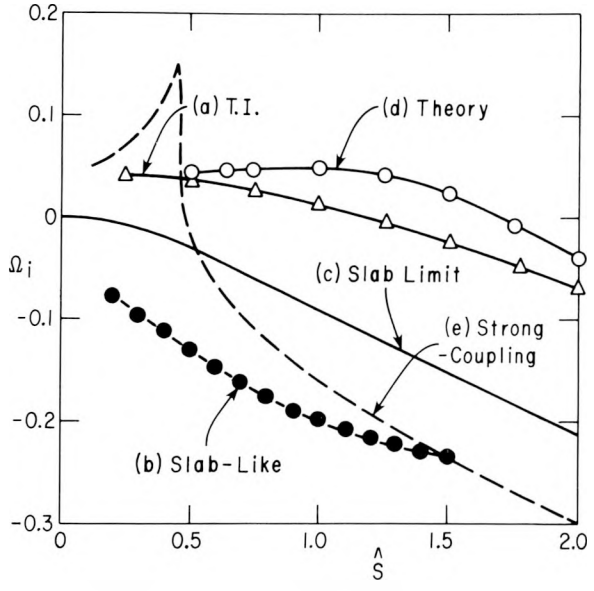

Figure 74. Plot of growth rate Ω_i (ω_i/ω_{*e}) versus shear $\hat{s}$.

$\sim a/Rq^2$. Above this critical value, one finds the onset of pressure-driven ballooning modes. Recently, however, it has been conjectured by several authors that, if beta were increased above this critical limit, a second region of stability could be found. These conjectures were based on a local analysis of ballooning modes in the vicinity of the magnetic axis, using model equilibria. We have confirmed this conjecture by using numerical techniques and have shown further that a second region of stability is found for all surfaces, not just those near the magnetic axis. Therefore, global stability is possible. We have also found that these high β equilibria with circular outer cross section are stable against internal kinks with q(0) down to at least 0.75. Representative results are shown in Fig. 75 for high toroidal mode numbers n.

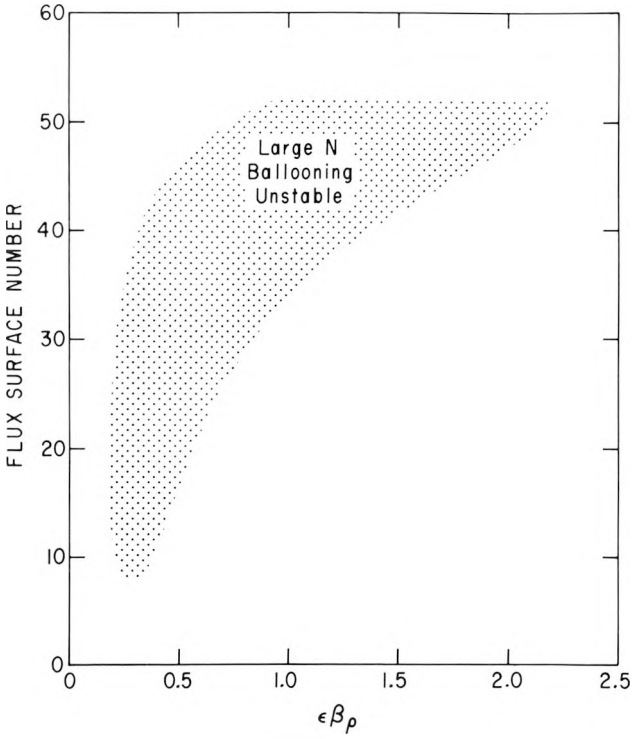

Figure 75. Flux surface stability vs. volume average beta for PLT parameters.

There are two questions that might be asked about these high β equilibria. First, are they stable to free surface kink modes and to nonideal modes? Secondly, how does one access these high β equilibria? Because of the large parameter space, we have not yet succeeded in giving a general answer to these questions. Results thus far, however, indicate that these high β equilibria are unstable to free surface kink modes but can be stabilized by a wall at a reasonable distance from the plasma. In addition, these equilibria are unstable to resistive modes. Defining accessibility to be the maintenance of stability to fixed boundary modes as one proceeds from low β to high β equilibria, we have not been able to find an accessible path from low β to high β for circular cross-section tokamaks except by going to very low values of shear (which is not desirable from the point of view of kink mode stability). However, accessibility has been achieved for D-shaped cross sections with reasonable values of shear.

Tearing Modes in a Plasma with Magnetic Braidings

Classical tokamak confinement calculations are based on the existence of magnetic surfaces almost everywhere. The experimentally observed enhanced electron thermal transport has led to speculation that the underlying process may be a breakup of the magnetic surfaces on a microscopic spatial scale. Even small radial perturbations in the magnetic field can have a large effect because of the enormous electron mobility parallel to the field lines. Electron excursions in the radial direction could then be principally the result of their co-wandering with the field lines. Recently, theoreticians have investigated this speculation from two complementary points of view. One approach has been to prescribe the statistical properties of the magnetic field and calculate the associated diffusion of test particles. The other has concentrated on determining the fluctuating magnetic field associated with some microinstability of the drift-Alfvén type. Self-consistent calculations await future fundamental theoretical advances.

We have investigated the additional effects that stochastic braiding of field lines may be expected to have on non-ideal, macroscopic tearing modes—modes which have been associated with minor and major disruptions in tokamak discharges. The basic idea is that there is an anomalous transport of parallel electron momentum in addition to the anomalous particle and energy transport. We have modeled this effect through the introduction of an anomalous elec-

tron viscosity. Estimates of the anomalous viscosity consistent with the observed enhanced thermal diffusion rate indicate that the viscosity has a much larger effect than does the (observed) classical resistivity in the Ohm's law for narrow current channels ($\lesssim$ a few cm wide). Such sharply peaked current profiles are intrinsic to linear and early nonlinear stages of the development of tearing modes.

The complexity of analysis depends strongly on whether or not the rate of change of magnetic flux in the narrow tearing layer, linearly or nonlinearly, is comparable to or much less than the rate of current diffusion across the layer. The first situation prevails for modes with azimuthal mode numbers m = 1, whereas the second obtains for m $\geqslant$ 2.

For the m = 1 mode, we have calculated the linear growth rate of the kink-tearing mode with viscosity the non-ideal effect. Dimensional analysis yields large growth rates. For m $\geqslant$ 2 modes, we have recovered previous analytical results for the linear growth rate and have extended the analysis to the quasilinear regime. This nonlinear calculation of the time evolution of the magnetic island width $w(\tau)$ shows that viscosity accelerates growth until the island reaches a thickness at which the resistive and viscous current diffusion rates are comparable. For current experimental parameters on PLT, this width is a few centimeters. Subsequent growth occurs at the slower rate governed by resistivity. The net result is that viscosity results in an "impulsive" increase in island width Δw compared to the width $w(\tau)$ calculated for negligible viscosity. The variation of this incremental width with viscosity is shown in Fig. 76, which results from numerical solutions of the quasilinear equations.

One tempting speculation which could account for the disruptive instability is that there is a sudden onset of a large anomalous electron viscosity during the nonlinear resistive growth of a magnetic island. It is quite likely that, either because of nonlinear couplings or toroidal effects, a large magnetic island might itself generate very stochastic regions of magnetic field, especially close to the separatrix. If Δw is comparable to the minor radius, the disruptive instability may be triggered. This requires $\mu/\chi_e \sim 10^2$, where μ is the anomalous electron viscosity and χ_e is the measured anomalous thermal conductivity for the normal discharge. It is not implausible to speculate that just prior to disruption, μ becomes this large (especially if the large scale magnetic islands are themselves generating stochasticity). We conclude that the sudden onset of electron viscosity is an interesting candidate for an explanation of the disruptive instability.

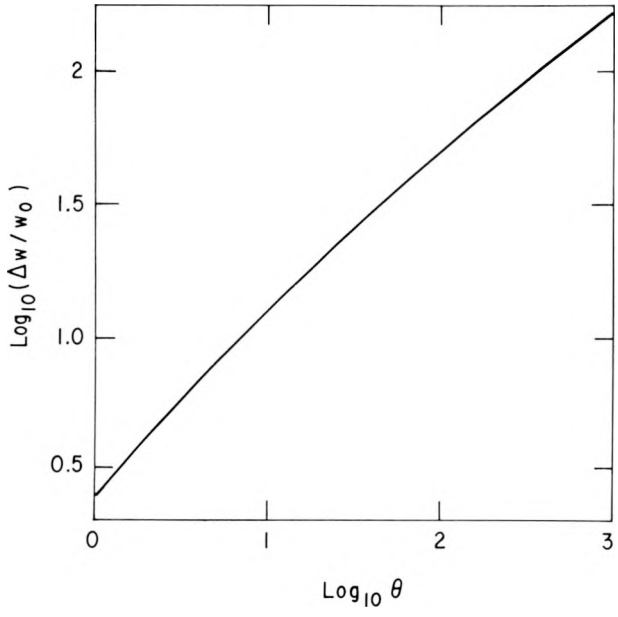

Figure 76. Increase Δw in island width due to viscosity. Here $\theta \equiv 8\,\pi\mu/\eta c^2\, w_o^2$ is the viscous rate of current diffusion across the initial island width w_o relative to the resistive rate.

Trapping of Cosmic Rays *

An astrophysical problem which involves considerable plasma physics concerns the origin of cosmic rays. For years a popular theory has been that they originate in the supernova explosion. But the supernova shock heats the ambient interstellar material originally surrounding the point at which the supernova occurs. This creates a rapidly expanding bubble of gas whose velocity of expansion is of order 10^4 km/s. The cosmic rays must penetrate through this bubble without too much loss of energy if the supernova origin theory is tenable.

Now the bubble is threaded with a roughly uniform field, strong enough that the gyration

*Supported by AFOSR Contract No. PR80-00656

radii of the cosmic rays are very small compared to the bubble size. Thus, it becomes impossible for the individual cosmic rays to cross this field. Each cosmic ray could individually stream along the field and escape, but, when considered collectively, they produce an instability in hydromagnetic waves. Further, the growth time of this instability is extremely short compared to the expansion time of the bubble. The hydromagnetic waves are driven unstable by a Doppler-shifted cyclotron resonance that in turn scatters the cosmic rays in pitch angle. As a result, the cosmic rays are trapped and suffer adiabatic energy losses to the waves. From general principles, the energy of a relativistic particle is proportional to the inverse scale size of the bubble. Since the bubble is observed to expand by a factor of many hundreds, the cosmic rays lose more than 99% of their energy to the waves. The waves themselves transfer their energy to the bubble by a nonlinear Landau damping process thereby accelerating it. Thus, in effect, if the trapping by plasma instabilities is a real process, then the idea that cosmic rays originate in the supernova explosion itself is not tenable.

There is one possible problem with the mechanism of trapping by these instabilities. When the cosmic rays approach pitch angles of nearly 90° they resonate with waves of shorter and shorter wave lengths. Such waves are cyclotron damped on the background plasma and are not unstable. Thus, the quasilinear scattering rate goes to zero, and the cosmic rays can only scatter through this critical pitch-angle region by means of higher-order nonlinear processes akin to trapping by the Alfvén wave. By carrying out an expansion in $\Delta\theta$, the small difference between the pitch angle and 90°, one can reduce the nonlinear problem to a single ordinary differential equation which is integrated numerically to obtain a wave trapping condition. Estimates for the Alfvén wave amplitudes show that they are sufficiently intense to produce the required wave trapping.

1-D Transport Code Modeling of the Limiter/Diverter Region in Tokamaks

Control of impurities is essential in high temperature tokamak experiments and proposed reactor designs. The poloidal divertor reduces the impurity of influx from the vessel wall to the main plasma by channeling incoming impurities into a separate chamber where they are collected by a divertor plate and by lowering the edge temperature of the plasma, which reduces the amount of wall material sputtered by charge exchange neutrals. In steady state the plasma loses some of its energy to the divertor plate and the remainder to the vessel walls by radiation, charge exchange, and a small amount of heat conduction and convection. Estimates of how much power is lost in each of these ways are important for evaluating how well the system protects the walls and for designing the divertor plates to withstand the necessary heat loads. In order to study the power balance in a tokamak with a divertor, we have incorporated a self-consistent model of the divertor (or limiter) region in the BALDUR 1-D transport code. This code has been used to model PDX, PLT, and ALCATOR for Ohmic and neutral beam heated cases.

Numerical results for PDX with 6 MW of deuterium neutral beam heating power into a D^+ plasma are illustrated in the figures. Figure 77 shows typical steady-state density and temperature profiles. The density and temperature decrease sharply near the separatrix with a fall-off distance of $\sim$ 1 cm. As expected from simple estimates, the edge density increases and the edge electron temperature decreases with increasing plasma density. The ion temperature at the edge is in the range 20-40 eV over a wide variation in plasma density. It appears that the edge value of T_i is strongly affected by the temperature of the recycling neutrals as well as by heat losses to the divertor or limiter resulting in a lower ion than electron temperature at the edge. In Fig. 78, we have graphed how the various power loss mechanisms to the divertor and the wall depend upon average plasma density. The losses to the divertor increase with increasing plasma density. Charge exchange becomes proportionately less important, and radiation, more important as $\bar{n}$ increases. At average densities of 2×10^{13} cm^{-3}, which corresponds to maximum plasma ion temperature, the divertor accounts for roughly half the power loss; the other half goes to the wall via charge exchange. At $\bar{n} = 10^{14}$ cm^{-3}, about 2/3 of the input power is channeled to the divertor, with charge exchange and radiation each accounting for some of the rest of the loss.

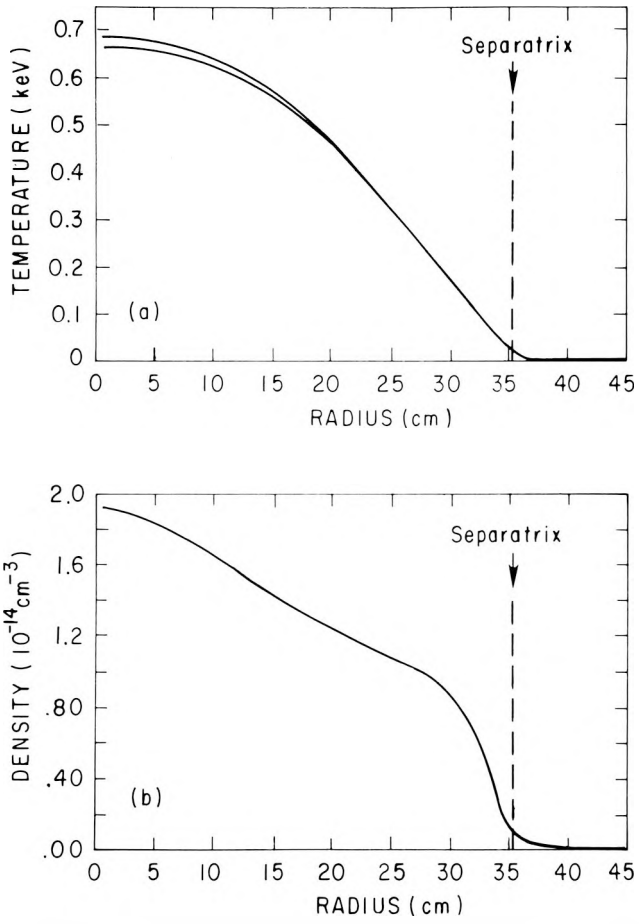

Figure 77. Temperature and density profiles in a one-dimensional computational model of a divertor.

The loading of the divertor or limiter plates depends upon the geometry. Our results indicate a maximum loading on the order of 1 kW/cm^2 for a poloidal divertor and several times more for a toroidal limiter. At higher densities the loading on the walls due to charge exchange neutrals becomes less severe, and relatively innocuous radiation losses take over. The relatively low ion temperature at the edge may ameliorate sputtering problems even at lower densities.

Physics Aspects of ETF/INTOR

In order to achieve their principle technical objectives, the Engineering Test Facility (ETF) and the International Tokamak Reactor

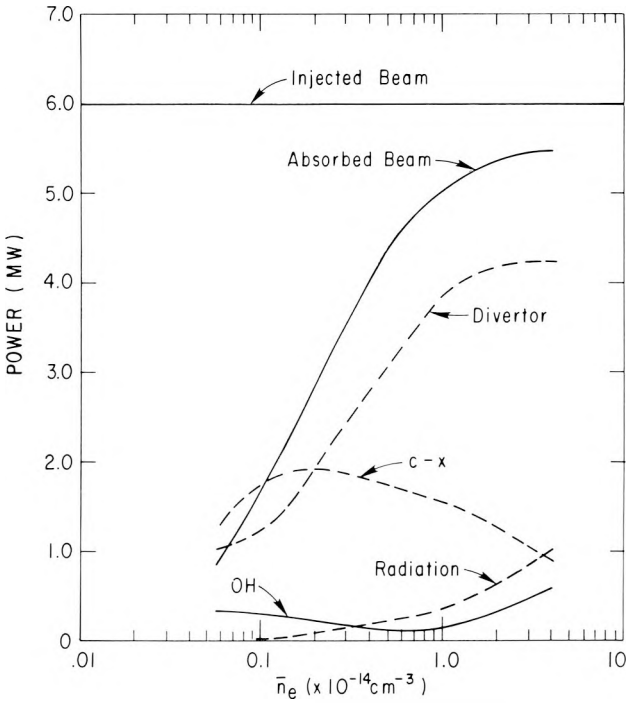

Figure 78. Average power input (solid lines) and power losses (dashed lines) versus average plasma density in a one-dimensional computational simulation of neutral beam heating of the PDX tokamak.

(INTOR) will require an ignited (or near ignited) plasma, sustained for pulse lengths of at least 100 seconds at a high enough plasma pressure to provide a neutron wall loading of at least 1.3 MW/m^2. The ignited plasma will have to be substantially free of impurities.

Achievement of ignition depends mainly on the confinement properties of the plasma. For the parameter range of present-day tokamak devices, the overall energy confinement time τ_E is found to obey an empirical scaling law of the form τ_E(s) = 5 x 10^{-19} $\bar{n}_e$ (cm^{-3}) a^2 (cm), with the dominant losses occurring through anomalous (i.e., nonclassical) cross-field electron thermal transport. Studies have been carried out of the requirements for reaching ignition in ETF/INTOR, on the basis of one-dimensional transport codes which model the particle and energy balance in a tokamak. Adopting a model for thermal transport based on the empirical scaling law for energy confinement discussed above, it has been found that ignition should be achieved in a pure DT plasma of minor radius in the midplane a = 1.2 m, vertical elongation factor κ

= 1.6, and field strength B = 5.0 T on axis. (The presently suggested device parameters, namely a = 1.3 m and B = 5.5 T, represent about 60% better $n\tau_E$ capability at fixed β.) These computations were for the case where the plasma is heated to ignition by 60-75 MW of neutral beam power at 150-200 keV energy injected nearly perpendicular to the main magnetic field.

Ignition occurs at $\langle\beta\rangle \simeq$ 4%, a value that includes contributions to the pressure from beam ions and alpha particles. The plasma temperature and $\langle\beta\rangle$ value rise during the burn phase, due to the increase in reaction rate with increasing temperature. Assuming parabolic density and temperature profiles, and taking B = 5.5 T, a burnphase value $\langle\beta\rangle$ = 5% (including a contribution of 1.5% from fast alpha particles and thermalized helium) provides the minimum specified neutron wall loading of 1.3 MW/m^2. Theoretical limitations on $\langle\beta\rangle$, arising from pressure-driven MHD "ballooning" and "kink" instabilities, permit stable equilibria up to about $\langle\beta\rangle$ = 5%, with fully optimized profiles, and certain present-day devices have already operated slightly into the theoretically-unstable regime.

Neutral-beam injection was selected as the primary heating option for ETF/INTOR. The injectors required represent a significant step beyond those that are being developed for the TFTR-generation of devices. In particular, to achieve a pulse length capability of about 10 seconds, it will probably be necessary to develop direct recovery systems (i.e., recovering the energy of the unneutralized beam ions), both to achieve an acceptable overall power efficiency, and to minimize power handling requirements on the ion beam dump. RF heating will be retained as an alternative to neutral beam heating in ETF/INTOR, because of its potential for technological advantages that will become even more important in a commercial reactor.

Computer calculations of the start-up of ETF/INTOR, calibrated against present-day experimental results, show that purely-ohmic start-up can be accomplished at low density (and very low impurity level) with a peak one-turn voltage around the plasma of only 100 volts, but such a voltage is about the limit of what can be provided. Thus, there is considerable incentive for lowering the start-up voltage by auxiliary electron cyclotron heating (at about 140 GHz) applied for the first approximately 100 msec.

The need to confine energetic ions (thermal ions, beam ions, and alpha particles) imposes severe requirements on the exact degree of axisymmetry of the toroidal confining field; i.e., on the "field ripple" that necessarily arises due to the discrete toroidal field coils. However, it seems that the requirements can be met by a 12-coil toroidal field system with coils of 8 m horizontal bore and 10 m vertical bore, provided the injectors are inclined at an angle of at least 15° to the perpendicular. If the field ripple could be adjusted upward, it would provide a mechanism for energy loss that increases sharply with increasing temperature. Accordingly, variable field ripple could provide an attractive technique for "burn control"; i.e., for preventing "run-away" of the plasma temperature due to the increase in reaction rate with increasing temperature.

Impurities represent the most serious threat to the achievement of ignition and a long burn pulse in ETF/INTOR, since the surface heat load on the first-wall and/or limiter will be much higher than in present-day tokamaks. Moreover, if the helium produced by the DT reactions is all retained in the plasma, the burn in ETF/INTOR will be quenched after about 30 seconds, unless the $\langle\beta\rangle$-value can increase significantly above 6%. It is the present consensus that some type of magnetic divertor will probably be needed in ETF/INTOR.

The bundle divertor, in which the main confining field is diverted in a single local region of the torus, is attractive from the point of view of assembly and maintenance. The main difficulty, in an ETF/INTOR-sized device, is that the requirements for achieving acceptably low field perturbation (ripple) on axis are in conflict with the requirement to provide adequate space for shielding the copper divertor coil(s). However, rapid progress is being made in developing satisfactory designs. Conventional poloidal divertors maintain the axisymmetry of the magnetic configuration, and employ an interior poloidal field coil to divert the field lines into a divertor chamber that passes all around the major circumference of the torus. However, the interior divertor coil was considered unworkable in the ETF/INTOR reactor environment. On the other hand, a poloidal divertor design with all poloidal field coils *outside* the toroidal field coils seems to be a viable concept, and calculations indicate that a divertor of this type should be capable of

performing the minimum functions required in ETF/INTOR; namely, to exhaust helium and to protect the plasma from limiter-generated impurities (Fig. 79).

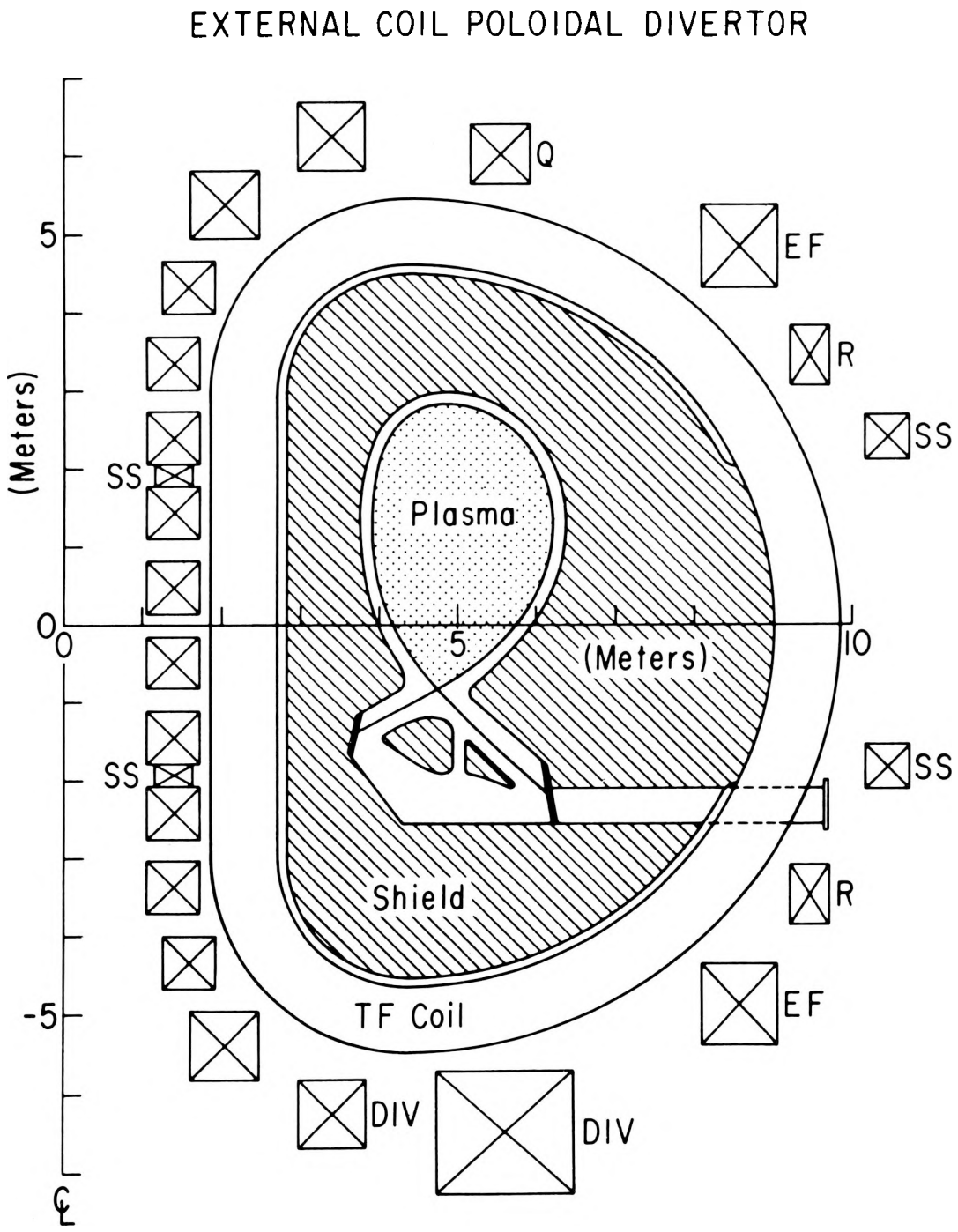

Figure 79. Proposed design of external-coil poloidal divertor.

Administration

OVERVIEW

Continued expansion of PPPL resulted in a marked increase in the Administration Department responsibilities.

The rapid growth in PPPL facilities necessitated the establishment of a Facilities Division under the Director for Administration. This Division includes the existing Facilities Planning and Construction Branch, the Plant Maintenance Branch, the Material Control Section, the Telecommunications Section, and responsibility for Security. This Division will provide the Laboratory with better integration of space planning, construction, and operation of facilities, and better prepare PPPL for assuming control of new facilities being constructed by DOE for TFTR.

Significant administrative changes during the year were in the area of Personnel. The PPPL Personnel Department assumed increased responsibility for auditing the Laboratory's Affirmative Action Program and for the processing of Group Insurance Major Medical claims; carried out a series of wage and salary surveys designed to provide management and staff with increased knowledge and awareness of compensations systems and practices; implemented revised job posting procedures; and designed the first PPPL in-house training and development program for supervisors and lead technicians.

STAFF

As of October 1978, the Laboratory's full-time staff totaled approximately 994, and by the close of FY79 this number had risen to 1054, divided as follows:

Faculty	4
Physicists	107
Engineers	191
Technicians	527
Others	225
Full Time Total	1,054

PLANT

As of October 1, 1979, the Plasma Physics Laboratory occupied a total of 584,634 gross square feet of building space in Government and University owned buildings at A, B, and C Sites on the Forrestal Campus of Princeton University.

	Government Owned (GSF)	University Owned (GSF)
A Site	28,910	141,580
B Site	0	86,210
C Site	327,934	0

Grand Total 584,634 GSF

During FY79 a number of facility addition and improvement projects were undertaken by the Laboratory. These were in addition to Line Item construction described under the heading of TFTR.

1. Lease of additional 20,000 GSF of hi-bay assembly space in the former Princeton-Penn Accelerator building at A Site – Occupied 5/79.
2. Experimental systems assembly and testing building – 3,600 GSF – $345,000 FY78 GPP – Completed 8/79.
3. Secondary unit substation #17 – $72,000 FY78 GPP – Completed 8/79.
4. A-Site sanitary sewer – $56,000 FY78 GPP Scheduled completion – 6/80.
5. Substation #18 – $270,000 FY78 GPP – Scheduled Completion – 3/80.
6. Emergency equipment facility – 4,000 GSF –$171,000 FY78 GPP – Scheduled completion – 6/80.
7. DAS computer room air conditioning modifications – $210,000 FY79 GPP – Completed 8/79.
8. Component assembly & storage building 15,000 GSF – $480,000 FY79 GPP – Scheduled completion – 4/80.
9. Laboratory building wing north addition 6,000 GSF – $477,000 FY79 GPP – Scheduled completion 9/80.
10. Landscaping & site improvements – $170,000 FY79 GPP – Scheduled completion 9/80.

PPPL LIBRARY

The primary objective of the PPPL Library for 1979 was an acceleration of the collection development program focused on Engineering acquisitions. A user survey provided guidance for an increase in the technology book collection by about 30% and in the journal collection by about

TABLE III. PPPL FINANCIAL SUMMARY ($K)

PROJECT	1975	1976/76A	1977	1978	1979
Operating (B/O)					
CLOSED CONFINEMENT:	15,037	27,634	23,073	23,883	22,887
PLT Fabrication	3,821	1,771	0	0	0
Operations (inc. ST)	3,540	8,060	7,304	8,082	6,891
Coil Test	157	615	314	0	0
Neut. Beam Pwr. Supp.	1,029	2,228	1,289	0	0
Test Stand	0	468	296	0	0
ICRF	50	72	1,035	1,022	1,164
PDX Fabrication	2,110	9,361	8,547	4,528	746
Operations	330	2,664	3,608	8,258	10,989
N.B.	0	0	0	894	2,805
ATC	2,370	1,560	0	0	0
FM-1	1,630	835	0	0	0
H-1	0	0	666[d]	522	292
Other	0	0	14[c]	577	0
DEVELOPMENT & TECHNOLOGY:	3,480	4,079	597	114	358
H-1	853	838	0[d]	0	0
Reactor Studies	266	427	456	0	0
Two Component Torus	2,160	2,814	0	0	0
Advanced Tokamak Studies	0	0	120	114	358
Other	201[a]	0	23[b]	0	0
RESEARCH:	2,614	3,788	3,005	3,170	3,903
Theory	1,848	2,530	2,008	2,378	2,459
Basic Experiments	766	1,000	668	638	1,161
User Service Center	0	258	329	154	282
REACTOR PROJECTS:	0	1,325	10,556	13,080	19,406
TFTR R&D	0	1,325	9,991	11,820	16,360
Research	0	0	241	640	975
Operations	0	0	324	620	2,071
TOTAL	21,131	36,826	37,233	40,249	46,555
Equipment (B/A)					
Capital Equipment Not Related to Construction	2,066	3,277	5,190	5,140	4,230
Construction (B/A)					
TFTR	400[e]	20,500	75,000	71,000	42,000
General Plant Projects	500	950	1,455	1,350	1,400

[a]Systems
[b]EPR RF Heating
[c]Ripple Injection Coil
[d]H-1 Moved from Development and Technology in 1977
[e]CP&D

15%. Tables IV and V show library holdings and interlibrary loans, respectively.

Reader Services

Computerized literature searching has been widely accepted by the staff with about 45-50 searches performed monthly. The main catalog of the Firestone Library was made available to the PPPL Library on microfilm.

TABLE IV. LIBRARY HOLDINGS

CATEGORY	FY78	FY79	% Increase
Monographs	3,225	3,382	4.9
Bound Journals	3,777	4,106	8.7
Reports	13,398	14,140	5.5
Microfiche	17,066	19,144	12.2

TABLE V. INTRALIBRARY LOAN

LIBRARY	FY78	FY79	% Decrease
Engineering	211	123	4.2
Math/Physics	83	83	0.0
Others	79	71	10.1

Intralibrary loans decreased as a result of the accelerated PPPL Library acquisitions program.

Graduate Education: Plasma Physics

Research in plasma physics, directed toward large-scale electric power generation via controlled thermonuclear energy, was initiated by Prof. Lyman Spitzer at Princeton University in 1951. Today, the Princeton Plasma Physics Laboratory (PPPL) is the largest center in the world for research dedicated to this field; the Laboratory is equipped with unexcelled research facilities and is also unusual in that it is directly associated with a major university. Graduate studies in plasma physics have been pursued at Princeton since 1959, and over 75 physicists have received doctoral degrees in this program. Many key positions in plasma research and technology at academic, industrial and government institutions are today held by Princeton/PPPL graduates. The teaching faculty for the plasma physics program, in Princeton University's Department of Astrophysical Sciences, currently numbers 19 members who offer a variety of courses to 35 students in residence. In addition, many PPPL staff members serve as advisors to graduate students who thereby receive training at the forefront of plasma research.

First-year graduate students typically take graduate courses given by the Physics Department in quantum mechanics, electricity and magnetism, and in statistical mechanics, together with the introductory plasma physics courses (AS 551 and 552). Second-year students typically take the intermediate-level plasma courses (AS 553 and 554), Professor Kruskal's applied mathematics course (AS 557), and such other courses as they select. Plasma physics courses are listed in Table VI. Staff members are listed in Table VII.

The academic work in the plasma physics program is thus broadly based in modern physics. The study of plasma physics requires the utilization of knowledge from electricity and magnetism, atomic physics, hydrodynamics, statistical mechanics and kinetic theory, and applied mathematics, together with diagnostic and data-handling methods from state-of-the-art laboratory physics. Techniques from many disciplines within theoretical and experimental physics find immediate application in plasma research and, by the same token, experience with plasmas can be transferred back to other areas in physics.

MAJOR ACTIVITIES

There is a strong interaction between the Plasma Physics Laboratory and the group of graduate students in the plasma physics program in the Department of Astrophysical Sciences at Princeton. Most of these students hold Assistantships in Research at PPL through which they participate in both the experimental and theoretical research at the Laboratory. First-year students this past year worked with the various

TABLE VI. PLASMA PHYSICS COURSES TAUGHT AND NAMES OF TEACHERS

	Fall 1978	
AS551	General Plasma Physics I	C. R. Oberman and S. Yoshikawa
AS553	Plasma Waves and Instabilities	T. H. Stix
AS557	Advanced Mathematical Methods in Astrophysical Sciences	M. D. Kruskal
AS558	Seminar in Plasma Physics	S. Yoshikawa
AS559	Nonlinear Interactions in Plasma	P. K. Kaw and J. A. Krommes
	Spring 1979	
AS552	General Plasma Physics II	R. M. Kulsrud and W. H. Tang
AS554	Irreversible Processes in Plasma	J. A. Krommes and C. R. Oberman
AS558	Seminar in Plasma Physics	S. Yoshikawa
AS560	Computational Methods in Plasma Physics	R. C. Grimm and H. Okuda

TABLE VII. PRINCETON PLASMA PHYSICS LABORATORY STAFF

FACULTY MEMBERS	TITLE
Thomas H. Stix	Professor of Astrophysical Sciences and Associate Director, PPPL, for Academic Affairs
Robert L. Dewar	Research Physicist and Lecturer in Astrophysical Sciences
Edward A. Frieman	Professor of Astrophysical Sciences
Harold P. Furth	Professor of Astrophysical Sciences
Melvin B. Gottlieb	Professor of Astrophysical Sciences
Raymond C. Grimm	Research Physicist and Lecturer with rank of Associate Professor in Astrophysical Sciences
Predhiman K. Kaw	Senior Research Physicist and Lecturer with rank of Professor
John A. Krommes	Research Staff and Lecturer in Astrophysical Sciences
Martin D. Kruskal	Professor of Mathematics and Astrophysical Sciences
Russell M. Kulsrud	Senior Research Physicist and Lecturer with rank of Professor in Astrophysical Sciences
Carl R. Oberman	Senior Research Physicist and Lecturer with rank of Professor in Astrophysical Sciences
Hideo Okuda	Research Physicist and Lecturer with rank of Associate Professor in Astrophysical Sciences
Francis W. Perkins, Jr.	Senior Research Physicist and Lecturer with rank of Professor
Gregory Rewoldt	Research Staff and Lecturer in Astrophysical Sciences
Marshall N. Rosenbluth	Visiting Lecturer with rank of Professor
Paul H. Rutherford	Senior Research Physicist and Lecturer with rank of Professor
William H. Tang	Research Physicist and Lecturer with rank of Associate Professor in Astrophysical Sciences
Schweickhard E. von Goeler	Senior Research Physicist and Lecturer with rank of Professor
Shoichi Yoshikawa	Senior Research Physicist and Lecturer with rank of Professor

experimental groups at PPL, including the PLT, PDX, ACT-1, Q-1, and H-1 groups, and second-year students assisted a number of members of the Theoretical Division. In addition, PPL physicists shared their expertise each week with the students at a student-run two-hour Tuesday afternoon seminar. The students are, of course, regular attendees at the Laboratory's own seminars and colloquia. All of this experience provides a natural transition to doctoral thesis research which, again, is carried out in collaboration with PPL staff members. A list of thesis projects, completed under the plasma physics program at Princeton, is given in Table VIII. Ongoing research projects are listed in Table IX.

TABLE VIII.
RECIPIENTS OF PH.D DEGREES

September 1979*

Edward J. Caramana Advisor: F. W. Perkins

Thesis: Effects of Impurity Radiation on Reversed Field Pinch Evolution

Employment: Los Alamos Scientific Laboratory, Los Alamos, New Mexico

*Mr. Caramana has been a visiting student in the Plasma Physics Laboratory working with Dr. Perkins. His Ph.D. degree was awarded by the University of Colorado.

TABLE IX. DOCTORAL THESES IN PROGRESS

Gary Allen — Advisor: M. Yamada
Thesis: Trapped-Particle Instability Simulations in a Linear Plasma

Cris Barnes — Advisor: J. Strachan
Thesis: Runaway Electron Studies on the Poloidal Divertor Experiment

Amitava Bhattacharjee — Advisor: R. L. Dewar
Thesis: Variational Principle for MHD equilibrium and Stability with Global Constraints

Kevin Brau — Advisor: V. Arunasalam
Thesis: Correlations in the Electron Temperature Fluctuation Spectrum in the PLT and PDX

Robert Chrien — Advisor: J. Strachan
Thesis: Confinement and Slowing Down of Fusion Reaction Ions in a Toroidal Plasma

David Eames — Advisor: N. Sauthoff
Thesis: The Role of Tungsten Radiation in Major Disruptions in PLT

Gerald Elder — Advisor: H. Hsuan
Thesis: Study of Wave Properties During Electron Cyclotron Heating Experiment

Robert Horton — Advisor: K-L Wong
Thesis: Generation of Plasma Current by Lower Hybrid Wave

Wen Ling Hsu — Advisor: M. Yamada
Thesis: Related Subjects of Spheromak Plasma

Michael Kotschenreuther — Advisors: J. Krommes and C. Oberman
Thesis: The Effect of Anomalous Viscosity Due to Drift Waves and Tearing Modes

Roger McWilliams — Advisors: R. W. Motley and F. W. Perkins
Thesis: The Role of Quasilinear Effects in Landau Damping of Lower-Hybrid Waves

Philippe Similon — Advisor: J. A. Krommes
Thesis: Nonlinear Theory of Drift Wave Turbulence

Eliezer Rosengaus — Advisor: R. L. Dewar
Thesis: Oscillation Center Transformation

Harold Thompson — Advisor: J. C. Hosea
Thesis: ICRF Probe Measurements

Donald Voss — Advisor: S. Cohen
Thesis: Wall Flux of Low Energy Neutrals in the PLT Tokamak

J. Randy Wilson — Advisor: K-L Wong
Thesis: Nonlinear Behavior of Lower-Hybrid Resonance Cones and Soliton Formation

Glen Wurden — Advisors: K-L Wong and M. Ono
Thesis: Laser Scattering on Lower-Hybrid Waves

Graduate Education: Fusion Reactor Technology

The Department of Chemical Engineering at Princeton University, in collaboration with the Princeton Plasma Physics Laboratory, offers a graduate program in fusion reactor technology for students interested in the engineering and technological aspects of power generation by controlled thermonuclear reactions. A coordinated program of study and research leads to the M.S.E. or Ph.D. degrees in chemical engineering.

The Program in Fusion Reactor Technology is closely integrated with the research activities of the Plasma Physics Laboratory and also has close links with the Center for Environmental Studies of the School of Engineering and Applied Science, which is concerned primarily with the environmental impact of energy technologies.

Applicants should have a strong background in science or engineering. While students will qualify for the masters or doctoral degree in chemical engineering, their theses or dissertations will be written in the field of fusion reactor technology. They may take relevant courses in plasma physics offered by the Department of Astrophysical Sciences, in material sciences offered by the Department of Aerospace and Mechanical Sciences, as well as those in fusion technology offered in the Department of Chemical Engineering.

In addition to the extensive research facilities of the Engineering Quadrangle and the libraries and Computer Center on the Main Campus, the library and research facilities of the Plasma Physics Laboratory are available to students in the Program.

MAJOR ACTIVITIES

The Chemical Engineering Department's participation in the national fusion effort goes back to 1955, with Professor E. F. Johnson's pioneering work in molten salt blankets for tritium generation. Several theses were produced in the sixties, but the Department did not establish a graduate program until 1973. By 1975 the program had grown to include 7 graduate students in residence. Currently four graduate students are in residence. Table X gives the Department's course offerings, and Table XI the Department's faculty members.

The twenty-four master's thesis and doctoral dissertation subjects treated during the history of the program can be categorized by topics as follows:

Molten Salts	7
Fast Neutrons	5
Radiolysis & Synfuels	3
Advanced Fuels, Plasma Heating, Use of Waste Heat	3
Chemical Engineering Miscellany	3
Hydrogen Permeation of Metals	2
Tritium Recovery	1

Table XII lists recently completed theses, and Table XIII theses in progress.

TABLE X. FUSION REACTOR TECHNOLOGY COURSE OFFERINGS

Chem. Eng. 351, 352 Junior Independent Work

Chem. Eng. 417 *Introduction to Fusion Power*
Engineering problems associated with controlled thermonuclear power. Stability of plasmas in linear and toroidal magnetic traps. Plasma heating and injection techniques. Systems analysis of heat transfer, fuel cycles, vacuum apparatus and magnet design parameters in fusion reactors. Three lectures. R. G. Mills

Chem. Eng. 451, 452 Senior Independent Work

Chem. Eng. 418 *Nuclear Engineering*
A survey of the applications of nuclear energy. Nuclear reactions including fission, slowing down and diffusion of neutrons; nuclear reactor theory; environmental effects of fission reactors. Introduction to fusion technology. Biology and chemical effects of radiation. Three lectures. Prerequisite: differential equations. R. C. Axtmann

Graduate

Chem. Eng. 550 *Fusion Reactor Technology*
A Study of contemporary problems in the development of nuclear fusion reactor systems. Plasma problems, fuel cycles, materials, blanket problems, energy extraction and power cycles, non-power uses of energy output, reactor control, environmental problems. Prerequisite: 417 or equivalent. R. G. Mills, staff

Plus Plasma Physics Courses in Astrophysical Sciences mentioned in Table VI (551, 552)
Plus Materials Courses in Mechanical and Aerospace Engineering (557, 558)

TABLE XI. FACULTY MEMBERS

Robert C. Axtmann	Professor of Chemical Engineering for Environment Studies
Carol K. Hall	Assistant Professor of Chemical Engineering
Ernest F. Johnson	Professor of Chemical Engineering
Robert G. Mills	Head, Engineering Program, Plasma Physics Laboratory. Lecturer in Chemical Engineering with Rank of Professor

TABLE XII. RECENT THESES

M.S.E.			
	D. C. Moreau	1976	Potentiality of the Proton-Boron Fuel for Controlled Thermonuclear Fusion
	Y. Immamura	1977	A Feasibility Study of LiF-BeF_2 and Chloride Salts as Blanket Coolants for Fusion Power Reactors
Ph.D.	J. D. Fish	1977	Radiolytic Production of Chemical Fuels in Fusion Reactor Systems
	A. S. Zarchy	1978	Limitations on Tritium Transport through Fusion Reactors

TABLE XIII. THESES IN PROGRESS

R. E. Buxbaum	Recovery of Tritium from Liquid Lithium using Yttrium
K. J. Lee	Alpha Particle Slowing Down Dynamics in a Fusion Plasma
H. H. Tseng	A Critical Examination of Molten Fluorides as Blanket Materials
M. H. Al-Morished	Reactor Materials

Table XIV. Principal Parameters of Experimental Devices

	Primary Facilities			Secondary Facilities					
	PLT	**PDX**	**TFTR***	**S-1***	**H-1**	**ACT-1**	**Q-1**	**QED**	**L-3**
R (m)	1.32	1.35	2.48	0.40	2.0**	0.59	1.2**	1.6**	3.5**
a (m)	0.43	0.45	0.85	0.25	0.05	0.1	.02	.01	0.05
I_P (MA)	0.65	0.5	2.5	0.5	–	–	–	–	–
B_T (T)	3.5	2.5	5.2	1.0	1.6	0.57	.7	.6	0.2
τ_{TF}	1.5 s	1.0 s	1.6 s	1 ms	dc	dc	dc	dc	dc
P_{aux} (MW)	2.5 (NB, 40 keV)	6 (NB, 50 keV)	33 (NB, 120 keV)	–	0.005 (LH)	0.001 (ECRH)	–	–	–
τ_{aux} (sec)	0.3	0.5	1.0	–	dc	dc	dc	dc	dc
$\bar{n}_{max}$ (cm^{-3})	10^{14}	10^{14}	10^{14}	3×10^{14}	4×10^{12}	2×10^{12}	10^{11}	10^{15}	10^{11}
T_{max}	7 keV	10 keV	20 keV	100 eV	10 eV	10 eV	.3 eV	15 eV	5 eV

*Under construction.
**Length of (linear) device.

Bibliography

PRINCETON LARGE TORUS (PLT)

Bitter, M., Hill, K., Sauthoff, N.R., Efthimion, P., Meservey, E.B., Roney, W., von Goeler, S., Horton, R., Goldman, M.A., Stodiek, W., "Dielectronic Satellite Spectrum of Helium-Like Iron (FE XXV)." *Physical Review Letters 43* (July 1979) 129-132. PPPL-1538 (April 1979) 17 pp.

Bitter, M., von Goeler, S., Horton, R., Goldman, M., Hill, K.W., Sauthoff, N.R., Stodiek, W., "Doppler-Broadening Measurements of X-ray Lines for Determination of the Ion Temperatures in Tokamak Plasmas." *Physical Review Letters 42* (January 1979) 304-307. PPPL-1490 (November 1978) 15 pp.

Colestock, P.L., Strachan, J.D., Ulrickson, M., Chrien, R., "Confinement of Fusion-Produced Tritium in the Princeton Large Torus." *Physical Review Letters 43* (September 1979) 768-772.

Davis, S.L., Medley, S.S., Brusati, M., "The Charge Exchange Analyzer for Mass Resolved Ion Temperature Measurements on PLT." PPPL-1478 (January 1979) 40 pp.

Dylla, H.F., Bol, K., Cohen, S.A., Hawryluk, R.J., Meservey, E.B., Rossnagel, S.M., "Observations of Changes in Residual Gas and Surface Composition with Discharge Cleaning in PLT." *Journal of Vacuum Science and Technology 16* (March/April 1979) 752-757. PPPL-1485 (October 1978) 27 pp.

Dylla, H.F., Cohen, S.A., Rossnagel, S.M., McCracken, G.M., Staib, Ph., "Glow Discharge Conditioning of a PDX Vacuum Vessel." *Journal of Vacuum Science and Technology 17* (January-February 1980) 286-290.

Eames, D.R., von Goeler, S., Sauthoff, N.R., Stodiek, W., "Observations of Several Disruptions in PLT Using Soft and Ultra-Soft X-ray Radiation." PPPL-1530 (March 1979) 52 pp.

Eubank, H.P., Goldston, R.J., Arunasalam, V., Bitter, M., Bol, K., Boyd, D., Bretz, N., Bussac, J.P., Cohen, S., Colestock, P., Davis, S., Dimock, D., Dylla, H., Efthimion, P., Grisham, L., Hawryluk, R., Hill, K., Hinnov, E., Hosea, J., Hsuan, H., Johnson, D., Martin, G., Medley, S., Meservey, E., Sauthoff, N., Schilling, G., Schivell, J., Schmidt, G., Stauffer, F., Stewart, L., Stodiek, W., Stooksberry, R., Strachan, J., Suckewer, S., Takahashi, H., Tait, G., Ulrickson, M., von Goeler, S., Yamada, M., Tsai, C., Stirling, W., Dagenhart, W., Gardner, W., Minon, M., Haselton, H., "Neutral Beam Heating Results for the Princeton Large Torus." *Physical Review Letters 43* (July 1979) 270-274.

Grisham, L.R., Eubank, H.P., Dylla, H.F., Goldston, R.J., Schilling, G., Stewart, L.A., Stooksberry, R.W., Ulrickson, M., "PLT Neutral Injector Performance." in *Proceedings of the IAEA Workshop on Neutral Injectors* (Culham Laboratory, Culham, 1978) to be published. PPPL-1484 (October 1978) 30 pp.

Hawryluk, R.J., Bol, K., Bretz, N., Dimock, D.L., Eames, D., Hinnov, E., Hosea, J.C., Hsuan, H.G.S., Jobes, F.C., Johnson, D.W., Meservey, E.B., Sauthoff, N.R., Schmidt, G.L., Suckewer, S., Ulrickson, M., von Goeler, S., "The Effect of Current Profile Evolution on Plasma-Like Interaction and the Energy Profile Confinement Time." *Nuclear Fusion 19* (October 1979) 1307-1317. PPPL-1534 (April 1979) 31 pp.

Hawryluk, R.J., Bol, K., Johnson, D.W., "Volt-Second Consumption During the Startup Phase of a Large Tokamak." *Nuclear Fusion 19* (November 1979) 1519-1522. PPPL-1508 (January 1979) 41 pp.

Hill, K., von Goeler, S., Bitter, M., Campbell, L., Cowan, R.D., Fraenkel, B., Greenberger, A.J., Horton, R., Hovey, J., Roney, W., Sauthoff, N.R., Stodiek, W., "Determination of Fe Charge-State Distributions in PLT by Bragg Crystal X-ray Spectroscopy." *Physical Review Letters 19* (April 1979) 1770-1779. PPPL-1457 (August 1978) 37 pp.

Hinnov, E., "Iron Radiation in Tokamak Discharges." in *Diagnostics for Fusion Experiments,* E. Sindoni and C. Wharton, editors, Pergamon Press, New York, (1979) pp. 139-148.

Hinnov, E., "Observed Resonance Lines of Highly Ionized Ti, Cr, Fe, and Ni in Tokamak Discharges." *Astrophysical Journal 230* (June 1979) L19.

Hinnov, E., "Radiation of Highly Ionized Atoms in the Diagnostics of Tokamak Plasmas," in *Proceedings of the U.S.-Japan Joint Seminar on Plasma Spectroscopy with Emphasis on Plasma Research in the Extreme Ultraviolet,* Kyoto University, 1979 (Department of Engineering Science, Kyoto University).

Hosea, J., "Regimes of Operation in the Princeton Large Torus," in *Physics of Plasmas Close to Thermonuclear Conditions,* D. Pfirsch, Editor (Pergamon Press, New York, 1981) to be published. PPPL-1589 (October 1979) 11 pp.

Hosea, J.C., Arunasalam, V., Bernabei, S., Bitter, M., Boyd, D., Bretz, N., Chrien, R., Cohen, S., Colestock, P., Davis, S., Dimock, D., Dylla, F., Eames, D., Efthimion, F., Eubank, H., Goldston, R., Grisham, L., Hinnov, E., Hsuan, H., Hwang, D., Jobes, F., Johnson, D., Kaita, R., Lawson, J.Q., Mazzucato, E., McNeill, D., Medley, S., Meservey, E., Mueller, D., Sauthoff, N., Stodiek, W., Stooksberry, R., Strachan, J., Suckewer, S., Tait, G., Thompson, H., von Goeler, S., "Fast Wave Heating in the Princeton Large Torus," in *Physics of Plasmas Close to Thermonuclear Conditions,* D. Pfirsch, Editor (Pergamon Press, New York, 1981) To be published. PPPL-1588 (October 1979) 14 pp.

Hosea, J., Bernabei, S., Colestock, P., Davis S.L., Efthimion, P., Goldston, R.J., Hwang, D., Medley, S.S., Mueller, D., Strachan, J., Thompson, H., "Fast Wave Heating of Two-Ion Plasmas in the Princeton Large Torus through Minority Cyclotron Resonance Damping ." *Physical Review Letters 43* (December 1979) 1802-1806. PPPL-1554 (July 1979) 16 pp.

Medley, S.S., Davis, S.L., "Charge Exchange Ion Temperature Measurements During High Power Neutral Beam Injection on PLT." PPPL-1507 (January 1979) 41 pp.

Post, D.E., Hulse, R.A., Hinnov, E., Suckewer, S., "Charge-Exchange Recombination for Highly-Ionized Iron," in *Proceedings of the XIth International Conference on the Physics of Electronic and Atomic Collisions, Kyoto, 1979,* K. Takayanagi, N. Oda, Editors (Kyoto, Society for Atomic Collision Research, 1979). Contributed Papers, p. 584.

Sauthoff, N.R., von Goeler, S., "Techniques for the Reconstruction of Two-Dimensional Images from Projections," *IEEE Transactions on Plasma Science, PS-7* (September 1979) 141-147. PPPL-1447 (August 1978) 29 pp.

Sauthoff, N.R., von Goeler, S., Eames, D.R., Stodiek, W., "Successor Oscillations of Internal Disruptive Instabilities in the PLT Tokamak." PPPL-1553 (June 1979) 17 pp.

Sauthoff, N.R., von Goeler, S., Eames, D.R., Stodiek, W., "Internal and External Disruptive Instabilities in the PLT Tokamak," in the *IAEA Symposium on Current Disruption in Toroidal Plasmas, Garching, 1979,* K. Lackner and H.P. Zehrfeld, Editors (Max-Planck-Institut für Plasmaphysik, Garching, 1979) IPP 3/51, Paper C5.

Strachan, J.D., Colestock, P., Eubank, H., Grisham, R., Hovey, J., Schilling, G., Stewart, L., Stodiek, W. Stooksberry, R., Young, K.M., "Measurement of the Neutron Spectra from Beam-Heated PLT Plasmas." *Nature 279* (June 1979) 626-628.

Suckewer, S., Eubank, H.P., Goldston, R.J., Hinnov, E., "Toroidal Plasma Rotation in the Princeton Large Torus Induced by Neutral Beam Injection." *Physical Review Letters 43* (July 1979) 207-210. PPPL-1542 (May 1979) 14 pp.

Suckewer, S., Fonck, R., Hinnov, E., "Observed Magnetic Dipole Transitions in the Ground-State Terms of Ti XIV, Ti XV, and Ti XVII." *Physical Review A 20* (March 1980) 924-927. PPPL-1591 (September 1979) 10 pp.

Suckewer, S., Hinnov, E., "Iron Forbidden Lines in Tokomak Discharges." *Physical Review A 20* (August 1979) 578-585. PPPL-1524 (March 1979) 26 pp.

Voss, D.E., Bol, K., Johnson, J.L., "Application of Numerical Equilibrium Calculations to Positioning of the Princeton Large Torus Plasma." PPPL-1483 (October 1978) 16 pp.

Voss, D.E., Cohen, S.A., "Low Energy Neutral Outflux from a PLT Tokamak," *Journal of Nuclear Materials* 94/95 (1980).

Voss, D.E., Cohen S.A., "UHV-Compatible Chopper Systems." *Journal of Vacuum Science and Technology 17* (January-February 1980) 303-305.

Wampler, W.R., Picraux, S.T., Cohen, S.A., Dylla, H.F., McCracken, G., Rossnagel, S.M., Magee, C.W., "Hydrogen Isotope Trapping in Materials Exposed in PLT." *Journal of Nuclear Materials 85/86* (December 1979) 983-987. PPPL-1537 (April 1979) 5 pp.

POLOIDAL DIVERTOR EXPERIMENT (PDX)

Jardin, S., "Stabilization of the Axisymmetric

Instability of the PDX Tokamak." *Physics of Fluids 21* (October 1978) 1851-1855. PPPL-1400 (December 1977) 20 pp.

Kaita, R., Davis, S.L., Medley, S.S., "Monte Carlo Simulation of Ion Trajectories in the Modified PDX Thermal Charge Exchange Analyzer." PPPL-1493 (December 1978) 17 pp.

Suckewer, S., Hinnov, E., Bol, K., Fonck, R., Hawryluk, R.J., Jacobsen, R.A., Meade, D.M., Okabayashi, M., Schmidt, G.L., Silver, E.H., Sinnis, J., "Titanium Density Measurements in the PDX Tokamak using Ti XVII Forbidden Line." *Nuclear Fusion 19* (December 1979) 1681-1684. PPPL-1563 (June 1979) 12 pp.

SMALLER DEVICES

Allen, G.R., Owens, D.K., Seiler, S.W., Yamada, M., Ikezi, H., Porkolab, M., "Parametric Lower Hybrid Instability Driven by Modulated Electron Beam Injection." *Physical Review Letters 41* (October 1978) 1045-1048. PPPL-1460 (August 1978) 13 pp.

McWilliams, R., Valeo, E.J., Motley, R.W., Hooke, W.M., Olson, L., "Steady-State Currents Driven by Collisionally Damped Lower Hybrid Waves." *Physical Review Letters 44* (January 1980) 245-248. PPPL-1584 (September 1979) 13 pp.

Motley, R.W., Bernabei, S., Hooke, W.M., "A Coaxial Lower Hybrid Plasma Source." *Reviews of Scientific Instruments 50* (December 1979) 1586-1589. PPPL-1509 (January 1979) 16 pp.

Motley, R.W., Bernabei, S., Hooke, W.M., McWilliams, R., Olson, L., "Penetration of Slow Waves into an Overdense Plasma." *Plasma Physics 21* (June 1979) 567-573. PPPL-1449 (June 1978) 16 pp.

Motley, R.W., Hooke, W.M., Anania, G., "Formation of Thermal Eddies During RF Heating of Plasma." *Physical Review Letters 43* (December 1979) 1799-1802. PPPL-1567 (July 1979) 13 pp.

Motley, R.W., and Hooke, W.M., "Active-Passive Waveguide Array for Wave Excitation in Plasmas." *Nuclear Fusion 20* (February 1980) 222-224. PPPL-1606 (November 1979) 10 pp.

Nishi, M., Yamada, M. Suckewer, S., and Rosengaus, E., "Measurements of Sputtering Yields for Low-Energy Plasma Ions." PPPL-1521 (April 1979) 29 pp.

Ono, M., "Cold Electrostatic Ion Cyclotron Waves and Ion-Ion Hybrid Resonances." *Physical Review Letters 42* (May 1979) 1267-1270. PPPL-1495 (December 1978) 13 pp.

Seiler, S., Yamada, M., "Ion-Beam-Driven Lower Hybrid Instability and Resultant Anamalous Beam Slowing." *Nuclear Fusion 19* (April 1979) 469-483. PPPL-1412 (January 1978) 62 pp.

Wilson, J.R., Wong, K.L., "Non-Linear Converging Resonance Cones." *Physics of Fluids 23* (March 1980) 566-572. PPPL-1549 (July 1979) 31 pp.

Wong, K.L., "Density Dependence of Electron Cyclotron Heating Rate in a Toroidal Octopole." *Physics of Fluids 21* (November 1978) 2108-2111.

Wong, K.L., "Experimental Observation of Current Generation by Uni-Directional Electron Plasma Waves." *Physical Review Letters 43* (August 1979) 438-441. PPPL-1464 (August 1978) 14 pp.

Wong, K.L., Wilson, J.R., Porkolab, M., "The Effect of Convective Loss on the Parametric Decay of Cold Electron Plasma Waves." *Physics of Fluids 23* (January 1980) 96-104. PPPL-1499 (February 1979) 38 pp.

TOKAMAK FUSION TEST REACTOR (TFTR)

Cecchi, J., "Tritium Permeation and Wall Loading in the TFTR Vacuum Vessel." *Journal of Vacuum Science and Technology 16* (January 1979) 58-70. PPPL-1422 (May 1978) 60 pp.

Das, S.K., Kaminsky, M., Tishler, R., Cecci, J., "Surface Damage and Sputtering of ATJ Graphite as Candidate Armor Plate Material for TFTR under D^+ Bombardment." *Journal of Nuclear Materials 85/86* (December 1979) 225-230.

Howe, H., Lind, K.E., "Environmental Control of Tritium Use at the Tokamak Fusion Test Reactor (TFTR)." PPPL-1494 (January 1979) 24 pp.

Kaita, R., Medley, S.S., "A Study of the Mass and Energy Resolution of the E B Charge Exchange

Analyzer for TFTR." PPPL-1582 (September 1979) 31 pp.

Kaminsky, M., Cecchi, J.L., Das, K.S., "Sputtering and Surface Damage of TFTR Protective Plate Candidate Materials by Energetic D^+ Irradiation." *Fusion Technology* (Pergamon Press, New York, 1979) 789-794.

Medley, S.S., "Vacuum System Design and Tritium Inventory for the TFTR Charge Exchange Diagnostic." PPPL-1551 (May 1979) 51 pp.

Ulrickson, M., "Material Studies Related to TFTR Limiters and Wall Armor." *Journal of Nuclear Materials 85/86* (December 1979) 231-235.

TFTR BLANKET MODULE

Jassby, D.L., Caldwell, C.S., Pettus, W.G., Schmotzer, J.K., Welfare, F., Womack, R. "Utilization of Fusion Neutrons in the Tokamak Fusion Test Reactor for Blanket Performance Testing and Other Nuclear Engineering Experiments." PPPL-1510 (January 1979) 51 pp.

Jassby, D.L., et al., in *Transactions of the American Nuclear Society,* Vol. 33 (November, 1979) 63 ff.

"TFTR Fusion Blanket Experiments." Princeton University Plasma Physics Laboratory and Babcock and Wilcox Company, Report EPRI TPS 79-705, Vol. I, Summary Report (July 1979).

GENERAL EXPERIMENTAL AND GENERAL ENGINEERING

Andrews, P.L., Goldston, R.J., "Scattering of Suprathermal Ions by Partially Ionized Impurities." PPPL-1513 (January 1979) 18 pp.

Bitter, M., von Goeler, S., Horton, R., Goldman, M.A., Hill, K., Sauthoff, N.R., Stodiek, W., "Doppler-Broadening Measurements of X-Ray Lines for Determination of the Ion Temperature in Tokamak Plasmas." *Physical Review Letters 42* (January 1979) 304-307. PPPL-1490 (November 1978) 15 pp.

Brown, G.M., Clarke, G.A., "Computerized Methods for J_{IC} Determination Using Unloading Compliance Techniques," in *Symposium on Computer Automation of Materials Testing,* Philadelphia, 1978 (American Society for Testing and Materials, Philadelphia, 1980) ASTM STP. 710.

Buchanan, C.H., "Energy Storage for Tokamak Reactor Cycles." PPPL-1511 (January 1979) 28 pp.

Buxbaum, R.E., Johnson, E.F., "The Use of Yttrium for the Recovery of Tritium from Lithium at Low Concentrations." PPPL-1548 (June 1979) 24 pp.

Cecchi, J.L., Johnson, B.M., Jones, K.W., Hinnov, E., Kruse, T.H., "Comparison of Tungsten and Gold Radiation from Beam-Foil Excitation and Tokamak-Produced Plasmas." *Physics Letters 70A* (March 1979) 320-322. PPPL-1479 (September 1978) 11 pp.

Christensen, U.R., "Time Varying Eddy Currents on a Conducting Surface in 3-D Using a Network Mesh Method." PPPL-1516 (April 1979) 35 pp.

Cohen, S.A. "Tokamak Plasma Diagnosis by Surface Physics Techniques." *Journal of Nuclear Materials 76/77* (September 1978) 68-77.

Cohen, S.A., McCracken, G.M., "A Model for Hydrogen Isotype Backscattering, Trapping and Depth Profiles in C and α-Si." *Journal of Nuclear Materials 84* (October 1979) 157-166. PPPL-1529 (March 1979) 34 pp.

Dimock, D., "Thomson Scattering," in *Diagnostics for Fusion Experiments,* E. Sindoni and C.B. Wharton, Editors (Pergamon Press, New York, 1979) 271-301.

Doll, D.W., Ulrickson, M., "An Evaluation of Coated Heat Sink Materials for Fusion Applications." *Journal of Nuclear Materials 85/86* (December 1979) 191-196.

Efthimion, P.C., Arunasalam, V., Bitzer, R., Campbell, L., Hosea, J.C., "A Fast-Scanning Heterodyne Receiver for Measurement of the Electron Cyclotron Emission from High-Temperature Plasmas." *Review of Scientific Instruments 50* (August 1979) 949-951. PPPL-1532 (March 1979) 12 pp.

Eubank, H.P., Murakami, M. "Recent Progress in Tokamak Experiments." *Physics Today 32* (May 1979) 25-32.

Furth, H.P., "U.S. Tokamak Research" in *9th European Conference on Controlled Fusion*

and Plasma Physics, Oxford, 1979. (Culham Laboratory, Culham, England, 1979) Invited Papers 309-320. PPPL-1598 (October 1979) 11 pp.

Goldston, R.J., "Radially Resolved Measurements of 'q' on the ATC Tokamak." *Physics of Fluids 21* (December 1978) 2346-2353. PPPL-1432 (April 1978) 35 pp.

Hawryluk, R.J., Suckewer, S., Hirshman, S.P., "Low-Z Impurity Transport in Tokamaks." *Nuclear Fusion 19* (May 1979) 607-632. PPPL-1473 (October 1978) 79 pp.

Johnson, B.M., Jones, K.W., Cecchi, J.L., Hinnov, E., Kruse, T.H., "Comparison of Tungsten and Gold Radiation from Beam-Foil Excitation and Tokamak-Produced Plasmas." *Physics Letters 70A* (March 1979) 320-322.

Johnson, B.M., Jones, K.W., Cecchi, J.L., Kruse, T.H., "Spectra from Foil-Excited Molybdenum Ions." *IEEE Transactions on Nuclear Science NS-26* (1979) 1317-1319.

Knutson, D.S., File, J., Marison, R.E., Rappe, G.H., "Non-Superconducting Magnet Structures for Near-Term Large Fusion Devices," in *5th International Conference on Structural Mechanics in Reactory Technology, Berlin 1979* (North Holland Publishing, Amsterdam, 1980) Vol. N, Pt. 1.

Langley, R.A., Colchin, R.J., Isler, R.C., Murakami, M., Simpkins, J.E., Cecchi, J.L., Corso, V.L., Dylla, H.F., Ellis, R.A., Jr., Nishi, M., "The ISX-A Graphite Limiter Experiment." *Journal of Nuclear Materials 85/86* (December 1979) 215-219.

McCracken, G.M., "Recycling and Surface Erosion Processes in Contemporary Tokamaks." PPPL-1536 (March 1979) 7 pp.

Magee, C.W., Cohen, S.A., Voss, D.E., Brice, D.K., "Depth Distributions of Low Energy Deuterium Implanted into Silicon as Determined by SIMS." PPPL-1575 (August 1979) 13 pp.

Moore, R., "Some Basic Problems with Copper Gasket Flanges." *Journal of Vacuum Science & Technology 16* (September/October 1979) 1575.

Nishi, M., Yamada, M., Suckewer, S., Rosengaus, E., "Measurements of Sputtering Yields for Low-Energy Plasma Ions." PPPL-1521 (April 1979) 29 pp.

Picraux, S.T., Cohen, S.A., Dylla, H.F., Wampler, W.R., "Ion Beam Analysis of Surface Modifications in Tokamaks." *IEE Transactions on Nuclear Science NS-26* (February 1979) 1277-1280.

Post, D.E., "Impurity Radiation Losses in Fusion Plasmas," in *Nagoya Seminar on Atomic Processes in Fusion Plasmas, Nagoya, 1979* (Nagoya, Institute of Plasma Physics, 1979) IPPJ-AM-13. pp. 38-43.

Rossnagel, S.M., Dylla, H.F., Cohen, S.A., "AES Study of the Adsorption of O_2, CO, Co_2, and H_2O on Indium," *Journal of Vacuum Science and Technology 16* (March/April 1979) 558-561. PPPL-1486 (October 1978) 13 pp.

Suckewer, S., Fishman, H., "Conditions for Soft X-Ray Lasing Action in a Confined Plasma Column." PPPL-1577 (September 1979) 43 pp.

Takahashi, H., "ICRF Heating and Wave Generation in the ATC Tokamak. Part I: Wave Generation, Propagation, and Absorption." PPPL-1545 (April 1979) 89 pp.

Weissenburger, D.W., Christensen, U.R., "Transient Eddy Currents on Finite Plane and Toroidal Conducting Surfaces." PPPL-1517 (April 1979) 58 pp.

FUSION POWER

Jassby, D.L., "Maximum Neutron Yields in Experimental Fusion Devices." PPPL-1515. (February 1979) 18 pp.

Jassby, D.L., "Fusion-Neutron Production During Protium Beam Injection into Protium-Deuterium Plasmas." *Nuclear Instruments and Methods 158* (1979) 611-612.

Jassby, D.L., "Fusion-Supported Decentralized Nuclear Energy System." PPPL-1555 (April 1979) 25 pp.

Jassby, D.L., Workshop Summaries for 3rd US/USSR Symposium on Fusion/Fission Reactors. PPPL-1550. (July 1979) 54 pp.

Mills, R.G., *Introduction to Fusion Power* (Department of Chemical Engineering, Princeton University, Princeton, 2nd Edition 1979) 625 pp.

Mills, R.G., "Tokamak Reactors." *Mechanical Engineering 100* (July 1978) 412-416.

Mills, R.G., "Nuclear Fusion and the Breeder," in *"Proceedings of the Institute of Electrical and Electronics Engineers, 1977 Conference on U.S. Technological Policy Issues, Washington 1977.* (IEEE, New York, 1977.) pp. 55-56.

Mills, R.G., Tenney, R.H., Bathke, C.G., Price, Jr., W.G., Bohlke, W.H., Johnson, E.F., Todd, A.M.M., Buchanan, C.H., Gralnick, S.L., "A Systems Study of Tokamak Fusion-Fission Reactors." PPPL-1450. (November 1978) 550 pp.

Singer, C.E., Jassby, D.L., Hovey, J., "Ignition of an Overheated, Underdense Fusioning Tokamak Plasma." *Nuclear Fusion 20* (April 1980) 489-495. PPPL-1571 (August 1979) 25 pp.

DESIGN STUDIES

Gralnick, S.L., Luzzi, T., Bundy, J., "Vacuum Vessel Design for a Tokamak Ignition Test Reactor." PPPL-1497 (February 1979) 20 pp.

Jassby, D.L., Bolton, R.A., Price, W.G., Singer, C.E., Stewart, L.D., Bundy, J.J., Gralnick, S.L., Luzzi, T., Marino, J.D., Lind, K., "PITR—Princeton Ignition Test Reactor." PPPL-1525 (December 1979) 261 pp.

Jassby, D.L., File, J., Bronner, G., Clarke, J.R., Johnson, H.G., Martin, G.D., Murray, J.G., Okabayashi, M., Price, W.G., Jr., Rogoff, P., Singer, C.E., Stewart, L.D., Budny, J.J. Gralnick, S.L., Luzzi, T., Marino, J.D., Sedgeley, D., Eckels, P., Gaberson, P., Murphy, J., "SLPX—Superconducting Long-Pulse Tokamak Experiment." *IEEE Transactions on Magnetics, MAG-15* (January 1979) 847-850. PPPL-1488 (November 1978) 4 pp.

Jassby, D.L., File, J., Reardon, P.J., "SLPX—Superconducting Long-Pulse Experiment." Presented at the IAEA Technical Committee on the Engineering of Large Tokamak Experiments, Paris, France, 1-6 September 1978. PPPL-1481 (October 1978) 18 pp.

Jassby, D.L., File, J., Reardon, P.J., "SLPX—Superconducting Long-Pulse Experiment," in *Fusion Technology* (Pergamon Press, New York, 1979) pp. 83-89.

Okabayashi, M., Todd, A.M.M. "MHD Equilibrium and Stability of the Spheromak." PPPL-1580. (August 1979) 25 pp.

SPLX Superconducting Long-Pulse Experiment: Final Report on Scoping Study, Vol. 1 "Executive Summary," PPPL-1503 (November 1978) Vol. 2 "Superconducting Long-Pulse Experiment I," PPPL-1500 (November 1978), Vol. 3 "Superconducting Long-Pulse Experiment II," PPPL-1501 (November 1978), Vol. 4 "A D-T Burning Version of SPLX," PPPL-1502 (November 1978), Vol. 5 "Work Breakdown Structure," PPPL-1504 (November 1978).

THEORY

Auerbach, S.P., "Energy of Waves in a Plasma." *Physics of Fluids 22* (September 1979) 1650-1656. PPPL-1474 (August 1978) 25 pp.

Boozer, A.H., "Guiding Center Drift Equations." PPPL-1527 (March 1979) 16 pp.

Chance, M.S., Dewar, R.L., Frieman, E.A., Glasser, A.H., Greene, J.M., Grimm, R.C., Jardin, S.C., Johnson, J.L., Manickam, J., Okabayashi, M., Todd, A.M.M., "MHD Stability Limits on High-β Tokamaks," in *Proceedings of the 7th International Conference on Plasma Physics and Controlled Nuclear Fusion Research, Innsbruck, 1978* (International Atomic Energy Agency, Vienna, 1979) Vol. I, 677-687.

Chen, L., Chance, M.S., Cheng, C.Z., "Absolute Dissipative Drift-Wave Instabilities in Tokamaks." PPPL-1570 (July 1979) 14 pp.

Chen, L., Cheng, C.Z., "Theory of Drift Wave Eigenmodes in Toroidal Plasmas." PPPL-1562 (July 1979) 36 pp.

Chen, L., Cheng, C.Z., Frieman, E.A., Guzdar, P.N., Kaw, P.K., Lee, W.W., Nevins, W.M., Oberman, C.R., Okuda, H., Rewoldt, G., Rutherford, P.H., Tang, W.M., White, R.B., "Theory of Drift and Trapped-Electron Instabilities," in *Proceedings of the 7th International Conference on Plasma Physics and Controlled Nuclear Fusion Research, Innsbruck, 1978* (International Atomic Energy Agency, Vienna, 1979) Vol. I, 763-775.

Chen, L., Guzdar, P.N., Hsu, J.Y., Kaw, P.K., Oberman, C.R., White, R.B., "Theory of Dissipative Drift Instabilities in Sheared Magnetic Fields," *Nuclear Fusion 19* (March 1979) 373-387. PPPL-1423 (June 1978) 50 pp.

Cheng, C.Z., Chen, L., "Unstable Universal Drift Eigenmodes in Toroidal Plasmas." PPPL-1579 (August 1979) 16 pp.

DeLucia, J., Jardin, S.C., Todd, A.M.M., "An Interactive Metric Method for Solving the Inverse Tokamak Equilibrium Problem." PPPL-1564 (July 1979) 50 pp.

Dewar, R.L., "Exact Oscillation-Centre Transformations." *Journal of Physics A 11.* (1978) 9-26.

Dewar, R.L., Chance, M.S., Glasser, A.H., Greene, J.M., Frieman, E.A., "WKB Theory for High-n Modes in Axisymmetric Toroidal Plasmas." PPPL-1587 (September 1979) 13 pp.

Elder, G.B., Perkins, F.W., "Heating Tokamaks by Parametric Decay of Intense Extraordinary Mode Radiation." PPPL-1578 (August 1979) 35 pp.

Foote, E.A., Kulsrud, R.M., "Hydromagnetic Waves in High-Beta Plasmas." PPPL-1514 (February 1979) 44 pp.

Frankel, N.E., Hines, K.C., Dewar, R.L., "Energy Loss Due to Binary Collisions in a Relativistic Plasma." *Physical Review A 20* (November (1979) 2120-2129.

Furth, H.P., "Economic Theory of the Disruptive Instability," in *Proceedings of the IAEA Symposium on Current Disruption in Toroidal Devices,* Garching, 1979, K. Lackner and H.P. Zehrfeld, Editors (Max-Planck-Institut für Plasmaphysik, Garching, Germany, July 1979) IPP 3/31, Paper B-3.

Greene, J.M., "A Method for Determining a Stochastic Transition." *Journal of Mathematical Physics 20* (June 1979) 1183-1201. PPPL-1489 (November 1978) 76 pp.

Hassam, A.B., Kulsrud, R.M., "Convective Cells and Transport in Toroidal Plasmas." PPPL-1496 (December 1978) 36 pp.

Hassam, A.B., Kulsrud, R.M., "Time Evolution of Mass Flows in a Collisional Tokamak." *Physics of Fluids 21* (December 1978) 2271-2279. PPPL-1427 (April 1978) 43 pp.

Hirschman, S.P., Jardin, S.C., "Two-Dimensional Transport of Tokamak Plasmas." *Physics of Fluids 22* (April 1979) 731-742. PPPL-1482 (October 1978) 52 pp.

Jardin, S.C., Johnson, J.L., Greene, J.M., Grimm, R.C., "Dynamic Grid Method for Time Dependent Simulations of Axisymmetric Instabilities in Tokamaks." *Journal of Computational Physics 29* (October 1978) 101-126. PPPL-1359 (July 1977) 54 pp.

Johnson, J.L., Dalhed, H.E., Greene, J.M., Grimm, R.C., Hsieh, Y.Y., Jardin, S.C., Manickam, J., Okabayashi, M., Storer, R.G., Todd, A.M.M., Voss, D.E., Weimer, K.E., "Numerical Determination of Axisymmetric Toroidal Magnetohydrodynamic Equilibria." *Journal of Computational Physics 32* (August 1979) 212-234. PPPL-1463 (July 1978) 46 pp.

Karney, C.F.F., "Stochastic Ion Heating by a Lower Hybrid Wave: II." PPPL-1528 (April 1979) 68 pp.

Karney, C.F.F. "Velocity-Space Diffusion in a Perpendicularly Propagating Electrostatic Wave," in *International Workshop on Intrinsic Stochasticity in Plasmas, Cargese,* G. Laval, D. Gresillon, Editors (Editions de Physique, Orsay, France, 1980) 159-168.

Karney, C.F.F., Fisch, N.J., "Numerical Studies of Current Generation by Radio-Frequency Traveling Waves." *Physics of Fluids 22* (September 1979) 1817-1824. PPPL-1506 (January 1979) 39 pp.

Karney, C.F.F., Perkins, F.W., Sun, Y.C., "Alfvén Resonance Effects on Magnetosonic Modes in Large Tokamaks." *Physical Review Letters 42* (June 1979) 1621-1624.

Karney, C.F.F., Sen, A., Chu, F.Y.F., "Nonlinear Evolution of Lower Hybrid Waves." *Physics of Fluids 22* (May 1979) 940-952. PPPL-1452 (June 1978) 38 pp.

Kaw, P.K., Guzdar, P.N., "The Universal Mode Revisited." PPPL-1573 (August 1979) 13 pp.

Kaw, P.K., Guzdar, P.N., "Quadratic Form for Resistive Drift Modes in a Slab with Magnetic Shear." PPPL-1526 (March 1979) 6 pp.

Kaw, P.K., Valeo, E.J., Rutherford, P.H., "Tearing Modes in a Plasma with Magnetic Braiding." PPPL-1561 (July 1979) 17 pp.

Krommes, J.A., "Plasma Transport in Stochastic Magnetic Fields. II: Principles and Problems of Test Electron Transport." Presented at the Oji Seminar on Nonequilibrium Statistical Mechanics, Kyoto, 1978. *Progress of Theoretical Physics,* Supplement No. 64 (1978).

Krommes, J.A., "Renormalized Compton Scattering and Nonlinear Damping of Collisionless Drift Waves." PPPL-1543 (May 1979) 46 pp.

Krommes, J.A., "Self-Consistent Kinetic Theory of Stochasticity," in *International Workshop on Intrinsic Stochasticity in Plasmas, 1979.*

Cargese (Editions de Physique, Orsay, France, 1980) 193-203. PPL-AF-89 (August 1979).

Krommes, J.A., Kleva, R.G., "On a Renormalized Weak Plasma Turbulence Theory." *Physics of Fluids 22* (November 1979) 2168-2177. PPPL-1522 (February 1979) 40 pp.

Kulsrud, R.M., "The Plasma Physics of Trapping of Cosmic Rays Around Supernova." Presented at the 16th International Cosmic Ray Conference, Kyoto, Japan, August 1979. PPPL-1558 (June 1979) 5 pp.

Kulsrud, R.M. "Stochastic Acceleration by Hydromagnetic Turbulence." PPPL-1518 March 1979) 17 pp.

Kuo-Petravic, G., Petravic, M., "A Program Generator for the Incomplete *LU* Decomposition-Conjugate Gradient (ICCG) Method." *Computer Physics Communications 18* (September 1979) 13-25. PPPL-1435 (April 1978) 29 pp.

Lee, Y.C., Chen, L., "Analytical Theory of Drift Waves and Drift Alfvén Waves in Tokamaks." PPPL-1512 (January 1979) 14 pp.

Lee, Y.C., Chen, L., Nevins, W.M., "Stability of Drift-Wave Eigenmodes with Arbitrary Radial Wavelengths." PPPL-1544 (May 1979) 11 pp.

Lee, W.W., Nevins, W.M., Okuda, H., White, R.B., "Unstable Drift Waves in a Sheared Magnetic Field." *Physical Review Letters 43* (July 1979) 347-350. PPPL-1519 (March 1979) 14 pp.

Lee, Y.C., Chen, L., "Analytical Theory of Drift Waves and Drift Alfvén Waves in Tokamaks." *Physical Review Letters 42* (March 1979) 708-11. PPPL-1512 (January 1979) 14 pp.

Mazzucato, E., Coppi, B., "Transport of Electron Thermal Energy in High Temperature Plasmas." *Physics Letters 71A* (May 1979) 337-340. PPPL-1533 (April 1979).

Monticello, D.A., White, R.B., Rosenbluth, M.N., "Feedback Stabilization of Magnetic Islands in Tokamaks," in *Proceedings of the 7th International Conference on Plasma Physics and Controlled Nuclear Fusion Research, Innsbruck, 1978* (International Atomic Energy Agency, Vienna, 1979) Vol. 1, 605-614. PPPL-1477 (September 1979) 12 pp.

Monticello, D.A., White, R.B., Nonlinear Drift Tearing Modes." PPPL-1547 (May 1979) 25 pp.

Mynick, H.E., "Guiding-Center Hamiltonian for Arbitrary Gyration." *Physical Review Letters 43* (October 1979) 1019-1022.

Mynick, H.E., "Guiding-Center Hamiltonian for Figure-8 Particles in Axisymmetric Field-Reversed Configurations." PPPL-1576 (September 1979) 22 pp.

Mynick, H.E., Krommes, J.A., "Particle Diffusion by Magnetic Perturbations of Axisymmetric Geometries." *Physical Review Letters 43* (November 1979) 1506-1509. PPPL-1581 (August 1979) 12 pp.

Okuda, H., "Strong Plasma Turbulence and Anamalous Diffusion in a Magnetic Field." PPPL-1531 (April 1979) 33 pp.

Okuda, H., Cheng, C.Z., "Numerical Simulation of Trapped Electron Instabilities in Toroidal Geometry." *Physical Review Letters 41* October 1978) 1116-1119. PPPL-1454 (June 1978) 13 pp.

Okuda, H., Lee, W.W., Cheng, C.Z., "Electrostatic and Magnetostatic Particle Simulation Models in Three Dimensions." *Computer Physics Communications 17* (June 1979) 233-238. PPPL-1461 (July 1978) 22 pp.

Okuda, H., Lee, W.W., Lin, A.T., "Plasma Diffusion Due to Magnetic Field Fluctuations." *Physics of Fluids 22* (October 1979) 1899-1906. PPPL-1498 (January 1979) 34 pp.

Okuda, H., Lin, A.T., Lin, C.C., Dawson, J.M., "Splines and High Order Interpolations in Plasma Simulations." *Computer Physics Communications 17* (June 1979) 227-231.

Petravic, M., Kuo-Petravic, G., "An ILUCG Algorithm which Minimizes in the Euclidean Norm" *Journal of Computational Physics 32* (August 1979) 263-269. PPPL-1458 (July 1978) 13 pp.

Post, E.D., Goldston, R.J., Grimm, R.C., Hawryluk, R.J., Hirshman, S.P., Hsieh, Y.Y., Hulse, R.A., Jassby, D.L., Jensen, R.V., McKenney, A., Meade, D.M., Mikkelsen, D.R., Ogden, J.M., Okabayashi, M., Rutherford, P.H., Schmidt, J.A., Seidl, F.G.P., Suckewer, S., Tenney, F., Mirin, A.A., McCoy, M.G., Killeen, J., Rensik, M.E., Shumaker, D.E., Tarter, C.B., "Computational Studies of Impurity Effects, Impurity Control, and Neutral Beam Injection in Large Tokamaks," in *Proceedings of the 7th International Conference on Plasma Physics and Controlled Nuclear Fusion Research, Innsbruck,*

1978 (International Atomic Energy Agency, Vienna, 1979) Vol. I, 471-485. PPPL-1476 (September 1978) 20 pp.

Pytte, A., Boozer, A.H., "Neoclassical Transport in Helically Symmetric Plasmas." PPPL-1552 (May 1979) 28 pp.

Rechester, A.B., Rosenbluth, M.N., White, R.B., "Calculation of the Kolmogorov Entropy for Motion Along a Stochastic Magnetic Field." *Physical Review Letters 42* (May 1979) 1247-1250. PPPL-1523 (March 1979) 11 pp.

Rutherford, P.H., "Tearing Modes in Tokamaks," in *Symposium and Workshop on Physics of Plasmas Close to Thermonuclear Conditions, Varenna, Italy, 1979* (Editrice Compositori, Bologna, to be published) Vol. I, 129-142.

Rutherford, P.H., "Impurity-Driven Rippling Modes in Tokamaks," in *Symposium and Workshop on Physics of Plasmas Close to Thermonuclear Conditions, Varenna, Italy, 1979* (Editrice Compositori, Bologna, to be published) Vol. I, 143-158.

Sato, T., "Strong Plasma Acceleration by Slow Shocks Resulting from Magnetic Reconnection." PPPL-1559 (July 1979) 59 pp.

Sato, T., Okuda, H., "Ion Acoustic Double Layers." PPPL-1565 (July 1979) 13 pp.

Singer, C.E., Post, D.E., "Sputtering Data Requirements for Tokamak Transport Codes," in *Proceedings of Workshop on Sputtering Caused by Plasma (Neutral Beam) Surface Interaction, Argonne, 1979* (Department of Energy, Washington, April 1980) CONF 190775. 1.1-1.4.

Stix, T.H., "Stochasticity and Superadiabaticity in Radio-Frequency Plasma Heating." PPPL-1539 (April 1979) 49 pp.

Strauss, H.R., Park, W., Monticello, D.A., White, R.B., Jardin, S.C., Chance, M.S., Todd, A.M.M., Glasser, A.H., "Stability of High Beta Tokamaks to Ballooning Modes." PPPL-1535 (April 1979) 13 pp.

Tang, W.M., White, R.B., Guzdar, P.N., "Impurity Effects on Ion-Drift-Wave Eigenmodes in a Sheared Magnetic Field." PPPL-1541 (May 1979) 29 pp.

Todd, A.M.M., Manickam, J., Okabayashi, M., Chance, M.S., Grimm, R.C., Greene, J.M., Johnson, J.L., "Dependence of Ideal MHD Kink and Ballooning Modes on Plasma Shape and Profiles in Tokamaks." *Nuclear Fusion 19* (June 1979) 743-752. PPPL-1470 (August 1978) 38 pp.

Valeo, E.J., Kaw, P.K., Monticello, D.A., White, R.B., "Stability of Helically Symmetric Equilibrium to Ideal MHD Perturbations." PPPL-1487 (November 1978) 19 pp.

White, R.B., "An Interactive Code for Solving Differential Equations Using Phase Integral Methods." *Journal of Computational Physics 31* (June 1979) 409-424. PPPL-1428 (March 1978) 33 pp.

White, R.B., Monticello, D.A., Rosenbluth, M.N., "Reply to the Comments on 'Simulation of Large Magnetic Islands': A Possible Mechanism for a Major Tokamak Disruption." *Physical Review A 18* (December 1978) 2735.

White, R.B., Park, W., Monticello, D.A., Strauss, H., "High Beta Tearing and Ballooning Modes in Tokamaks," in *IAEA Symposium on Current Disruptions in Toroidal Devices, Garching, 1979,* K. Lackner and H.P. Zohrfeld, Editors (Max-Plack-Institut für Plasmaphysik, Garching, 1979) IPP 3-51 paper D 4.

White, R.B., Waddell, B.V., Rosenbluth, M.N., Monticello, D.A., Carreras, J., "Nonlinear Numerical Algorithms for Studying Tearing Modes," in *Theoretical and Computational Plasma Physics, Trieste, 1977* (International Atomic Energy Agency, Vienna, 1978) 79-91.